Kaolinite Surface Charges Developed in Cyclohexane in the Presence of Bitumen

by

Hanyu Zhang

A thesis submitted in partial fulfillment of the requirements for the degree of

Doctor of Philosophy

in

Materials Engineering

Department of Chemical and Materials Engineering
University of Alberta

Abstract

Non-aqueous extraction (NAE) process was explored as an alternative to the Clark hot water extraction process (CHWE) to recover bitumen from Alberta oil sands. The upshot of the NAE process is that it eliminates the latter's environmental issues concerning high fresh water and energy consumptions. Significant efforts have been devoted to improving the performance of NAE over the past several decades. However, the inability to remove fine mineral solids from bitumen to produce a refinery-ready bitumen product remains one of the major challenges that prevent the NAE process from being commercially viable.

A novel approach to address this challenge involves using an external electric field to remove fine solids from NAE bitumen product. However, there is limited research on this concept, and fundamental questions regarding the charging mechanism of fine mineral particles in nonpolar organic solvents with dissolved bitumen remain largely unanswered. In this work, we focused on kaolinite, a representative clay mineral, to investigate its charging mechanism in cyclohexane suspension with the presence of bitumen by electrophoretic deposition experiments and several analytical methods, including phase analysis light scattering (PALS) zeta potential measurement, Fourier transform infrared (FTIR) spectroscopy, X-ray photoelectron spectroscopy (XPS), and electrochemical quartz crystal microbalance with dissipation (EQCM-D) measurements.

Electrophoretic deposition and zeta potential measurement showed that kaolinite particles remained uncharged in cyclohexane but acquired charges when coated with bitumen. FTIR spectra of the deposited films on the electrodes showed that carboxyl groups were the primary contributor to the negative charges of kaolinite deposited on the anode. XPS

analyses showed that the deposited organic-coated kaolinite films on the cathode had a higher nitrogen content, and the films deposited on the anode showed carbon and sulfur species with higher oxidation states that were associated with oxygen.

Subsequently, we conducted experiments to investigate the charging of kaolinite in cyclohexane with the addition of bitumen and compared it with adding a surfactant Span 80. It turned out pristine kaolinite suspended in cyclohexane remained uncharged, but the addition of bitumen induced negative charges and the addition of Span 80 caused positive charges on kaolinite. The removal of Span 80 eliminated the positive charges, suggesting that Span 80 stabilized negative charges by reverse micelles and made kaolinite positively charged. This is consistent with classical charging mechanism in nonpolar solvents. Notably, removing bitumen did not affect the negative charge on kaolinite, indicating that it is the coated bitumen rather than dissolved bitumen that made kaolinite get charged in cyclohexane.

Analysis of the kaolinite deposited on the cathode after filtering the cyclohexane-bitumen-kaolinite suspension and re-pulping kaolinite showed that it contained a lower carbon content than the kaolinite dispersed in the suspension before electrophoretic deposition. This implied that it was the desorption of a small fraction of adsorbed bitumen on kaolinite surface that caused the kaolinite to carry a net negative charge. Indeed, when the bitumen-coated kaolinite was dispersed in toluene, which is a stronger solvent than cyclohexane, more kaolinite was found to deposit on the anode than from cyclohexane. In contrast, when the bitumen-coated kaolinite was dispersed in *n*-pentane, which is a weaker solvent than cyclohexane, much less kaolinite was found to deposit on the anode. EQCM-D measurement showed that an applied external electric field could indeed induce bitumen

desorption from the bitumen layer previously adsorbed on kaolinite surface.

The findings from this work provided a new perspective on fine particles charging mechanism in nonpolar liquid, revealed the functions of bitumen in kaolinite charging when it is suspended in cyclohexane, and could guide the development of electric field-enhanced fine solids removal technology for nonaqueous extraction of oil sands.

Preface

Below is a statement of my contributions to co-authored papers contained in this thesis:

Chapter 3 has been published as "Zhang H, Tan X, Wang K, Liu Q. Electrodeposition of bitumen-, asphaltene-, or maltene-coated kaolinite from cyclohexane suspensions. Fuel. March 1, 2022. 311:122582." I was responsible for designing and performing the experiments, analyzing the data, and writing the paper draft. Tan X and Wang K were involved in the supervision, experimental design, equipment construction, and data analysis. Liu Q was the supervisory author and contributed to experiment design, data interpretation, and manuscript editing and composition. All the authors contributed to the discussion and commented on the manuscript.

Chapter 4 has been submitted to Chemical Engineering Journal as "Zhang H, Wang K, Wang D, Li J, Xiang B, Tan X, Liu Q. Kaolinite surface charges developed in cyclohexane suspension with dissolved Span 80 or bitumen: electrodeposition and adsorption/desorption studies." I was responsible for designing and performing the experiments, analyzing the data, and writing the paper draft. Wang K was involved in equipment construction, experimental design, and data analysis. Wang D was responsible for measuring the zeta potential of kaolinite particles in water at different pH and analyzing the data. Li J was involved in performing the electrochemical QCM-D measurement and Xiang B was responsible for analyzing the QCM-D data. Tan X was involved in supervision and experimental design. Liu Q was the supervisory author and contributed to experiment design, data interpretation, and manuscript editing and composition. All the authors contributed to the discussion and commented on the manuscript.

The Appendix contains a paper published in the journal Fuel as "Zhang H, Tan X, Liu Q. Fine solids removal from non-aqueous extraction bitumen: A literature review. Fuel. March 15, 2021. 288:119727." This is a review paper and provides a complete background of the research work carried out in this thesis. I was responsible for conceptualization and writing the paper draft. Tan X was involved in supervision, conceptualization, and resource support. Liu Q was the supervisory author and contributed to conceptualization, resources support, and review and edit the draft. All the authors contributed to the discussion and commented on the manuscript.

Acknowledgements

With a heart full of gratitude, I would like to express my sincere gratitude and my deepest respect to my esteemed supervisors Dr. Qi Liu and Dr. Xiaoli Tan for their continuous guidance, encouragement, and support throughout the whole period of my Ph.D. study. Dr. Liu is not only very knowledgeable and intelligent, but also extremely patient and compassionate. If I become a good teacher in the future, it must be because I was inspired and influenced by Dr. Liu's words and deeds. Dr. Tan is always very knowledgeable and patient, providing me with lots of guidance and advices to my research work. This work could not have been finished without their significant input.

I would like to acknowledge the valuable assistance and suggestions provided by our research group research associate Dr. Kaipeng Wang, as well as IOSI lab technicians Lisa Brandt and Brittany Mackinnon. Their support in the lab and with my research work has been invaluable.

My gratitude also extends to my colleagues and group members Xianfeng Sun, Daowei Wang, Xuyang Liu, Dong Wang, Menatalla Ahmed, Haoran Sun, Xue Wang, Hongbiao Tao, Hao Li, Shahrad Khodaei Booran, Jingqiao Li, Chao Wang and Chao Deng for all their help and collaborations during my Ph.D. study. The camaraderie we shared during my Ph.D. study has been a source of strength and inspiration.

I am also thankful to my dear friend Rui Fan for his continuous encouragement and the inspiration he has provided during my moments of doubt.

I would also like to acknowledge the financial support to this research provided by the Natural Sciences and Engineering Research Council of Canada (NSERC) and the

scholarship provided by China Scholarship Council (CSC) during my Ph.D. study at the University of Alberta.

Finally, I would like to express my heartfelt gratitude to my parents and my brother for their unyielding support, unwavering encouragement, and boundless love. I could not have achieved this milestone without them, and my gratitude to them is beyond words. I also thank fate for its shelter and this era for its benediction.

Table of Contents

List of Tables

List of Figures

Nomenclature and Acronym

λ_B	Bjerrum length
k_B	Boltzmann constant
T	Absolute temperature in Kelvin
e	Elementary charge
ε_0	Vacuum dielectric constant
ε_r	Relative dielectric constant
θ	The fraction of surface coverage
C_0	Atomic concentration of carbon on kaolinite surface
C_{coated}	Atomic concentration of carbon on the surface of samples, which are bitumen-coated kaolinite, asphaltene-coated kaolinite, and maltene-coated kaolinite
C_{bulk}	Atomic concentration of carbon in bitumen, asphaltene, or maltene
Δm	Mass change
Δf	Frequency shift
ΔD	Dissipation change

AER	Alberta Energy Regulator
ACK	Asphaltene-coated kaolinite
AOT	Sodium di-2-ethylhexylsulfosuccinate
BCK	Bitumen-coated kaolinite
CHWE	Clark hot water extraction process
CMC	Critical micelle concentration
$CyNMe_2$	Cyclohexyldimethylamine
DC	Direct current

Dilbit	Diluted-bitumen-product
EDL	Electric double layer
EQCM-D	Electrochemical quartz crystal microbalance with dissipation
FFT	Fluid fine tailings
FTIR	Fourier transform infrared spectroscopy
IEP	Isoelectric point
IL	Ionic liquid
ILAS	Ionic liquid assisted solvent extraction
IOSI	Institute for Oil Sands Innovation
KB	Filter cake from cyclohexane suspension of kaolinite treated with bitumen
KS	Filter cake from cyclohexane suspension of kaolinite treated with Span 80
MCK	Maltene-coated kaolinite
MFT	Mature fine tailings
NAE	Non-aqueous extraction
OLOA 11000	Polyisobutylene succinimide
PALS	Phase analysis light scattering
PEG-PPG-PEG	poly(ethylene glycol)-block-poly(propylene glycol)-block-poly(ethylene glycol)
PFT	Paraffinic froth treatment
PMMA	Poly(methyl methacrylate)
PZC	Point of zero charge
QCM-D	Quartz crystal microbalance with dissipation
SAGD	Steam assisted gravity drainage

SESA	Solvent extraction spherical agglomeration
SHS	Switchable hydrophilicity solvent
SHSE	Switchable hydrophilicity solvent extraction
Span 80	Sorbitan monooleate
UV-Vis	Ultraviolet-visible spectroscopy
XPS	X-ray photoelectrons spectroscopy
XRD	X-ray diffraction analysis
XRF	X-ray fluorescence analysis
$Zr(Oct)_2$	Zirconyl 2-ethyl hexanoate

Chapter 1 Introduction

1.1 Background

1.1.1 Oil sands

Oil sands are natural sedimentary mixture of crude bitumen, rock matrix, other associated minerals, and water [1], and they are a non-conventional petroleum source. Canada has the largest oil sands resource in the world, which is also one of the largest proven crude oil reserves in the world [2, 3]. Canada's oil sands are mainly present in the northeastern part of the province of Alberta in three areas: Athabasca Wabiskaw-McMurray, Cold Lake Clearwater, and Peace River Bluesky-Gething [1]. According to the 2020-2021 annual report from Alberta Energy Regulator (AER) [4], the proven crude oil reserves from Alberta oil sands are 161 billion barrels.

1.1.2 Bitumen recovery from oil sands

Surface mining and in-situ are two main bitumen recovery methods used in commercial operations based on the overburden thickness of oil sands ore. In 2018, an average of 1.35 million barrels of bitumen per day were produced from surface mining, and 1.56 million barrels of bitumen per day were produced from in-situ production [5]. In-situ method is used for deep buried deposit. Steam assisted gravity drainage (SAGD) is the dominant in-situ bitumen recovery method. In this method, pairs of horizontal wells are drilled into the lower part of an oil sands formation with different depth. Steam is injected into the upper well to heat the surrounding oil sands formation and reduce the viscosity of bitumen. The bitumen then drains into the lower well and is pumped to the surface. Surface mining is used for shallow oil sands formations that are less than 75 m deep [6]. For economic

reasons, only the deposits containing more than 7 wt. % bitumen are extracted in current commercial surface mining operations [7]. Typically, surface mined oil sands in Alberta contain about 9-13 wt.% bitumen, 84-89 wt.% mineral solids (mainly clays and quartz sands), and 3-7 wt.% water [7, 8]. Bitumen is extracted from the surface mined oil sands using water-based extraction method, schematically shown in **Figure 1.1.** The mined oil sands are crushed and mixed with warm water and caustic soda (NaOH). Bitumen is released from the sands and clay by the turbulent agitation in mixers and hydrotransport pipelines, and the entrained air bubbles attach to the bitumen droplets. When the slurry reaches the primary separation vessels in extraction plant, the aerated bitumen droplets float to the pulp surface to form bitumen froth that typically contains 60 wt.% bitumen, 30 wt.% water, and 10 wt.% fine solids and clay [9]. Most of the solids in the oil sands settle to the bottom and form primary tailings that are sent to tailing ponds. The bitumen froth is sent to a froth treatment plant where it is diluted with solvents to remove fine solids and water. The cleaned bitumen is sent to upgrading and/or refinery plants for further processing to produce final oil products [10].

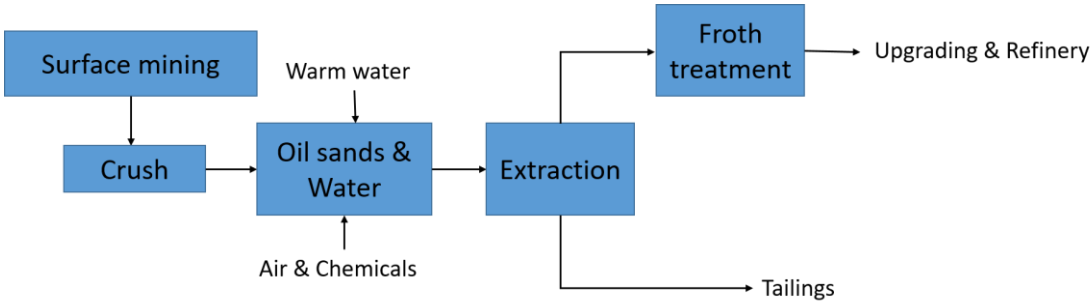

Figure 1.1 Simplified scheme for surface mined oil sands processing using water-based extraction method.

Numerous petroleum products have been produced from the bitumen that is extracted from surface mined oil sands by water-based bitumen extraction process in the past several decades; and the water-based extraction process itself has undergone many technological changes and achieved great improvement in efficiency, economics, and environmental performance. However, there are still problems with water-based extraction process due to the inherent issues of this extraction process. For example, large amounts of warm fresh water are needed in the water-based extraction process. Although about three quarters of process water are recycled, it takes about 3 barrels of fresh river water to produce 1 barrel of oil, for the extraction process runs at 17 to 21 barrels of water per barrel of bitumen [11, 12]. In addition to the high energy consumption for heating up this large amount of water (to about 50℃ to meet the requirement of the process [13]), the enormous demand of fresh water makes the oil production to be limited by the water supply capacity of the water source [13]. High energy consumption also brings environmental problems such as high greenhouse gas emissions. Besides, a large portion of the process water is trapped in the slow-settling mature fine tailings (MFT) in the tailings ponds. It is estimated that several decades are needed to release the trapped process water from MFT [3]. With increasing oil sands production, the tailings ponds area has been steadily increasing, causing all sorts of environmental problems and concerns [14].

The non-aqueous extraction (NAE) process has been proposed to overcome the issues of water-based bitumen extraction by partially or completely replacing water with organic solvents. As illustrated in **Figure 1.2**, in an NAE process, surface mined oil sands ore is crushed and mixed with an organic solvent to dissolve bitumen. After a follow up solid-liquid separation, a bitumen product stream and a dry stackable extraction solid waste

stream are generated. No water is needed, thus eliminating the inherent issues associated with the water-based bitumen extraction process. NAE of Alberta oil sands has been studied since the 1960s [15, 16] and has been on and off in lockstep with changing political, economic, and environmental climate of the industry over the past 50 years. To this day, there has not been a commercial NAE process. In addition to the non-technical factors that are difficult to predict or control, the NAE process has two technical challenges that need to be overcome before it can be seriously considered. One is the recovery of organic solvent from the extraction solid waste, and the other is the clean-up of the generated bitumen product so that it meets market specs regarding water and mineral solids content [17, 18].

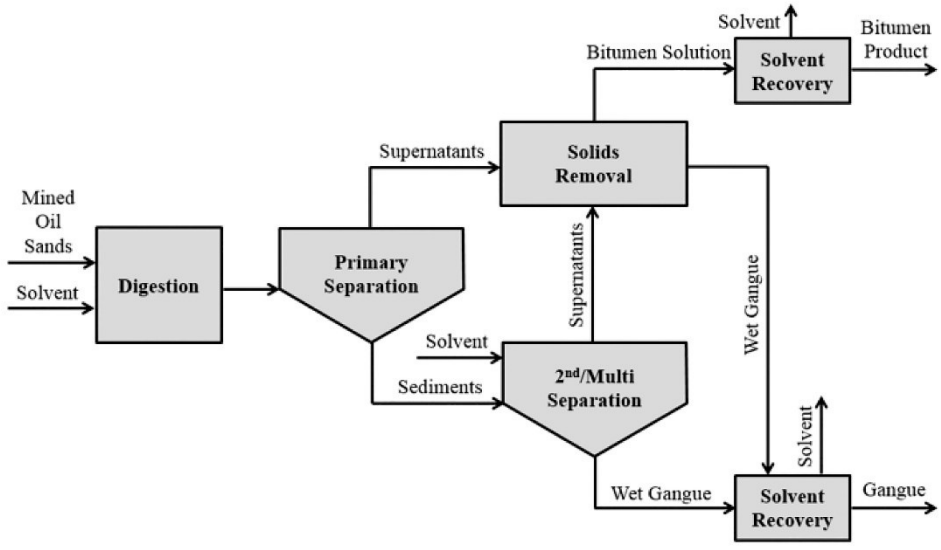

Figure 1.2 Simplified schematic flow diagram for an NAE process (adapted from Chen and Liu [19]).

For economic and environmental reasons, the solvent contained in the NAE solid waste stream as well as in the bitumen product needs to be recovered and re-used. The solvent is

more valuable than bitumen so that its loss to the solid waste should be avoided. Unrecovered solvent in the solid waste also poses an environmental hazard. Solvent migration, diffusion, and evaporation from fines-dominated NAE extraction solid waste that also contains residual bitumen are challenging scientific problems, so that although complete solvent recovery by a high temperature under vacuum is technically possible, how to make the process economical and less energy-intensive is a major challenge [20].

The bitumen product from an NAE process will unavoidably contain water (e.g., from oil sands connate water) and fine clay solids. The bitumen product needs to be cleaned to contain less than 0.5 wt.% combined solids and water to be transported by pipelines and less than 0.03 wt.% solids to be used as direct feed to high conversion refineries [17, 18]. However, fine solids in NAE bitumen products are very difficult to remove because the particle sizes are small, ranging from 10 nm to 10 μm [17, 20, 21]. These small sized particles in NAE bitumen are susceptible to Brownian motion [22]. Therefore, the fine particles can remain suspended indefinitely in solvent-diluted bitumen. To make matters worse, the fine mineral particles in NAE bitumen are mostly coated by organic matters (mainly asphaltenes) [23]. This can occur before mining or during nonaqueous extraction of the mined oil sands. The organic layer coated on mineral solid surfaces can extend outward in good solvents of asphaltenes, leading to a steric repulsion which prevents particles from aggregating [3, 24].

1.1.3 Fine particles removal from NAE bitumen products

In order to reduce the mineral solids content of NAE bitumen product, many fine solids removal methods have been studied, which are based on the physical, chemical, and

physicochemical properties of the solvent-bitumen-fines system. These methods can be divided into two categories. One category of the methods aims at directly obtaining bitumen product with low solids content by modifying the NAE process. These modified NAE processes mainly include so-called solvent extraction spherical agglomeration (SESA) process, ionic liquid assisted solvent extraction (ILAS) process, and switchable hydrophilicity solvent extraction (SHSE) process, which have been reviewed in detail in our previous published review paper [13] (attached in Appendix).

Another category of the methods is to remove the fine solid particles from the solvent-diluted-bitumen-product (abbreviated as dilbit following industry convention from this point onward) after the NAE extraction. Since the usual industrial solid-liquid separation methods such as filtration and centrifugation are only suitable for slurries with particle size larger than about 100 μm [25], and since the organic coating keeps the fine particles dispersed in dilbit, these methods are ineffective in removing the fine solids from dilbit unless the suspended fine solids can be destabilized to form aggregates, or other forces (e.g. electrostatic force, magnetic force, etc.) are applied to assist with the solid-liquid separation. Therefore, these post extraction fine solids removal methods focus on improving solid-liquid separation efficiency by adding chemical additives to form aggregates in combination with the application of novel solid-liquid physical separation techniques. Adding polymer flocculants, antisolvent, and small amount of water droplets can help the fine solids in NAE bitumen form aggregates that can be more readily removed. In addition, the fine solids in NAE bitumen product can also be removed by filtration after hydrothermal treatment or filtration in a magnetic or an electric field. This research is motivated by the electrostatic filtration method to remove fine solids from dilbit. It has

been described in a recent patent by Cullinane et al. [26]. In this process (**Figure 1.3)**, the dilbit is passed through a coarse filter. The filtrate from the filter is pumped to an electrostatic separator where the fine solids in the dilbit can be removed. The electrostatic separator is a hollow container that is filled with glass beads. The electric field is applied by a pair of electrodes, with one electrode located in the center while the counter electrode surrounds the shell of the container. During the separation process, the potential difference between the electrodes can be maintained across the glass beads bed and/or the separation volume, which can lead to a spatially varying electric field because of the dielectric character of the glass beads [27]. When the NAE dilbit flows through this electric field, the dispersed fine solids, which are assumed charged, would be retained by the glass beads and removed from the flow. After the electrostatic separation, the clean bitumen with 0.1 wt.% fine solids content is sent for solvent recovery. Heat exchanges are used to control the temperature during the process. When the filter media reaches its maximum capacity, the applied voltage is turned off and the filter media are flushed with solvent. Inert fluid (such as nitrogen) can be used to purge the residue from the electrostatic separator between filtration and wash cycles in order to avoid product and solvent loss.

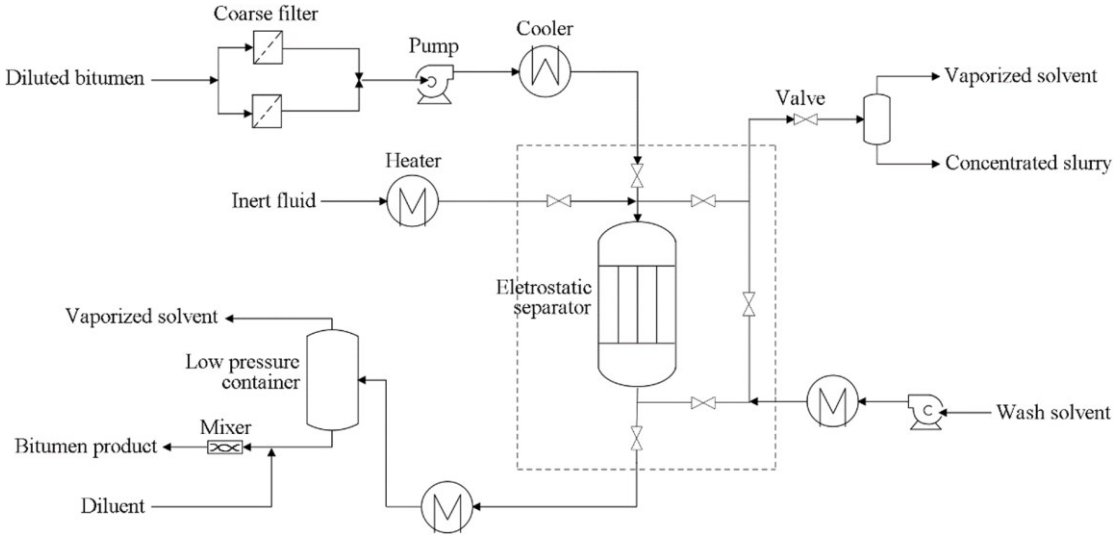

Figure 1.3 Flowsheet of fine solids removal process from NAE bitumen by electrostatic filtration patented by Cullinane et al. [26].

Using an external electrostatic field to enhance fine solids removal from NAE bitumen product is a novel concept but reported work is scarce. Many questions remain. One of the fundamental questions concerns the development of charges on the surface of fine solids in NAE bitumen product. Unlike in an aqueous suspension, how mineral particles become charged in organic solvents with very low dielectric constants, and how do dissolved species in such solvents affect the charge are still poorly understood subjects. Therefore, a detailed investigation on the development of surface charges on fine solids in solvent-diluted NAE bitumen and on how the dissolved bitumen affects these charges is required to answer these questions.

1.2 Research Objective and Approach

The main objective of this research is to investigate the development of fine solids surface charges in an organic solvent with dissolved bitumen, analyze the charging mechanism,

and explore the influencing factors. Kaolinite, the dominant clay mineral in NAE bitumen [18], was used to represent the fine solids. Cyclohexane was used as the organic solvent because it has been reported as the most promising solvent for NAE process due to its high efficiency in both bitumen and solvent recovery and in the quality of the extracted bitumen product [18]. Bitumen or bitumen subfractions (asphaltene and maltene) were added to the kaolinite-cyclohexane system to simulate the NAE bitumen product.

The charges carried by kaolinite particles in cyclohexane suspension were detected by electrophoretic deposition under a DC voltage of 1500 V. At a fixed deposition time, the amount of kaolinite deposited on either the anode or the cathode not only revealed the signs but also the magnitude of the surface charges carried by kaolinite. The composition of the kaolinite-cyclohexane suspension was changed to examine the effects of the different additives, and kaolinite was either used directly or previously coated with bitumen. The kaolinite surface charges in cyclohexane were also quantified by zeta potential measurement. Fourier transform infrared spectroscopy (FTIR) and X-ray photoelectron spectroscopy (XPS) were used to study the chemical composition of the kaolinite before and after electrophoretic deposition, which helped to explore the charging mechanism of kaolinite in cyclohexane suspensions.

1.3 Thesis Organization

This thesis is organized into five chapters:

Chapter 1 provides a general introduction to the background, motivation, objectives, and organization of the thesis.

Chapter 2 reviews the relevant literature concerning nonaqueous extraction (NAE) of oil sands, NAE bitumen product quality, past studies about particle charging in nonpolar solvents, and electrophoretic deposition. Part of this chapter has been published in the journal *Fuel*: Zhang H, Tan X, Liu Q. 2021. Fine solids removal from non-aqueous extraction bitumen: A literature review. Fuel. 288:119727. A copy of the published paper is attached in the Appendix.

Chapter 3 investigates the electrophoretic deposition of bitumen-, asphaltene-, and maltene-coated kaolinite from cyclohexane suspensions. Fourier transform infrared spectroscopy (FTIR) and X-ray photoelectron spectroscopy (XPS) were used to analyze the chemical composition of the coating layer on the kaolinite particles that were electrophoretic deposited both on the anode and the cathode. The relations between the chemical composition of the coating layer and particle surface charge in cyclohexane were explored. This chapter has been published in the journal *Fuel*: Zhang H, Tan X, Wang K, Liu Q. 2022. Electrodeposition of bitumen-, asphaltene-, or maltene-coated kaolinite from cyclohexane suspensions. Fuel. 311:122582.

Chapter 4 analyzes the influence of the addition of bitumen and a surfactant, Span 80 (sorbitan monooleate), on the surface charges of fresh kaolinite particles suspended in cyclohexane. The results showed that, with the addition of bitumen, the main contributor to kaolinite surface charge in cyclohexane is the bitumen that adsorbed on kaolinite surface, rather than the bitumen dissolved in the solution. The results of CHNS elemental composition analysis and electrochemical QCM-D measurement indicated that the selective dissolution of charge-carrying species from the bitumen coating layer induced by an external electric field was responsible for kaolinite particles charge in cyclohexane.

Span 80, on the other hand, induced kaolinite surface charges by forming reverse micelles which stabilized counter charges. Therefore, when Span 80 was removed from the solution, the kaolinite surface charges disappeared, but when bitumen was removed from the solution, the kaolinite surface charges remained in the electrophoretic deposition experiment. This chapter has been submitted to *Chemical Engineering Journal* as a research paper and is currently under review: Zhang H, Wang K, Wang D, Li J, Xiang B, Tan X, Liu Q. Kaolinite surface charges developed in cyclohexane suspension with dissolved Span 80 or bitumen: electrodeposition and adsorption/desorption studies.

Chapter 5 contains the conclusion of this thesis work, the overall discussion of the research results, original contributions, and the proposed future work.

References

[1] Masliyah JH, Czarnecki J. Xu Z. Introduction to the Athabasca oil sands. In: Handbook on theory and practice of bitumen recovery from Athabasca oil sands, volume I: theoretical basis. Kingsley Knowledge Pub; 2011. p. 1-39.

[2] Jin Y, Liu W, Liu Q, Yeung A. Aggregation of silica particles in non-aqueous media. Fuel 2011; 90 (8): 2592-7.

[3] Wang D, Tao H, Wang K, Tan X, Liu Q. The filterability of different types of minerals and the role of swelling clays in the filtration of oil sands tailings. Fuel 2022; 316: 123395.

[4] Alberta Energy Regulator, Alberta energy regulator, available at: https://static.aer.ca/prd/documents/reports/AER2020-21AnnualReport.pdf.

[5] Canadian Association of Petroleum Producers CAPP, 2019 Crude Oil Forecast, Markets and Transportation, available at: https://www.capp.ca/wp-content/uploads/2019/11/2019_Crude_Oil_Forecast_Markets_and_Transportation-338794.pdf.

[6] Regulator-ERCB AE. Alberta's Energy Reserves 2007 and Supply/Demand Outlook 2008-2017. Calgary: Energy Resources Conservation Board. 2008.

[7] Masliyah JH, Czarnecki J. Xu Z. Physical and chemical properties of oil sands. In: Handbook on theory and practice of bitumen recovery from Athabasca oil sands, volume I: theoretical basis. Kingsley Knowledge Pub; 2011. p. 173-256.

[8] Romanova UG, Valinasab M, Stasiuk EN, Yarranton HW, Schramm LL, Shelfantook WE. The effect of oil sands bitumen extraction conditions on froth treatment performance. Journal of Canadian Petroleum Technology. 2006 Sep 1; 45 (09).

[9] Rao F, Liu Q. Froth treatment in Athabasca oil sands bitumen recovery process: A review. Energy & fuels. 2013 Dec 19; 27 (12): 7199-207.

[10] Masliyah J, Zhou ZJ, Xu Z, Czarnecki J, Hamza H. Understanding water‐based bitumen extraction from Athabasca oil sands. The Canadian Journal of Chemical Engineering. 2004 Aug; 82 (4): 628-54.

[11] Oil Sands Magazine, Water usage, available at: https://www.oilsandsmagazine.com/technical/environment/water-usage

[12] Hooshiar A, Uhlik P, Liu Q, Etsell TH, Ivey DG. Clay minerals in nonaqueous extraction of bitumen from Alberta oil sands: Part 1. Nonaqueous extraction procedure. Fuel processing technology. 2012 Feb 1; 94 (1):80-5.

[13] Zhang H, Tan X, Liu Q. Fine solids removal from non-aqueous extraction bitumen: A literature review. Fuel. 2021 Mar 15; 288: 119727.

[14] Avagyan AB. Environmental building policy by the use of microalgae and decreasing of risks for Canadian oil sand sector development. Environmental Science and Pollution Research. 2017 Sep; 24 (25): 20241-53.

[15] Poettmann FH, Kelly JT. Use of a soluble oil in the extraction of hydrocarbons from oil sands. US Patent 3,392,105; 1968.

[16] West RC. Non-aqueous process for the recovery of bitumen from tar sands. US Patent 3,131,141; 1964.

[17] Pal K, Nogueira Branco LDP, Heintz A, Choi P, Liu Q, Seidl PR, et al. Performance of solvent mixtures for non-aqueous extraction of Alberta oil sands. Energy Fuels 2015; 29 (4): 2261–7.

[18] Nikakhtari H, Wolf S, Choi P, Liu Q, Gray MR. Migration of fine solids into product bitumen from solvent extraction of Alberta oilsands. Energy Fuels 2014; 28 (5): 2925–32.

[19] Chen Q, Liu Q. Bitumen coating on oil sands clay minerals: a review. Energy Fuels 2019; 33 (7): 5933-43.

[20] Nikakhtari H, Vagi L, Choi P, Liu Q, Gray MR. Solvent screening for non-aqueous extraction of Alberta oil sands. Can J Chem Eng 2013; 91 (6):1153–60.

[21] Hooshiar A, Uhlik P, Ivey DG, Liu Q, Etsell TH. Clay minerals in nonaqueous extraction of bitumen from Alberta oil sands: Part 2. Characterization of clay minerals. Fuel Process Technol 2012; 96: 183–94.

[22] Russel W. Brownian motion of small particles suspended in liquids. Annu Rev Fluid Mech 1981; 13 (1): 425–55.

[23] Bensebaa F, Kotlyar LS, Sparks BD, Chung KH. Organic coated solids in Athabasca bitumen: Characterization and process implications. Can J Chem Eng 2000; 78 (4): 610–6.

[24] Liu J, Cui X, Huang J, Xie L, Tan X, Liu Q, et al. Understanding the stabilization mechanism of bitumen-coated fine solids in organic media from non-aqueous extraction of oil sands. Fuel 2019; 242: 255–64.

[25] Kaminsky HA, Etsell TH, Ivey DG, Omotoso O. Distribution of clay minerals in the process streams produced by the extraction of bitumen from Athabasca oil sands. Can J Chem Eng 2009; 87 (1): 85–93.

[26] Cullinane JT, Minhas BS. Electrostatic filtration of fine solids from bitumen. US Patent 9,752,079; 2017.

[27] Ohsawa A, Morrow R, Murphy AB. An investigation of a dc dielectric barrier discharge using a disc of glass beads. J Phys D Appl Phys 2000; 33 (12):1487.

Chapter 2 Literature Review

2.1 The Composition of Nonaqueous Extracted Dilbit

In the nonaqueous extraction (NAE) process, water is replaced by solvents to extract bitumen from oil sands. In addition to conventional solvents, such as cyclohexane, toluene, and n-pentane, some new synthetic solvents are also used in NAE process. For example, ionic liquid (IL) has been reported used themselves or together with conventional solvents to recover bitumen from oil sands [1-3]; and switchable hydrophilicity solvents (SHS) were also used to extract bitumen as reported in literature [1, 4]. Since there has been no commercial NAE operation, the NAE bitumen products mentioned in this review are all from the laboratories. **Figure 2.1** shows a schematic of IL enhanced NAE process. IL is mixed with oil sands to extract bitumen. In most laboratorial practices, organic solvent is also added as co-solvent to the oil sands. The mixture forms distinct layers after stirring and centrifugation that consists of bitumen and solvent at the top, middle layer of IL and bottom layer of sands. The dilbit can be collected by centrifugation and decantation, and the IL both at middle and bottom layer can be recovered using water. In the dilbit, obviously bitumen and solvent are the most important component and have the most content. Small amounts of IL have been reported to be present in the dilbit due to experimental manipulation [5, 6]. The solids content in dilbit various in different reports. According to Painter's et al. [5] and Li's et al. reports, there were no Fourier transform infrared (FTIR) detectable solids contained in dilbit. However, Tourvieille et al. [7] argued that there should be about 0.9 wt.% solids containing in the dilbit according to the result of their work. Since they all used 1-ethyl-3-metyl-imidazolium tetrafluoroborate ([Emim][BF_4]) as one of the ILs in their works and Touryieille et al. followed the same

reagents and conditions used by Painter et al. It may be the difference between oil sands samples that causes the difference in solids content (Touryieille's et al. work was published in 2017, the oil sands ore used in their work was sampled in 2008 and kept in a sealed container. The ore has most likely undergone aging, which made it much more difficult to process). The detailed mineral composition of the solids and the content of potential water in dilbits were not mentioned in the literature. In addition to the IL assisted NAE process with solvent additives, there are laboratorial practices extracting bitumen from oil sands using ionic liquid without solvent additives although rarely reported [2, 8, 9]. In those processes, only ionic liquid is mixed with oil sands. Bitumen is separated from oil sands together with ionic liquid. Berton et al. [9] used different ILs and ILs mixture with various amounts extract bitumen from oil sands. Under the best conditions, the solids content in dilbit can be less than 1 wt.%. In addition, the dilbit contained considerable amount of IL, only 75 % of the IL was recovered from dilbit.

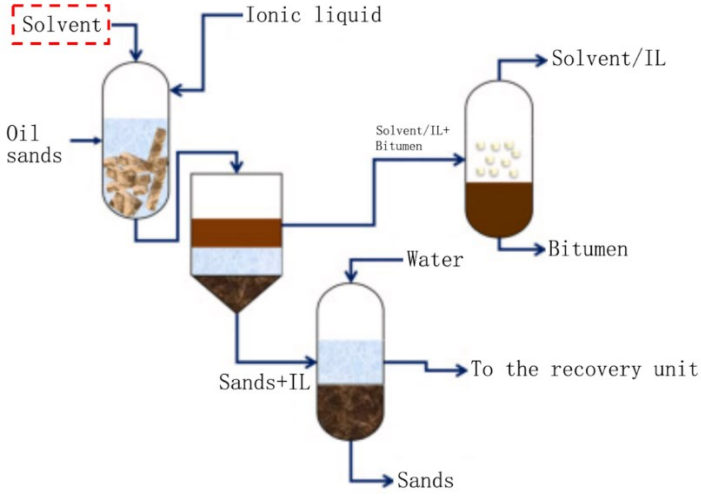

Figure 2.1 A schematic of ionic liquid promoted bitumen extraction from oil sands. It should be noted that in some reports no "solvent" was used in addition to ionic liquid [8, 9] (adapted and reproduced from Joshi and Kundu [3])

Compared with IL, SHS is relatively less used for NAE process. **Figure 2.2** shows a process for extracting bitumen from oil sands using a CO_2-responsive SHS cyclohexyldimethylamine ($CyNMe_2$). As shown in **Figure 2.2**, Holland et al. [10] used $CyNMe_2$ in its hydrophobic form to extract bitumen from oil sands. Solids and bitumen/ $CyNMe_2$ mixture were separated by decanting. The solids were washed with $CyNMe_2$ and carbonated water. The bitumen/ $CyNMe_2$ mixture was treated with water and CO_2 to extract the $CyNMe_2$ by converting it to the hydrophilic form bicarbonate salt [$CyNMe_2H$] [HCO_3]. The washed bitumen was then collected by decantation. CO_2 was removed from the bicarbonate salt solution by heating and treating with either N_2 or air, so the bicarbonate salt converted to hydrophobic $CyNMe_2$ and can be separated from water. The results of their large-scale tests (using 500 g samples of oil sands) showed that the dilbit contained 74 wt.% bitumen, 12 wt.% SHS, and 14 wt.% water. No solids were found in the dilbit according to their report. Similar to IL assisted NAE process, there is also different opinion on the solids content in dilbit. Sui et al. [11] used three different SHS (triethylamine, $CyNMe_2$, and N,N-dimethylbenzylamine) together with toluene extract bitumen from oil sands. It was found that the effect of the amine structure on dilbit quality was negligible, and the solids content in dilbit was about 0.12 mg/mL. That is to say, although toxic [12, 13] IL and SHS can improve the performance of NAE process, there is no consensus in the literature that the use of these synthetic solvents in NAE process can produce dilbit without solids. In addition, the cost problem brings great obstacles to the industrial application of IL and SHS in NAE process [10, 14]. For now, the possibility that IL assisted solvent extraction and SHS extraction can be applied in industry is much lower than the NAE process using conventional solvents. Therefore, this review mainly focuses on the

composition of dilbit from "conventional" NAE processes, i.e., extraction processes in which conventional solvents are used.

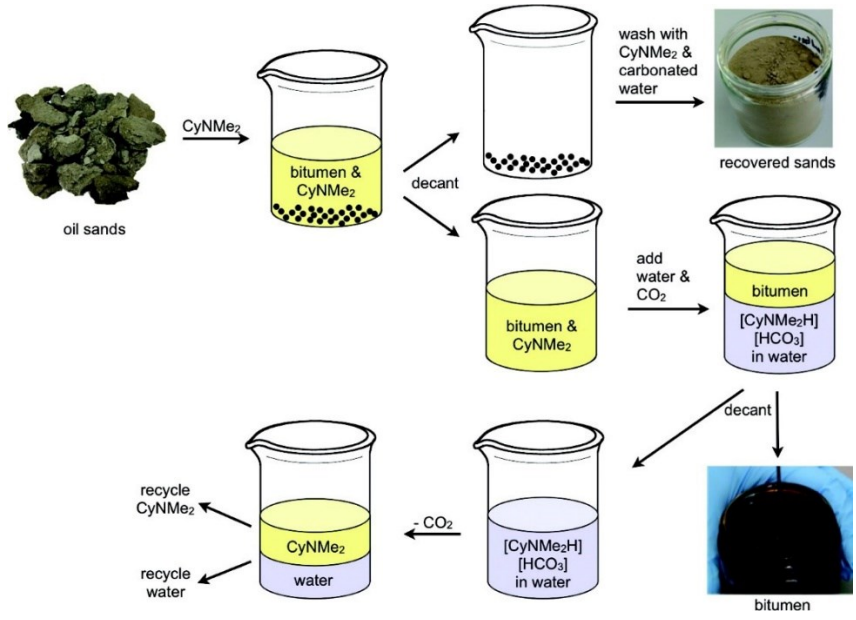

Figure 2.2 Schematic of a process for extracting bitumen from oil sands using CO_2-responsive SHS $CyNMe_2$ (adapted from Holland et al. [10]).

The composition of dilbit from conventional NAE process depends on the oil sands ore, solvent, experimental protocol, and other factors. Prior to solvent recovery from the NAE dilbit, the main component of the product should be the solvent that is used, and its content depends on the dosage of the solvent used in extraction. Over the past decade or so the Institute for Oil Sands Innovation (IOSI) has funded many projects to study NAE processes. **Figure 2.3** shows a typical NAE extraction flowsheet that has been developed from these studies. In this flowsheet, the "1st supernatant" and the "Centrifuge supernatant" are considered the NAE bitumen product. Since the oil sands ore to solvent ratio is typically kept at 60: 40 (15-19), the solvent content in the final NAE bitumen product usually ranges from 82 wt.% to 88 wt.% [18].

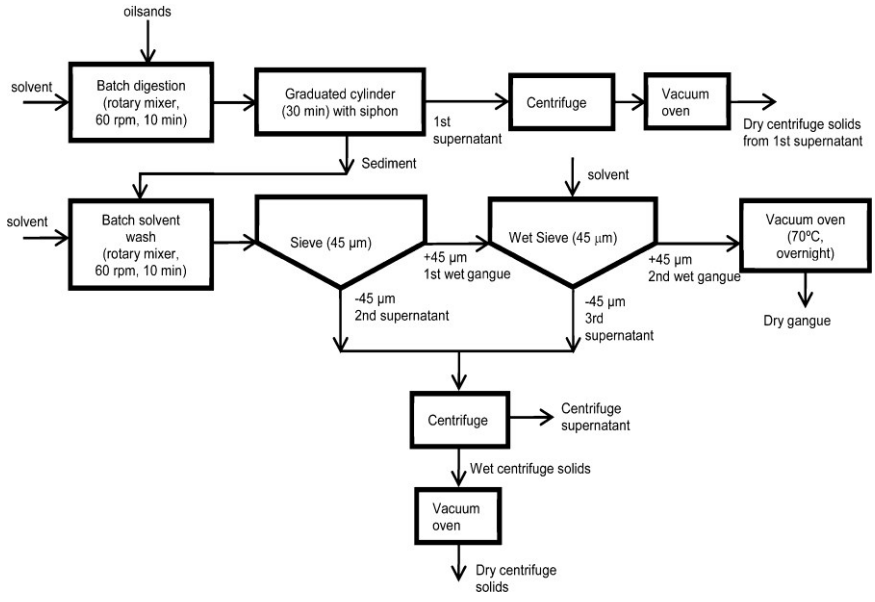

Figure 2.3 A typical flowsheet of NAE process used in laboratory (adapted from Nikakhtari et al. [17]).

After removing the solvent by rotary evaporation, the NAE bitumen product contains about 95 wt.% bitumen, varying somewhat depending on the grade of the oil sands ore, solvent used, and solvent-to-bitumen ratio. The remaining mass in the bitumen product is made up of fine solids and water. Understandably, the higher the oil sands ore grade, the higher the bitumen content and the lower the fine solids and water content in the NAE bitumen product. The type of solvent also has a significant effect on the bitumen content in the product. According to reported studies [15, 18, 20], the bitumen content in the product is higher when using ethylbenzene, isoprene, cyclohexane and cyclopentane as solvent than using methylcyclopentane and n-pentane as solvent. In addition to bitumen content, another important performance index is bitumen recovery. Previous studies [17, 21] have shown cyclohexane to be a suitable solvent to use in NAE extraction of Alberta oil sands due to high bitumen recovery, high bitumen content and low fine solids content

in product bitumen, as well as high solvent recovery rate from the NAE extraction gangue.

Although fine solids and water are the minor components in NAE bitumen, they are deleterious to the quality of the bitumen product. Few studies have focused on the study of water in NAE bitumen, and it is simply recognized as a harmful component and its content, combined with fine solids in bitumen product, should be less than 0.5 wt.% to meet pipeline transport requirement [15, 17, 22]. On the other hand, the fine solids in NAE bitumen have attracted more attention. Studies have been carried out to investigate the content, particle size distribution, mineralogical composition, and aggregate structure of fine solids in NAE bitumen product. The focus of those studies is to remove the fine solids from the bitumen product. The fine solids contents in NAE bitumen product are typically between 0.5 wt.% and 3 wt.%. Although "fine solids" in oil sands industry generally refer to mineral solids with diameters less than 45 μm, the fine solids in NAE bitumen that are problematic to remove are usually much smaller than 45 μm. They normally have particle sizes ranging from 10 nm to 10 μm [19, 22].

Table 2.1 shows the mineralogical composition of the fine solids in NAE bitumen from a specific oil sands ore. In reality, the composition will be different depending on the source of the ore, the extraction-separation equipment and specific operating parameters used in the operation, and the solvent used in the process [15, 17, 20, 23-26)]. Yet it has been widely accepted that the fine solids are mainly comprised of quartz, kaolinite and illite clays together with significant amounts of organic materials and trace amounts of siderite, pyrite, calcite and chlorite. Mixed layer swelling clays, such as illite-smectite and kaolinite-smectite, have not been extensively studied in NAE bitumen but are believed to be present in low quantities. The detection and study of these swelling clays are more

complicated than conventional powder X-ray diffraction analysis (XRD). The presence of these swelling clays could be problematic due to their unique high cation exchange capacity, high charge density and high specific surface areas [1, 17, 19, 27-29]. Nikakhtari and coworkers [17] extracted bitumen from Alberta oil sands using the NAE process described in **Figure 2.3**, and they did a comprehensive study of fine solids in the bitumen product. They reported that the fine solids in NAE bitumen product had a relatively high organic material content, at about 25 wt.%. The fine solids were also highly hydrophobic with an average contact angle of 80 – 88°, indicating that the fine solids were coated by an organic layer. However, the coating layer did not cover all the surface of fine solids, because strong signals of silicon and aluminum were detected on the surface of fine solids by XPS measurement, and this indicated there were exposed inorganic minerals on the surface.

Table 2.1 Mineralogical composition of fine solids in NAE bitumen product from an Alberta oil sands (adapted from Nikakhtari et al. [17]).

Mineral	Weight % (normalized)
Non-clays	
Quartz	38.6
Potassium feldspar	8.0
Calcite	2.4
Dolomite	0.8
Siderite	3.2
Pyrite	0.7
Hematite	0.2
Anatase	0.2
Total non-clays	**54.1**
Clays	
Kaolinite (disordered)	27.2
Illite	16.8
Chlorite	1.8
Total clays	**45.9**
Total	**100**

Nikakhtari and coworkers [17] concluded that the fine solids that were coated by organic matters were possibly natural Janus particles [30], with one side coated by organic matters while the other side uncoated; or the organic coating may be more randomly distributed rather than uniformly distributed on the fine solids surface. This hypothesis of incomplete coverage is plausible, and it has also been proven by other researchers [31-33]. Clearly, to account for the high carbon content and incomplete surface coverage at the same time, the organic coating layer must be patchy and very thick. The organic matters may also form aggregates with mineral fine solids [19] or exist independently in the system as insoluble organic particles.

2.2 Fine Solids Removal Methods from NAE Dilbit

Many methods have been attempted to remove fine solids from NAE dilbit. One of them is to aggregate suspended fine solids in NAE dilbit by adding polymer flocculants and then remove the fine solids with mechanical separation processes [22]. Polymer flocculants have been widely used to remove fine particles in wastewater treatment, pulp and paper industry [34]. In the oil sands industry, they have been used in the treatment of fluid fine tailings (FFT) and mature fine tailings (MFT) [35]. Dixon et al. [36] reported their study about fine solids removal from NAE dilbit by polymer flocculants. In their work, several polymers were selected and screened for flocculation behavior using kaolinite suspended in toluene solution of bitumen. Sedimentation experiments were carried out to observe the performance of the flocculants. They suggested that in order to improve the effectiveness of separation of solids from bitumen and to reduce the energy consumption of the following physical separation, the polymer flocculants should be hydrophobic for improving solubility in oil and should contain polar or charged groups for bonding to fine

solids. However, the sedimentation results showed that the addition of the polymers did not significantly enhance fine solids removal. This highlighted the challenges of polymer selection. Up to now, there is no report of fine solids removal method using polymer flocculants that achieves a good performance of removing solids from NAE dilbit. More studies are needed to select or develop new polymers to remove fine solids from NAE dilbit efficiently. A fundamental understanding of how polymer flocculants would behavior in complex mixture of bitumen, solvent, and solids would also help improve the fine solids removal method.

Antisolvent (i.e., refers to a poor solvent of asphaltene, which can precipitate asphaltene from solution) has also been used to aggregate and remove solids from NAE dilbit [25]. With the addition of antisolvent in dilbit, asphaltene molecules tend to bind together and therefore form "network" structured aggregates [37]. This process can trap and collect fine solids, which can be removed together with the precipitated asphaltene [38]. The suspended fine solids can also function as nuclei for asphaltene precipitation when an antisolvent is added [39]. The precipitation and aggregation of asphaltene by an antisolvent has been used in the treatment of bitumen froth generated by the CHWE process to remove water and fine solids from the bitumen. The process is called paraffinic froth treatment (PFT) [40]. PFT performances well in froth treatment and can result in virtually solids free bitumen product [41]. However, the disadvantage of lower bitumen recovery caused by the precipitation of asphaltene is an unavoidable issue of PFT. Graham et al. [25] used a similar process to remove fine solids from NAE extracted bitumen. Pentane was used to precipitate asphaltenes and remove fine solids from heptane extracted bitumen. Unfortunately, this process failed to meet the ideal requirement for fine solids content of

the bitumen product. In addition, using one solvent for bitumen extraction while another for fine solids removal would bring complication for industrial application.

In addition to polymer flocculants and antisolvents, water can also be used in fine solids removal from NAE dilbit. When water is added to the dilbit, it will disperse into water droplets under agitation. The water droplets can collect the fine particles and form large aggregates that are easier to settle. Alquist et al. were awarded a patent for a bitumen extraction process from oil sands using organic solvents in 1980 [42], in which the fine solids suspended in dilbit were removed by added water containing a cationic surfactant. According to the patent, the solids content in final dilbit can be reduced to about 0.2 wt.% under the optimal conditions. However, Farnand et al. [38] suggested that surfactant usually led to the formation of stable water-in-oil emulsions which were detrimental to the separation of fine solids particles. In contrast, water-soluble organic compounds with low molecular weight, such as resorcinol, formic acid, catechol, and chloral hydrate, can modify the surface wettability of the bitumen-coated particles suspended in diluted bitumen, making these particles amenable for collection by water droplets which can then be readily separated. The water-soluble low molecular weight organic compounds performed well in assisting water droplets to collect fine particles, but the concentrations of these compounds needed to be extremely high (>50 wt%) in the aqueous solution in order to achieve satisfactory degree of fine solids removal. Farnand et al.'s work also proposed a combination technique of using the water-soluble additive and antisolvent, which showed a dramatic improvement in settling rate of the fine solids at much lower reagent dosages. The solids content in bitumen product decreased to 0.1 wt.% [38]. However, such a process would require a two-solvent system as the authors used naphtha

in the NAE process and an antisolvent in the fine solids removal process. Liu et al. [43] explored this method and put forward a two-stage agglomeration process to separate fine bitumen-coated silica particles from cyclohexane by modifying the particle's surface using the amphiphilic polymer poly(ethylene glycol)-block-poly(propylene glycol)-block-poly(ethylene glycol), i.e., PEG-PPG-PEG, and then adding small amount of water to collect the surface modified particles to form large aggregates. The two-stage method required small amount of the amphiphilic polymer and performed better than one-stage addition of only the polymer or only water. Since the system was cyclohexane suspension of bitumen-coated silica without extra bitumen added, the solids content in the supernatant after treatment can be lowered to 100 ppm. Malladi [44] studied the influence of velocity and size of the collector (water) droplets on particle capture efficiency using a microfluidic aspiration device. Although the particles used in the research, hollow glass beads, were different from bitumen-coated particles, the results provided reference for an understanding of influencing factors on the performance of the water droplets collection process.

The other method for removing fine solids from NAE dilbit is filtration in an electric field. This method has been introduced in Chapter 1 of this thesis and the process in a recent patent was described in **Figure 1.3**. This research is motivated by the method of fine solids removal from NAE dilbit using external electric field. We tried to explore the charging mechanism of particles in nonpolar solvent by investigating cyclohexane suspension of kaolinite in the presence of bitumen. A fundamental understanding of why and how particles get charged in nonpolar media in the presence of bitumen could benefit the electrostatic filtration method to remove fine solids from dilbit.

2.3 Charging Mechanism of Particles in Nonpolar Solvents

Particles carry charges in most cases when they are dispersed in water, and the charging mechanisms have been analyzed extensively. However, when particles are dispersed in nonpolar solvents, the situation is more complicated. Before reviewing previous studies on the charging mechanism of particles in nonpolar solvents, it is advantageous to briefly review the mechanisms by which particles are charged in water.

The widely accepted mechanisms for particles to acquire surface charges in water include unequal dissolution of lattice-forming ions, hydrolysis of broken surface bonds, isomorphic substitution in the crystal lattice (mostly with clays), and adsorption from solution [45]. One example of the unequal dissolution of lattice-forming ions is silver iodide (AgI) particle, a sparingly soluble salt (the solubility product in water is 8.5×10^{-17}). If Ag^+ and I^- are dissolved unequally due to the influence of the solvent environment, the AgI particles would carry charges consistent with the ion that is dissolved less. For example, AgI is usually synthesized from silver nitrate ($AgNO_3$) and potassium iodide (KI). With excess $AgNO_3$ during the synthesis, the additional Ag^+ would inhibit the dissolution of Ag^+ from AgI, resulting in more I^- than Ag^+ dissolving from AgI. In this case, AgI particles would carry positive charges. In contrast, if more KI is added during synthesis, then AgI particles would carry negative charges. **Figure 2.4** shows that when more I^- is dissolved, AgI carries positive charges.

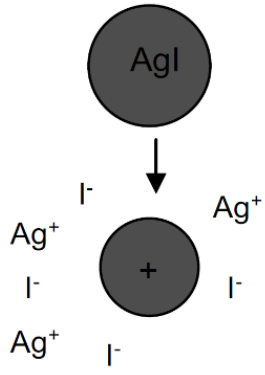

Figure 2.4 A schematic diagram of AgI particle acquiring a net charge in water by unequal dissolution of lattice-forming ions (adapted from Cosgrove et al. [45]).

Figure 2.5 shows the process of silica surface acquiring charges in water by hydrolysis of broken surface bonds. The broken silica can react with water and form hydroxyl groups (silanol groups) at the surface. Subsequent reaction of the silanol groups with H^+/OH^- in water would lead to net surface charges. It becomes positively charged by obtaining H^+ in water when the water is acidic and there are abundant H^+ (for silica specifically, the pH value should be less than 2 [46]). At above pH 2, the silanol groups tend to react with OH^- to form H_2O by losing H^+ and thus leaving the silica negatively charged.

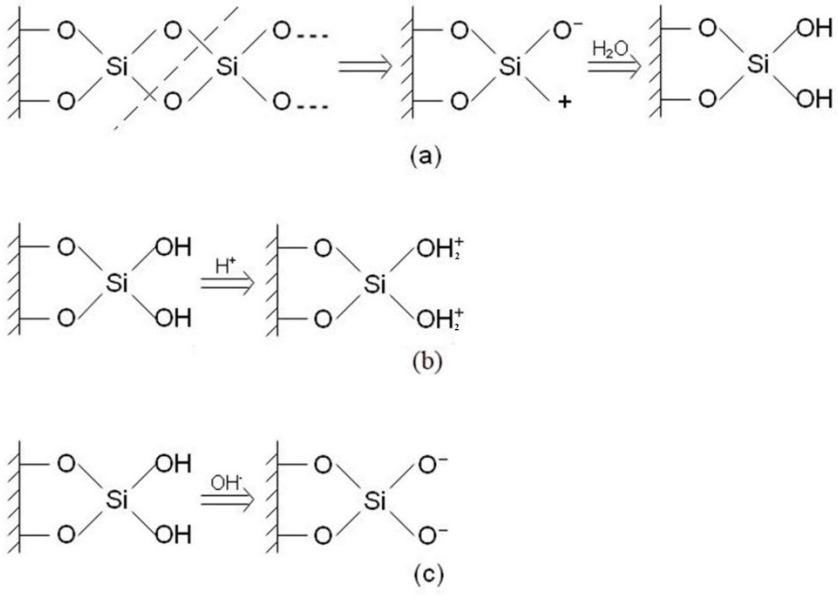

Figure 2.5 Schematic diagram showing the hydrolysis of broken silica surface bonds. (a) breakage of silica surface and interaction with water; (b) positive charge of the hydrated surface at high acidity; (c) negative charge of the hydrated surface at high alkalinity (Drawn based on the description in reference [46]).

The isomorphic substitution is the substitution of lattice ions of clay by a similar sized cations but with a different valence. It generally leads to a negative charge on the basal plane of clay due to lower valence substitution, such as the substitution of Si^{4+} by Al^{3+}, and the substitution of Al^{3+} by Mg^{2+}, Zn^{2+}, or Fe^{2+} [45].

Particles can also become charged in water by adsorbing large macromolecular organic matter [47] or ionic surfactants [48] with charges from solution. For example, ink particles are carbon black, which is hydrophobic, but they can acquire anionic charge due to the adsorption of anionic surfactants and thus disperse in water.

With a particle charged in water, the counter ions will surround the particle surface and

form a so-called electric double layer (EDL). **Figure 2.6** is a diagram of an EDL with a negatively charged core particle. As can be seen, the EDL consists of Stern layer and diffuse layer that surround a charged particle. The Stern layer consists of counter ions (positive ions in the figure) attracted to the particles surface and closely attached to it by the electrostatic force. Diffuse layer is a water film that contains free ions with a higher concentration of the counter ions. These ions are affected by the electrostatic force of the charged particle. In addition, when the charged particle moves in water (the dispersion medium), a layer of the surrounding liquid remains attached to the particle. The boundary of this layer is slipping plane. Zeta potential is the value of electric potential at the slipping plane.

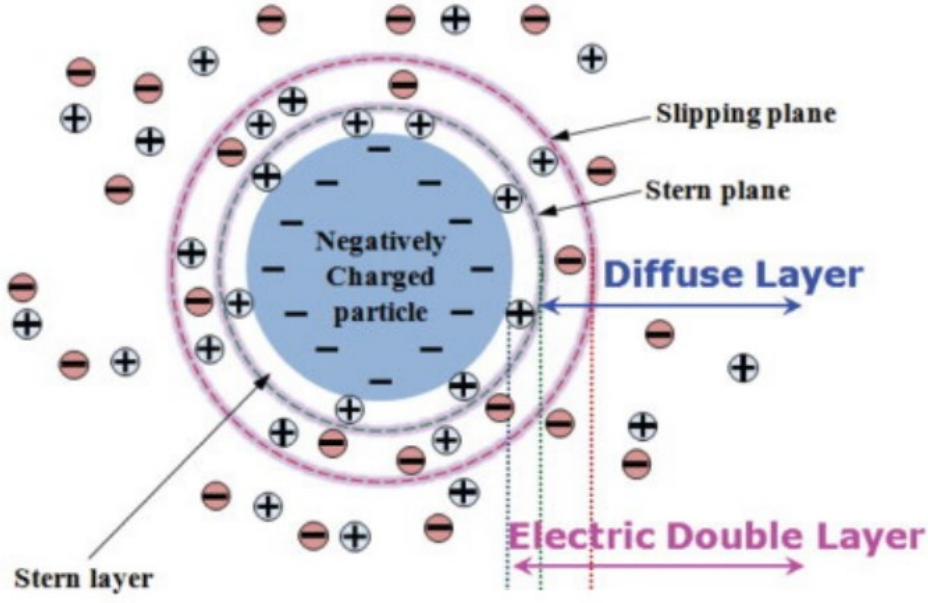

Figure 2.6 Diagram of electric double layer (adapted and reproduced from Park and Seo [49]).

When particles are suspended in a nonpolar solvent, the solvent molecules are incapable of “solvating” ions or ionic compounds due to their low dielectric constant. Therefore, particles are unlikely to acquire charges by unequal dissolution or through “solvolysis” of surface groups. On the other hand, the other two particle charging mechanisms in water, namely the isomorphic substitution in the crystal lattice and adsorption from solution, could lead to particle surface charge in nonpolar solvents. The isomorphic substitution in the crystal lattice of clay has nothing to do with the suspending solvents in which they are submerged. If particles can absorb charged components from the nonpolar solvents, they obviously would be charged. However, even though the particles could acquire charges by isomorphic substitution and adsorption, it is still an open question whether they are able to keep the net charges without being neutralized by the counter charges and counter ions.

As mentioned earlier, in an aqueous solution the counter ions are stabilized by hydration due to the high dielectric constant of water. **Table 2.2** shows the dielectric constants of water and some common nonpolar organic solvents. As can be seen the dielectric constants of the nonpolar organic solvents are much lower than water, therefore they do not have a strong affinity to ions and ionic species like water, and would not be able to stabilize the ions and ionic compounds to maintain the net charge of the particles. This can be understood by calculating the Bjerrum length (λ_B), which is defined as the distance at which the Coulombic energy between two elementary charges is equal to thermal energy (k_BT) [50]. If the distance between two opposite elementary charges is less than the Bjerrum length, the thermal energy would not be able to overcome the electrostatic attraction between the charges, so that the two elementary charges would associate with each other to form a neutral entity. Therefore, the distance between two opposite

elementary charges must always be maintained at larger than the Bjerrum length to keep them both charged. Bjerrum length is given by [51]:

$$\lambda_B = \frac{e^2}{4\pi\varepsilon_0\varepsilon_r k_B T} \quad (2.1)$$

where ε_r is the relative dielectric constant of the solvent, and T is the absolute temperature in Kelvin. The other parameters are constant: e is the elementary charge (≈ 1.602×10^{-19}C), ε_0 is the vacuum dielectric constant (≈ 8.85×10^{-12} F·m^{-1}), and k_B is the Boltzmann constant (≈ 1.38×10-23 J·K^{-1}). According to the data in **Table 2.2**, the Bjerrum length λ_B in water (ε_r ≈ 80) is about 0.7 nm when the temperature is 293.2 K, a distance that can be easily achieved by the hydration shell of monovalent ions. For example, although influenced by various factors [52], the thickness of hydration shell of monovalent ions such as Na^+ and K^+ are commonly about 0.35 nm [53]. Therefore, the counter ions surrounding charged particles in water can be kept in the EDL rather than collapsing on the particles surface to neutralize the charge. In comparison, the λ_B in a nonpolar solvent such as cyclohexane (ε_r ≈ 2) is about 28 nm, much larger than the λ_B in water. Therefore, the hydration shell of charged species in water can prevent them from neutralizing each other by electrostatic attraction. In nonpolar solvents with low dielectric constants, on the other hand, it is difficult to keep the oppositely charged species apart beyond the required Bjerrum length due to the lack of "solvation". It is possible that charges could develop on particle surfaces in nonpolar solvents, but they would immediately re-associate with the oppositely charged species to form neutral entities [54]. Therefore, the presence of stable solvated free ions or charged species is the most important precondition for particles to acquire a net charge in nonpolar solvent. For charged species that are not large enough to keep the charges beyond

the Bjerrum length from opposite charges, it is possible to stabilize the charged species through “large charged structural entities” formed by “dielectric molecules” that contain dipole moments displaced far away from the geometrical center, as proposed by Kraus et al. in 1930s [55, 56]. The “large charged structural entities” are reverse micelles formed by surfactants in nonpolar solvents. Kraus and coworkers just stopped short of linking the “large charged structural entities” to reverse micelles.

Table 2.2 Relative dielectric constant of common solvents at 293.2 K (adapted from Wohlfarth et al. [57]).

Solvent	**Relative dielectric constant**
Hexane	1.887
Heptane	1.921
Octane	1.948
Decane	1.985
Dodecane	2.012
Cyclohexane	2.024
Hexadecane	2.046
1,4-Dioxane	2.219
Bezene	2.283
Toluene	2.379
Water	80.100

Reverse micelle is an aggregate formed by surfactant molecules in nonpolar solvents. Surfactants are amphiphilic molecules with “hydrophilic head group” and hydrophobic “tail” as described in **Figure 2.7** [58]. When surfactant molecules with high enough concentration are dissolved in nonpolar solvents, the hydrophilic head groups are concentrated in the core and the hydrophobic tail groups point outward to keep the hydrophilic groups away from the nonpolar solvent. The surfactant aggregates formed in this way have a reverse structure to surfactant micelles formed in water (with hydrocarbon

tails gathering inside and hydrophilic heads pointing outward), so that they are called "reverse micelles". **Figure 2.8** shows simplified depictions of micelles and reverse micelles.

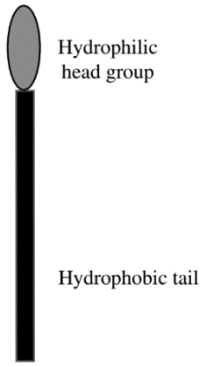

Figure 2.7 Schematic diagram of the basic surfactant molecule structure (adapted from Myers [58]).

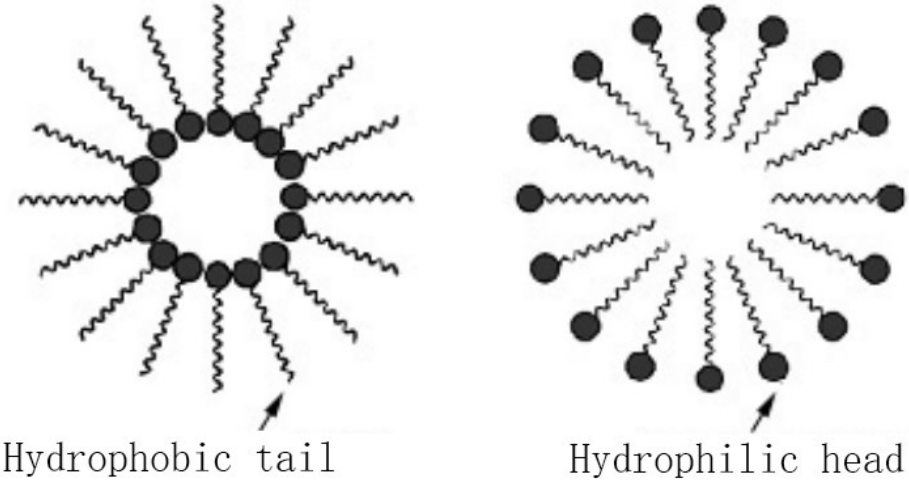

Figure 2.8 Schematic representation of a reverse micelle (left) formed in nonpolar solvents and a micelle (right) formed in water (adapted from Baruwati et al. [59]).

As shown in **Figure 2.8**, if reverse micelles can hold a charge in their center to form charged reverse micelles, the long hydrophobic tails could be able to keep the distance between the encapsulated charge and countercharges larger than Bjerrum length in the nonpolar solvent. This eliminates the re-association and neutralization of the charges. Sometimes the reverse micelles cannot completely eliminate the re-association of opposite charges when their size is below the Bjerrum length. In this case the reverse micelles can reduce electrostatic attraction between the opposite charges to form "ion-pairs". These "ion pairs" can dissociate to release "free ions" so that an equilibrium is established between the neutral ion pair and the free ions [54].

These functions of reverse micelles will allow the presence of "electrolyte" or free ions/charges in nonpolar solvents, thus providing conditions for the particles to carry net charges. The early studies on reverse micelles were mainly focused on neutral reverse micelle formation [60-62]. When charged reverse micelles gained more interest, they became accepted as the favored types of species to stabilize free charges in nonpolar solvents [63]. Indeed, charging of particles in nonpolar solvents in the presence of surfactants has been studied extensively afterwards. Ponto et al. [64] plotted a typical charging curve of particles in nonpolar solvents showing the influence of surfactant concentration on particles' electrophoretic mobility (**Figure 2.9**) based on the reported research work in literature [65-68]. These studies indicated, according to the investigation of electrophoretic mobility, particles are not charged in nonpolar solvents until the concentration of surfactant reaches a certain value. This value is called critical micelle concentration (CMC). Reverse micelle is thought to be formed in nonpolar solvents when the surfactant concentration is higher than CMC. There are some controversies regarding

CMC of surfactants in nonpolar solvents, which will be discussed in the next paragraph. When CMC is exceeded, particles charging increases with the increase of surfactant concentration and reaches a maximum. After that, the particle surface charges begin to decrease because of electrostatic screening caused by the increase in the charge-carrying reverse micelle concentration [69-73].

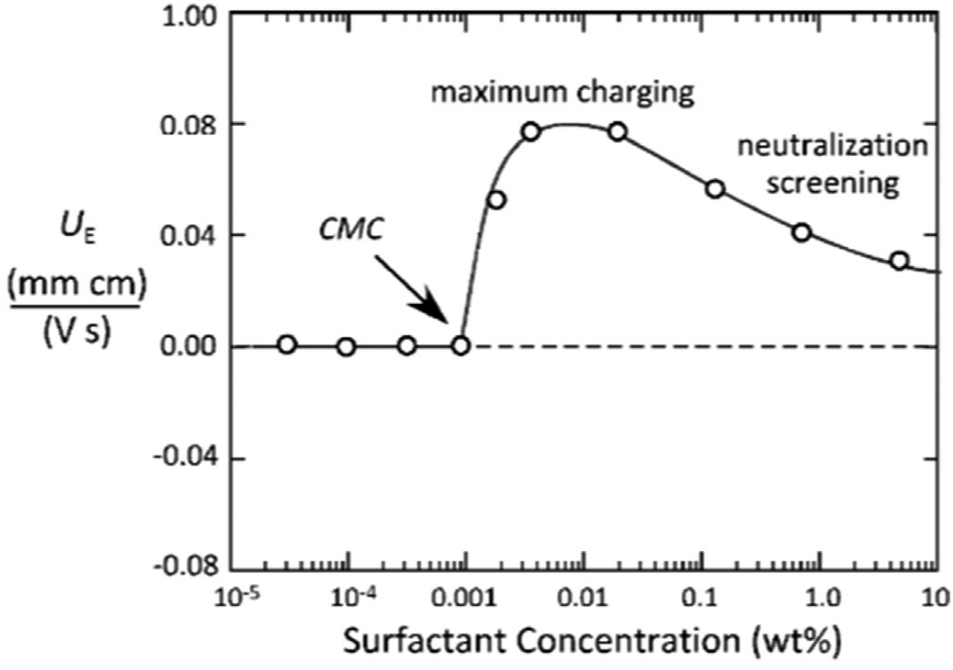

Figure 2.9 Typical charging curve for particles in nonpolar solvents with the addition of surfactants (adapted from Ponto et al. [64]).

However, different from the concept of critical micelle concentration (CMC) in water at which the micelles start to form [74], the formation of reverse micelles in nonpolar solvents does not always appear to start at a distinct concentration [70, 75, 76]. The existence of CMC is controversial for surfactants in nonpolar solvents. In aqueous solutions, when the concentration of a surfactant is increased, many physical properties of the aqueous solution (such as surface tension, turbidity, molar conductivity) change sharply over a narrow range

of concentration [23]. However, the solution properties of the nonpolar system always change gradually with the surfactant concentration [76]. There are also reports that aggregates of surfactant molecules in nonpolar solvents form at low concentrations in the form of doublets, triplets, and "pre-micellar" aggregates [75, 77-80]. In addition, the analysis about CMC of reverse micelles was also related to a small amount of water in their systems by many researchers. Eicke and Christen [81] analyzed the formation of sodium di-2-ethylhexylsulfosuccinate (AOT) reverse micelles in H_2O/AOT/i-C_8H_{18} system using infrared and vapor pressure osmometric measurements. The result suggested that water should be a pre-requisite for the micellization of surfactant in nonpolar solvents, and the CMC depended on the amount of added water. To enable the measurement of reverse micelles' properties by adding water or other polar solvents is a common method in many reports [82-86]. These nonpolar systems with the addition of water should be more accurately described as microemulsions. In this thesis, no water was intentionally added. Although the nonaqueous systems may be in contact with water vapor when the surface is in contact with air, there should be only trace amount of water in the systems, so that only the reported studies using systems with a minimal amount of water are suitable references.

When the charged reverse micelles are present in a nonpolar solvent in the form of "free ions" or ionizable "ion pairs", solid particles suspended in this nonpolar solvent may carry charges in the system (As described in **Figure 2.9**, the reverse micelles formed by surfactant can indeed make particles charged in nonpolar solvents, and the electrophoretic mobility depends on surfactant concentration). Many studies have focused on the charging mechanism of particles in solvent-surfactant suspensions. One of the reported charging mechanisms is preferential adsorption. Roberts and coworkers [87] studied the charge of

poly(methyl methacrylate) (PMMA) spheres dispersed in nonpolar solvents (decane and dodecane) solutions of AOT and zirconyl 2-ethyl hexanoate ($Zr(Oct)_2$). They concluded that the particle charges were developed by the competitive adsorption of both positively and negatively charged reverse micelles, as shown in **Figure 2.10**. If the positively charged reverse micelles are preferentially adsorbed on particle surface, the particle will be positively charged due to excess of positive charges on surface. If the particle adsorbs more negatively charged reverse micelles, it will be negatively charged. Preferential adsorption mechanism provides one way to explain why the particle potential, after reaching the maximum value, decreases with the increase of surfactant concentration. Cao et al. investigated the charging of polystyrene particles suspended in dodecane with the addition of different concentrations of AOT. **Figure 2.11** provides a schematic description about the influence of surfactant concentration on particle surface charges. At low surfactant concentrations (but still above the concentration to form reverse micelle), polystyrene particles tend to adsorb preferentially negatively charged reverse micelles compared with positively charged reverse micelles, so the particles carry net negative charges; At high surfactant concentrations, more reverse micelles are present, and the particles that carry negative charges would adsorb more positively charged reverse micelles under this condition. This will decrease the particle surface charge and may even neutralize the charges. The preferential adsorption mechanism is also used to explain the charging of nonpolar media suspensions of silica, alumina, titania, and carbon black with the addition of surfactants [63, 88-92].

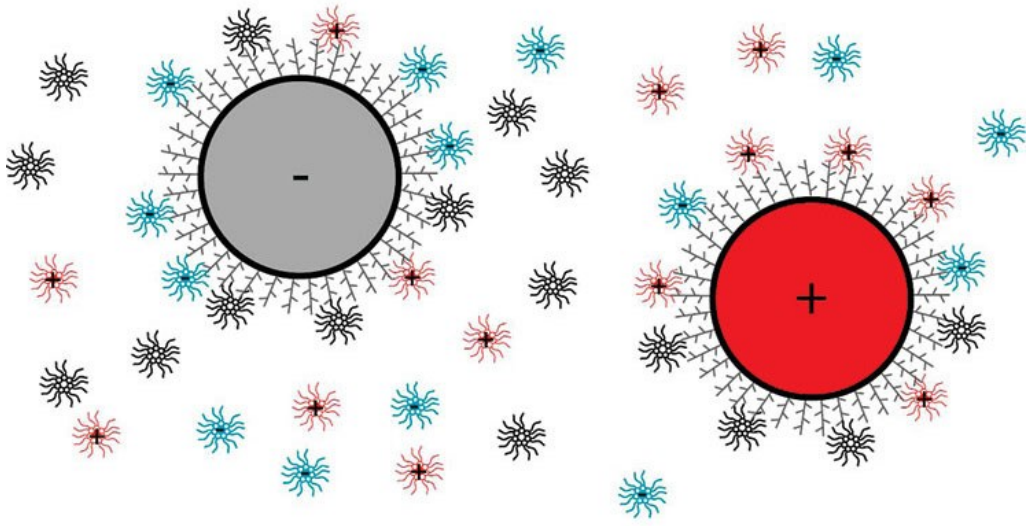

Figure 2.10 Schematic diagram of particles obtain different charges by competitive adsorption of oppositely charged micelles (adapted from Roberts et al. [87]).

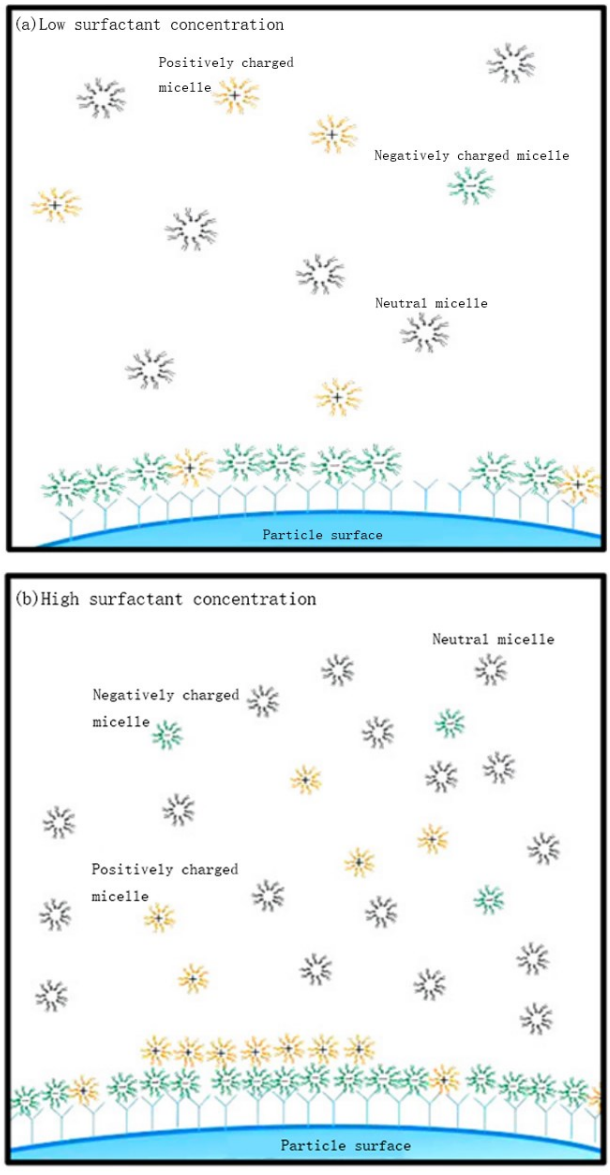

Figure 2.11 Schematic diagram of preferential adsorption of charged reverse micelles on particle surface in an organic solvent at (a) low surfactant concentration, where the negative reverse micelles are preferentially adsorbed, and (b) high surfactant concentration, where positively charged reverse micelles are preferentially adsorbed (adapted from Cao et al. [89]).

Briscoe and Horn [93] suggested another charging mechanism of particles in nonpolar

solvents with dissolved surfactants. They measured the surface forces between charged mica in *n*-decane solution of AOT using modified surface force apparatus and analyzed the charging mechanisms. According to their investigation and analysis, there was always a very small amount of water in the nonpolar liquid even when procedures were taken to avoid introducing water into the system. During their experiment, the trace amount of water in the system would accumulate at the hydrophilic mica surface and form aggregates with the adsorbed AOT. This very small amount of water could provide a hydration environment for K^+ ions from the mica surface. The hydration of K^+ reduces its electrostatic attraction to the negative lattice charge of mica so the hydrated K^+ ions may dissociate from mica lattice to form surface aggregates. Indeed, reverse micelles in nonpolar media have been shown to be exchangeable ions [94-97]. Briscoe and Horn suggested that the same ion change could happen between surface aggregates and reverse micelles in the bulk. This would lead to K^+ being solubilized into the nonpolar solution, leaving mica negatively charged. Mica has a more complex chemical structure than the oxides and carbon black mentioned previously. This surface dissolution mechanism involving a small amount of water is not suitable to explain the charging of silica, titania, alumina, and carbon black particles in nonpolar solvents.

The most widely accepted charging mechanism of particles in nonpolar solvents is the acid-base interaction mechanism introduced by Fowkes [98]. Acid-base interactions are originally defined in aqueous system. Acid was defined as anything that can increase the concentration of hydronium H^+, whereas base was identified as anything that can increase the concentration of hydroxyl OH^- in the solution [99]. The definition of acid and base was extended beyond the restriction of their relationship with water by Brønsted [100] and

Lowry independently [101] in 1923. Acid was defined as something that can donate protons during an interaction, whereas base was defined as a substance that can accept protons. The acid (or base) defined in this system was called Brønsted-Lowry acid (base) or proton acid (base). A further extension of the acid and base definition was introduced by Lewis in the same year in 1923 [102]. The Lewis acid was something that could act as an electron-pair accepter and the Lewis base was an electron-pair donor. This extension of definition removed the limitation of proton transfer during acid-base interaction. Brønsted-Lowry definition of acid-base interaction is very convenient in aqueous system, while Lewis description is more universally applicable [103, 104].

With regards to the characterization and ranking of acids and bases, the isoelectric point (IEP) is the most widely used parameter for acid-base properties characterization of mineral particles [64, 104]. Mineral particles acquire charges in aqueous suspensions, and the extent of the charge can be determined by zeta potential measurement. The concentration of ions that make the zeta potential equal to zero is the IEP. In aqueous solutions, H^+ and OH^- are recognized as potential determining ions, so the IEP is expressed in terms of pH value, which is determined by zeta potential measurements at different pH. A similar quantity that is often used together with or in place of IEP is the point of zero charge (PZC), which is the concentration of potential determining ions (not limited to H^+ and OH^- ions) making particles surface charge to equal zero. PZC is usually determined by titration. Usually the PZC and IEP are not equal. When mineral particles are dispersed in water, the PZC would equal to IEP if no specific adsorption of other species exists except H^+ and OH^- ions. The PZC of kaolinite is commonly believed to be between pH 6 and pH 6.5, although the reported PZC range of kaolinite is wide [105-109]. The difference of

reported kaolinite PZC or IEP may arise from the differences in composition of samples of different origins [106, 107].

The surfactants' acid-base property can be quantified by the empirical effective pH (pH_{Eff}) [64], which is determined using different minerals covering a wide range of PZC or IEP. **Figure 2.12** describes how the pH_{Eff} of a specific surfactant is determined. The maximum particle charges of the different minerals (with known PZC or IEP) are measured in an organic solvent in the presence of reverse micelles formed by the surfactant to be tested. The empirical pH_{Eff} of the surfactant is identified as the PZC or IEP of the mineral whose maximum surface charge is zero. Sorbitan monooleate (Span 80), AOT, and polyisobutylene succinimide (OLOA 11000) are most commonly reported oil soluble surfactants in the study of particle charging in nonpolar solvent. The pH_{Eff} of Span 80, AOT, and OLOA 11000, according to relevant reports [64, 67, 70], are 0, 5, and 9, respectively. Gacek and Berg [67] reported that the pH_{Eff} of a given surfactant appears to be unique when the relative dielectric constant of the dispersing nonpolar solvent is around 2 and the content of trace water is very low (< 100 ppm). Therefore, in nonpolar solvents, such as cyclohexane, that contains very small amount of water, the acid-base property of surfactants and mineral particles can be determined accurately and directly by comparing the surfactants' pH_{Eff} to the mineral's measured PZC or IEP.

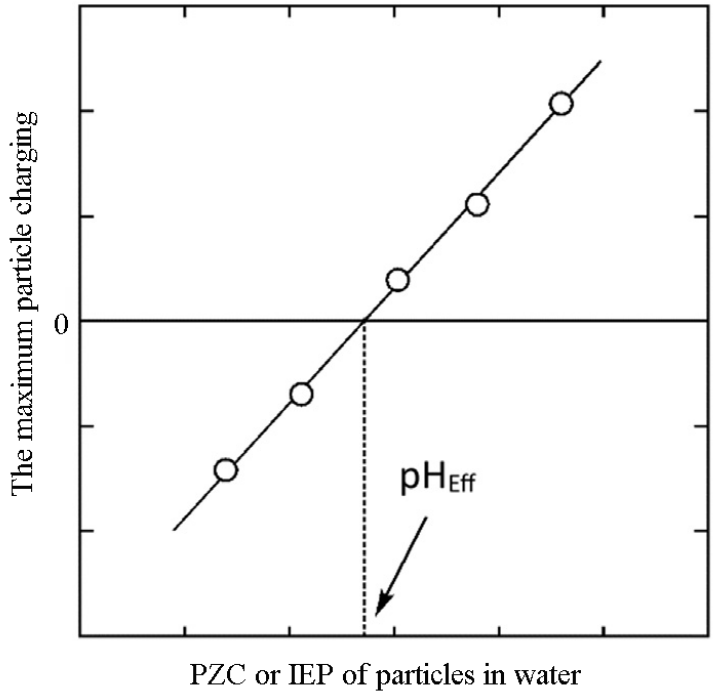

Figure 2.12 A schematic illustration of how empirical effective pH (pH_{Eff}) of a specific surfactant is identified. The x-axis is the PZC or IEP expressed in terms of pH value, the y-axis shows the maximum charges of particles with different IEPs with a given reverse-micelle-forming surfactant. The pH_{Eff} of this surfactant is the x-intercept of the trend line (adapted from Ponto and Berg [64]).

With the comparable relative acidity and basicity of the surfactant and mineral, acid-base mechanism can be used to explain how particles acquire charges in nonpolar suspensions with the addition of a surfactant. As shown in **Figure 2.13**, the mineral particles acquire charges through a process involving three steps: first, the polar head of a neutral surfactant molecule adsorbs onto particle surface to form an acid-base adduct. Then in the second step, charge transfer occurs between the surfactant molecule and particle surface according to their acid-base properties. The direction of charge transfer depends on the relative

acidity (or basicity) of the surfactant and the mineral, indicated by their pH_{EFF} and IEP, respectively. For example, if the surfactant's pH_{EFF} is lower than the mineral's IEP, then the surfactant would be a stronger acid than the mineral, and the charge transfer would happen by moving negative charges (electron donors) from mineral surface to the surfactant. Finally, in the third step, the charged surfactant molecule desorbs from mineral surface and is stabilized by reverse micelles, leaving the mineral particle to carry a net opposite charge [63, 64, 70, 98, 110].

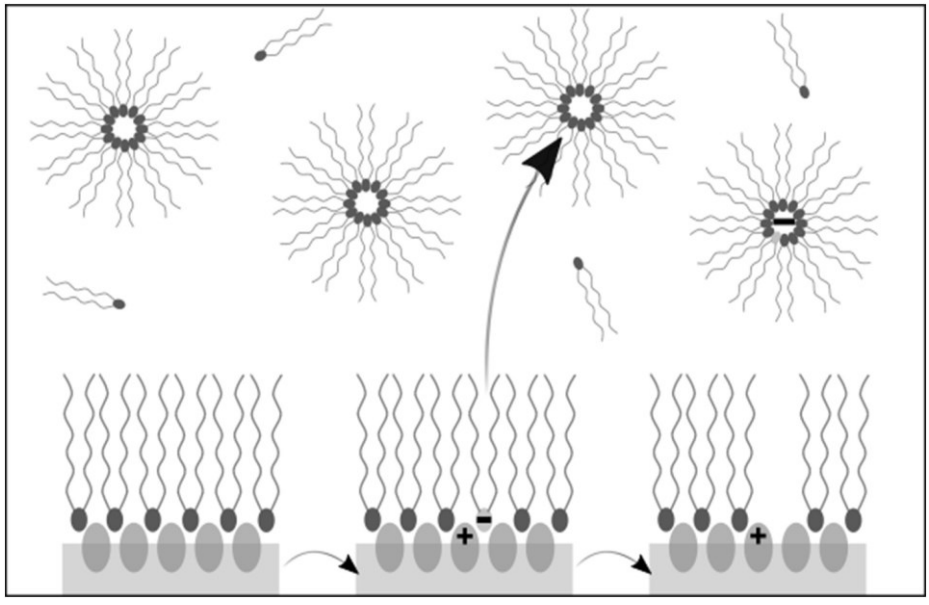

Figure 2.13 A schematic diagram that shows the process of particles acquiring charges by acid-base mechanism (adapted from Ponto and Berg [64]).

2.3 Electrophoretic Deposition

Electrophoretic deposition is a process of depositing charged particles onto oppositely charged electrodes under an applied DC electric field [111, 112]. As described in **Figure 2.14**, if the particles are positively charged, they will deposit on the cathode during the

electrophoretic deposition. Similarly, the negatively charged particles will deposit on the anode. This phenomenon has been known for more than 200 years since clay particle movement induced by an electric field in water was observed by Russian scientist Ruess in 1808. The first description of the practical use of electrophoretic deposition technology was in the production of emitters for vacuum electron tube by depositing thoria particles on platinum cathode patented in 1933 [112]. Electrophoretic deposition is also called electrodeposition in general [113, 114], although the latter often refers to electroplating [115, 116]. Technically speaking, electrophoretic deposition is different from electroplating, and **Table 2.3** presents the distinction between them.

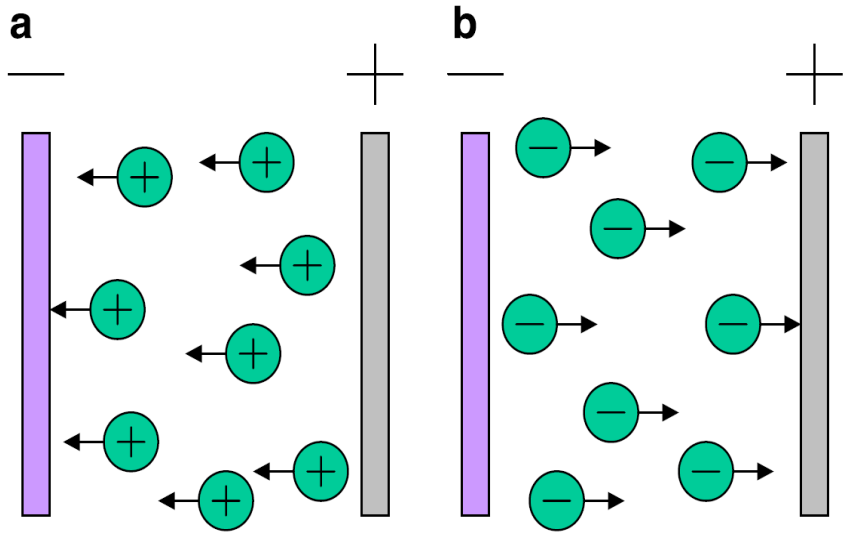

Figure 2.14 A schematic diagram that shows electrophoretic deposition process. (a) positively charged particles depositing on the cathode, (b) negatively charged particles depositing on the anode (adapted from Besra and Liu [112]).

Table 2.3 The distinction between electrophoretic deposition and electroplating (adapted from Besra and Liu [112] with modification).

Property	**Electrophoretic deposition**	**Electroplating**
Moving species	Particles, droplets	Ions
Charge transfer on deposition	None	Ion reduction, ion oxidation
Required conductance of liquid medium	Low	High
Preferred liquid	Organic	Water

Electrophoretic deposition is recognized as a materials processing technique and has been successfully used for preparing thick films of modified silica [117], carbon nanotube film [118], oxide nanorods [118], nano-size zeolite membrane [119], luminescent materials [120-122], gas diffusion electrodes [123], and superconductors [124, 125]. This technique has also been used to coat hydroxyapatite on metal substrate for biomedical applications [126, 127], produce biofilms [128], manipulate biological entities [129], and develop advanced biomaterial structures [130]. The most extensive application of electrophoretic deposition is in the field of processing of advanced materials [112]. In addition, some researchers used electrophoretic deposition method to investigate the deposition of asphaltene particles from model oils (synthetic oils) and analyze asphaltene surface charges in oil. One of the apparatuses for asphaltene electrophoretic deposition is shown in **Figure 2.15**. Two electrodes are placed parallel to each other and about half of the electrodes are submerged in the model oil with suspended asphaltene. The charges of asphaltene in different oils can be analyzed by changing the model oils and changing the method of loading samples.

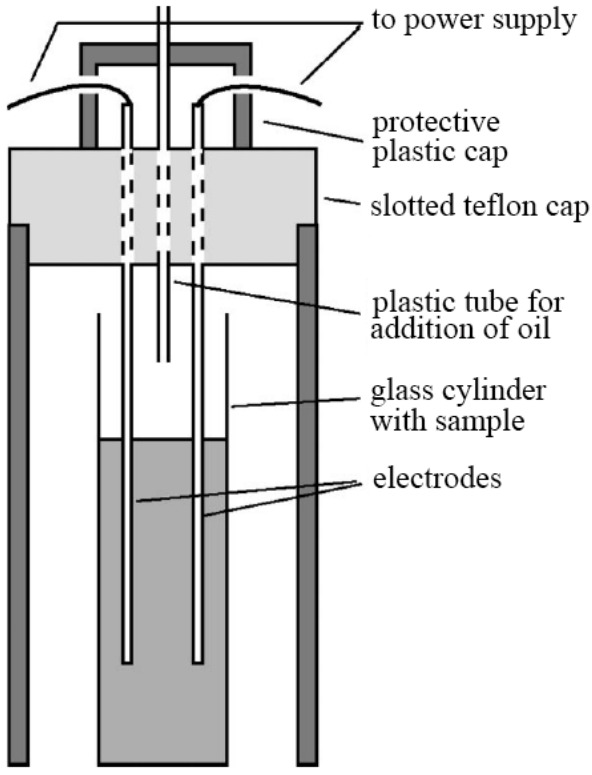

Figure 2.15 Schematic illustration of an electrophoretic deposition apparatus used for analyzing asphaltene charging in different model oils (adapted from Khvostichenko and Andersen [114]).

2.4 Quartz Crystal Microbalance with Dissipation to Study Bitumen Adsorption

Quartz crystal microbalance with dissipation (QCM-D) is an ultrasensitive technique that can measure mass changes at the nanogram scale. It has been widely used to monitor the adsorption and desorption process in real-time [131]. The working principle of QCM-D is based on the piezoelectric property of its quartz crystal sensor. The quartz crystal sensor oscillates when an alternating electric potential is applied. Under a given condition, the oscillation is influenced by the substance that adsorbs on the sensor. The mass variation on the sensor surface can be determined by monitoring the frequency and dissipation

changes on a quartz crystal sensor [132]. QCM-D has been widely used in the adsorption and desorption of polymers, DNA, and proteins on various substrates in liquid [133-137]. After Ekholm et al. first applied QCM-D to investigate the adsorption of asphaltenes and resins extracted from a North Sea crude oil on gold surface in 2001 [138], an increasing number of research groups have been studying the adsorption and desorption of crude oils and sub-components on various surfaces using QCM-D. Abudu and Goual [139] measured the adsorption of crude oil on gold, silica, stainless steel, and hydrophobic polystyrene surface in solvents with different degrees of asphaltene solubility using QCM-D. Xiang et al. [140] analyzed the desorption of bitumen from silica influenced by sodium citrate and sodium hydroxide using QCM-D. The results of QCM-D experiments indicated that bitumen desorption was significantly enhanced with the combined addition of sodium citrate and sodium hydroxide. Goual et al. used QCM-D to determine the electrophoretic deposited mass of bitumen compounds and model compounds (alcohol, acid, and amine) in toluene-based system with an external electric field. The nature of the charge carriers present in bitumen was identified in their work. Based on these studies, QCM-D is expected to measure the minute mass changes of bitumen that have been adsorbed onto the substrate surface.

References

[1] Lin F, Stoyanov SR, Xu Y. Recent advances in nonaqueous extraction of bitumen from mineable oil sands: a review. Organic Process Research & Development. 2017;21(4):492-510.

[2] Alade O, Mohammed I, Abdel-Azeim S, Shakil Hussain SM, Kamal MS, Mahmoud M, et al. Review on Applications of Ionic Liquids (ILs) for Bitumen Recovery: Mechanisms, Challenges, and Perspectives. Energy & Fuels. 2023.

[3] Joshi VA, Kundu D. Ionic liquid promoted extraction of bitumen from oil sand: A review. Journal of Petroleum Science and Engineering. 2021;199:108232.

[4] Yang Z, He C, Sui H, He L, Li X. Recent advances of CO2-responsive materials in separations. Journal of CO2 Utilization. 2019;30:79-99.

[5] Painter P, Williams P, Mannebach E. Recovery of bitumen from oil or tar sands using ionic liquids. Energy & Fuels. 2010;24(2):1094-8.

[6] Painter P, Williams P, Lupinsky A. Recovery of bitumen from Utah tar sands using ionic liquids. Energy & Fuels. 2010;24(9):5081-8.

[7] Tourvieille J-N, Larachi F, Duchesne C, Chen J. NIR hyperspectral investigation of extraction kinetics of ionic-liquid assisted bitumen extraction. Chemical Engineering Journal. 2017;308:1185-99.

[8] Abdelfatah E, Berton P, Rogers RD, Bryant SL. Low-temperature bitumen recovery from oil-sand reservoirs using ionic liquids. SPE Journal. 2019;24(05):2409-22.

[9] Berton P, Manouchehr S, Wong K, Ahmadi Z, Abdelfatah E, Rogers RD, et al. Ionic liquids-based bitumen extraction: enabling recovery with environmental footprint comparable to conventional oil. ACS Sustainable Chemistry & Engineering. 2019;8(1):632-41.

[10] Holland A, Wechsler D, Patel A, Molloy BM, Boyd AR, Jessop PG. Separation of bitumen from oil sands using a switchable hydrophilicity solvent. Canadian Journal of Chemistry. 2012;90(10):805-10.

[11] Sui H, Xu L, Li X, He L. Understanding the roles of switchable-hydrophilicity tertiary amines in recovering heavy hydrocarbons from oil sands. Chemical Engineering Journal. 2016;290:312-8.

[12] Latała A, Nędzi M, Stepnowski P. Toxicity of imidazolium and pyridinium based ionic liquids towards algae. Bacillaria paxillifer (a microphytobenthic diatom) and Geitlerinema amphibium (a microphytobenthic blue green alga). Green Chemistry. 2009;11(9):1371-6.

[13] Vanderveen JR, Durelle J, Jessop PG. Design and evaluation of switchable-hydrophilicity solvents. Green Chemistry. 2014;16(3):1187-97.

[14] Plechkova NV, Seddon KR. Applications of ionic liquids in the chemical industry. Chemical Society Reviews. 2008;37(1):123-50.

[15] Pal K, Nogueira Branco LdP, Heintz A, Choi P, Liu Q, Seidl PR, et al. Performance of solvent mixtures for non-aqueous extraction of Alberta oil sands. Energy & Fuels. 2015;29(4):2261-7.

[16] Geramian M, Liu Q, Ivey DG, Etsell TH. Influence of Oil Sands Composition on Bitumen Quality During Non-Aqueous Bitumen Extraction from the Athabasca Deposit. The Canadian Journal of Chemical Engineering. 2019;97(1):268-80.

[17] Nikakhtari H, Wolf S, Choi P, Liu Q, Gray MR. Migration of fine solids into product bitumen from solvent extraction of Alberta oilsands. Energy & fuels. 2014;28(5):2925-32.

[18] Hooshiar A, Uhlik P, Liu Q, Etsell TH, Ivey DG. Clay minerals in nonaqueous extraction of bitumen from Alberta oil sands: Part 1. Nonaqueous extraction procedure. Fuel processing technology. 2012;94(1):80-5.

[19] Hooshiar A, Uhlik P, Ivey DG, Liu Q, Etsell TH. Clay minerals in nonaqueous extraction of bitumen from Alberta oil sands: Part 2. Characterization of clay minerals. Fuel processing technology. 2012;96:183-94.

[20] Nikakhtari H, Vagi L, Choi P, Liu Q, Gray MR. Solvent screening for non-aqueous extraction of Alberta oil sands. The Canadian Journal of Chemical Engineering. 2013;91(6):1153-60.

[21] Liu J, Cui X, Huang J, Xie L, Tan X, Liu Q, et al. Understanding the stabilization mechanism of bitumen-coated fine solids in organic media from non-aqueous extraction of oil sands. Fuel. 2019;242:255-64.

[22] Zhang H, Tan X, Liu Q. Fine solids removal from non-aqueous extraction bitumen: A literature review. Fuel. 2021;288:119727.

[23] Masliyah JH, Czarnecki J, Xu Z. Handbook on theory and practice on bitumen recovery from athabasca oil sands. 2011.

[24] Wu J, Dabros T. Process for solvent extraction of bitumen from oil sand. Energy & Fuels. 2012;26(2):1002-8.

[25] Graham R, Helstrom J, Mehlberg R. A solvent extraction process for tar sand. 1987.

[26] Meadus FW, Sparks BD, Puddington IE, Farnand JR. Separating organic material from tar sands or oil shale. Google Patents; 1977.

[27] Meadus F, Bassaw B, Sparks B. Solvent extraction of athabasca oil-sand in a rotating mill Part 2. Solids—liquid separation and bitumen quality. Fuel Processing Technology. 1982;6(3):289-300.

[28] Kaminsky HA, Etsell TH, Ivey DG, Omotoso O. Distribution of clay minerals in the process streams produced by the extraction of bitumen from Athabasca oil sands. The Canadian Journal of Chemical Engineering. 2009;87(1):85-93.

[29] Kaminsky HA, Uhlik P, Hooshiar A, Shinbine A, Etsell TH, Ivey DG, et al., editors. Comparison of morphological and chemical characteristics of clay minerals in the primary froth and middlings from oil sands processing by high resolution transmission electron microscopy. Proceedings of the first international oil sands tailings conference; 2008.

[30] Hu J, Zhou S, Sun Y, Fang X, Wu L. Fabrication, properties and applications of Janus particles. Chemical Society Reviews. 2012;41(11):4356-78.

[31] Wang S, Liu Q, Tan X, Xu C, Gray MR. Study of asphaltene adsorption on kaolinite by X-ray photoelectron spectroscopy and time-of-flight secondary ion mass spectroscopy. Energy & fuels. 2013;27(5):2465-73.

[32] Wang S, Liu Q, Tan X, Xu C, Gray MR. Adsorption of asphaltenes on kaolinite as an irreversible process. Colloids and Surfaces A: Physicochemical and Engineering Aspects. 2016;504:280-6.

[33] Bensebaa F, Kotlyar LS, Sparks BD, Chung KH. Organic coated solids in Athabasca bitumen: Characterization and process implications. The Canadian Journal of Chemical Engineering. 2000;78(4):610-6.

[34] Gregory J, Barany S. Adsorption and flocculation by polymers and polymer mixtures. Advances in colloid and interface science. 2011;169(1):1-12.

[35] Vajihinejad V, Gumfekar SP, Bazoubandi B, Rostami Najafabadi Z, Soares JB. Water soluble polymer flocculants: synthesis, characterization, and performance assessment. Macromolecular Materials and Engineering. 2019;304(2):1800526.

[36] Dixon DV, Stoyanov SR, Xu Y, Zeng H, Soares JB. Challenges in developing polymer flocculants to improve bitumen quality in non-aqueous extraction processes: an experimental study. Petroleum Science. 2020;17:811-21.

[37] Madge D, Garner W. Theory of asphaltene precipitation in a hydrocarbon cyclone. Minerals engineering. 2007;20(4):387-94.

[38] Farnand J, Meadus F, Sparks B. Removal of intractable fine solids from bitumen solutions obtained by solvent extraction of oil sands. Fuel processing technology. 1985;10(2):131-44.

[39] Zahabi A, Gray MR, Dabros T. Kinetics and properties of asphaltene adsorption on surfaces. Energy & fuels. 2012;26(2):1009-18.

[40] Long Y, Dabros T, Hamza H. Stability and settling characteristics of solvent-diluted bitumen emulsions. Fuel. 2002;81(15):1945-52.

[41] Lin F, Pang CJ. Impact of a hybrid bitumen extraction process on the destabilization of resulting bitumen froth emulsion diluted with heptane. Minerals Engineering. 2020;145:106069.

[42] Alquist HE, Ammerman AM. Process for extracting bitumen from tar sands. Google Patents; 1980.

[43] Liu J, Cui X, Santander C, Tan X, Liu Q, Zeng H. Destabilization of fine solids suspended in oil media through wettability modification and water-assisted agglomeration. Fuel. 2019;254:115623.

[44] Malladi S. Removal of Particulate Fines from Organic Solvents Using Water as Collector Droplets: University of Toronto (Canada); 2015.

[45] Cosgrove T. Colloid science: principles, methods and applications: John Wiley & Sons; 2010.

[46] Lowe BM, Skylaris C-K, Green NG. Acid-base dissociation mechanisms and energetics at the silica–water interface: An activationless process. Journal of colloid and interface science. 2015;451:231-44.

[47] Bele M, Kodre A, Arčon I, Grdadolnik J, Pejovnik S, Besenhard J. Adsorption of

cetyltrimethylammonium bromide on carbon black from aqueous solution. Carbon. 1998;36(7-8):1207-12.

[48] Gupta SD, Bhagwat SS. Adsorption of surfactants on carbon black-water interface. Journal of dispersion science and technology. 2005;26(1):111-20.

[49] Park S-J, Seo M-K. Intermolecular force. Interface science and technology. 2011;18:1-57.

[50] Moritz R, Zardalidis G, Butt H-Jr, Wagner M, Müllen K, Floudas G. Ion size approaching the Bjerrum length in solvents of low polarity by dendritic encapsulation. Macromolecules. 2014;47(1):191-6.

[51] Bjerrum N. Untersuchungen über Ionenassoziation: AF Høst; 1926.

[52] Tansel B, Sager J, Rector T, Garland J, Strayer RF, Levine L, et al. Significance of hydrated radius and hydration shells on ionic permeability during nanofiltration in dead end and cross flow modes. Separation and Purification Technology. 2006;51(1):40-7.

[53] Volkov A, Paula S, Deamer D. Two mechanisms of permeation of small neutral molecules and hydrated ions across phospholipid bilayers. Bioelectrochemistry and bioenergetics. 1997;42(2):153-60.

[54] Dukhin A, Parlia S. Ions, ion pairs and inverse micelles in non-polar media. Current opinion in colloid & interface science. 2013;18(2):93-115.

[55] Kraus CA, Hooper GS. The Dielectric Properties of Solutions of Electrolytes in a Non-Polar Solvent. Proceedings of the National Academy of Sciences. 1933;19(11):939-43.

[56] Geddes JA, Kraus CA. Properties of electrolytic solutions. XVIII. Molecular polarisations and polar moments of some electrolytes in benzene solutions. Transactions of the Faraday Society. 1936;32:585-93.

[57] Wohlfarth C. CRC Handbook of Phase Equilibria and Thermodynamic Data of Aqueous Polymer Solutions: CRC Press; 2012.

[58] Myers D. Surfactant science and technology: John Wiley & Sons; 2020.

[59] Baruwati B. Studies on the synthesis, characterization, surface modification and

application of nanocrystalline nickel ferrite. India Institute of Chemical Technology Hyderabad. 2007.

[60] Nelson S, Pink R. 322. Solutions of metal soaps in organic solvents. Part III. The aggregation of metal soaps in toluene, iso butyl alcohol, and pyridine. Journal of the Chemical Society (Resumed). 1952:1744-50.

[61] Singleterry C, Weinberger LA. The Size of Soap Micelles in Benzene from Osmotic Pressure and from the Depolarization of Fluorescence1. Journal of the American Chemical Society. 1951;73(10):4574-9.

[62] Kaufman S, Singleterry CR. The critical range for micelle formation by an oil-dispersible soap in a hydrocarbon solvent. Journal of Colloid Science. 1952;7(5):453-64.

[63] Smith GN, Eastoe J. Controlling colloid charge in nonpolar liquids with surfactants. Physical Chemistry Chemical Physics. 2013;15(2):424-39.

[64] Ponto BS, Berg JC. Clay particle charging in apolar media. Applied Clay Science. 2018;161:76-81.

[65] Gacek M, Bergsman D, Michor E, Berg JC. Effects of trace water on charging of silica particles dispersed in a nonpolar medium. Langmuir. 2012;28(31):11633-8.

[66] Gacek M, Brooks G, Berg JC. Characterization of mineral oxide charging in apolar media. Langmuir. 2012;28(5):3032-6.

[67]Gacek MM, Berg JC. Investigation of surfactant mediated acid–base charging of mineral oxide particles dispersed in apolar systems. Langmuir. 2012;28(51):17841-5.

[68] Michor EL, Berg JC. Temperature effects on micelle formation and particle charging with span surfactants in apolar media. Langmuir. 2015;31(35):9602-7.

[69] Hsu MF, Dufresne ER, Weitz DA. Charge stabilization in nonpolar solvents. Langmuir. 2005;21(11):4881-7.

[70] Gacek MM, Berg JC. The role of acid–base effects on particle charging in apolar media. Advances in Colloid and Interface Science. 2015;220:108-23.

[71] Sainis SK, Merrill JW, Dufresne ER. Electrostatic interactions of colloidal particles

at vanishing ionic strength. Langmuir. 2008;24(23):13334-7.

[72] Espinosa CE, Guo Q, Singh V, Behrens SH. Particle charging and charge screening in nonpolar dispersions with nonionic surfactants. Langmuir. 2010;26(22):16941-8.

[73] Keir RI, Quinn A, Jenkins P, Thomas JC, Ralston J, Ivanova O. Electrokinetic properties of copper phthalocyanine pigment dispersions. Journal of Imaging Science and Technology. 2000;44(6):528-33.

[74] Mattei M, Kontogeorgis GM, Gani R. Modeling of the critical micelle concentration (CMC) of nonionic surfactants with an extended group-contribution method. Industrial & Engineering Chemistry Research. 2013;52(34):12236-46.

[75] Ruckenstein E, Nagarajan R. Aggregation of amphiphiles in nonaqueous media. The Journal of Physical Chemistry. 1980;84(11):1349-58.

[76] Shrestha LK, Sato T, Aramaki K. Phase behavior and self-organized structures of diglycerol monolaurate in different nonpolar organic solvents. Langmuir. 2007;23(12):6606-13.

[77] Eicke H. Aggregation and micellization. Top Curr Chem. 1980;87:85-9.

[78] Ravey J, Buzier M, Picot C. Micellar structures of nonionic surfactants in apolar media. Journal of colloid and interface science. 1984;97(1):9-25.

[79] Shrestha LK, Kaneko M, Sato T, Acharya DP, Iwanaga T, Kunieda H. Phase behavior of diglycerol fatty acid esters− nonpolar oil systems. Langmuir. 2006;22(4):1449-54.

[80] Shrestha LK, Sato T, Acharya DP, Iwanaga T, Aramaki K, Kunieda H. Phase behavior of monoglycerol fatty acid esters in nonpolar oils: Reverse rodlike micelles at elevated temperatures. The Journal of Physical Chemistry B. 2006;110(25):12266-73.

[81] Eicke HF, Christen H. Is water critical to the formation of micelles in apolar media?? Helvetica Chimica Acta. 1978;61(6):2258-63.

[82] Alexandridis P, Andersson K. Reverse micelle formation and water solubilization by polyoxyalkylene block copolymers in organic solvent. The Journal of Physical Chemistry B. 1997;101(41):8103-11.

[83] Kawai T, Hamada K, Shindo N, Kon-No K. Formation of AOT reversed micelles and W/O microemulsions. Bulletin of the Chemical Society of Japan. 1992;65(10):2715-9.

[84] Giddings LD, Olesik SV. A study of AOT reverse micelles in liquids at ambient and high pressure. Langmuir. 1994;10(9):2877-83.

[85] Manoj KM, Jayakumar R, Rakshit S. Physicochemical studies on reverse micelles of sodium bis (2-ethylhexyl) sulfosuccinate at low water content. Langmuir. 1996;12(17):4068-72.

[86] Falcone RD, Correa NM, Biasutti MA, Silber JJ. Properties of AOT aqueous and nonaqueous microemulsions sensed by optical molecular probes. Langmuir. 2000;16(7):3070-6.

[87] Roberts GS, Sanchez R, Kemp R, Wood T, Bartlett P. Electrostatic charging of nonpolar colloids by reverse micelles. Langmuir. 2008;24(13):6530-41.

[88] McNamee CE, Tsujii Y, Matsumoto M. Interaction forces between two silica surfaces in an apolar solvent containing an anionic surfactant. Langmuir. 2004;20(5):1791-8.

[89] Cao H, Cheng Y, Huang P, Qi M. Investigation of charging behavior of PS particles in nonpolar solvents. Nanotechnology. 2011;22(44):445709.

[90] Dukhin AS, Goetz PJ. How non-ionic “electrically neutral” surfactants enhance electrical conductivity and ion stability in non-polar liquids. Journal of Electroanalytical Chemistry. 2006;588(1):44-50.

[91] Patel MN, Smith Jr PG, Kim J, Milner TE, Johnston KP. Electrophoretic mobility of concentrated carbon black dispersions in a low-permittivity solvent by optical coherence tomography. Journal of colloid and interface science. 2010;345(2):194-9.

[92] Smith PG, Patel MN, Kim J, Milner TE, Johnston KP. Effect of surface hydrophilicity on charging mechanism of colloids in low-permittivity solvents. The Journal of Physical Chemistry C. 2007;111(2):840-8.

[93] Briscoe WH, Horn RG. Direct measurement of surface forces due to charging of solids immersed in a nonpolar liquid. Langmuir. 2002;18(10):3945-56.

[94] Mukherjee K, Moulik S, Mukherjee D. Langmuir1993, 9, 1727− 1730. Google

Scholar There is no corresponding record for this reference.

[95] Eicke H-F. Surfactants in nonpolar solvents. Micelles. 1980:85-145.

[96] Eicke H-f, Shepherd JC, Steinemann A. Exchange of solubilized water and aqueous electrolyte solutions between micelles in apolar media. Journal of colloid and interface science. 1976;56(1):168-76.

[97] Rharbi Y, Winnik MA. Solute exchange between surfactant micelles by micelle fragmentation and fusion. Advances in colloid and interface science. 2001;89:25-46.

[98] Pugh RJ, Matsunaga T, Fowkes FM. The dispersibility and stability of carbon black in media of low dielectric constant. 1. Electrostatic and steric contributions to colloidal stability. Colloids and Surfaces. 1983;7(3):183-207.

[99] Arrhenius S. Über die Dissociation der in Wasser gelösten Stoffe. Zeitschrift für physikalische Chemie. 1887;1(1):631-48.

[100] Brönsted JN. Einige bemerkungen über den begriff der säuren und basen. Recueil des Travaux Chimiques des Pays-Bas. 1923;42(8):718-28.

[101] Lowry T. The uniqueness of hydrogen. Journal of the Society of Chemical Industry. 1923;42(3):43-7.

[102] Lewis GN. Valence and the Structure of Atoms and Molecules: Chemical Catalog Company, Incorporated; 1923.

[103] Berg JC. The importance of acid-base interactions in wetting, coating, adhesion and related phenomena. Nordic Pulp & Paper Research Journal. 1993;8(1):75-85.

[104] Sun C, Berg JC. A review of the different techniques for solid surface acid–base characterization. Advances in Colloid and Interface Science. 2003;105(1-3):151-75.

[105] Sposito G. Surface-reactions in natural aqueous colloidal systems. Chimia. 1989;43(6):169-76.

[106] Yukselen Y, Kaya A. Zeta potential of kaolinite in the presence of alkali, alkaline earth and hydrolyzable metal ions. Water, Air, and Soil Pollution. 2003;145(1):155-68.

[107] Yukselen-Aksoy Y, Kaya A. A study of factors affecting on the zeta potential of kaolinite and quartz powder. Environmental Earth Sciences. 2011;62(4):697-705.

[108] West LJ, Stewart DI, editors. Effect of zeta potential on soil electrokinesis. Geoenvironment 2000: Characterization, Containment, Remediation, and Performance in Environmental Geotechnics; 2000: ASce.

[109] Dwari R, Mishra B. Evaluation of flocculation characteristics of kaolinite dispersion system using guar gum: a green flocculant. International Journal of Mining Science and Technology. 2019;29(5):745-55.

[110] Pugh R, Fowkes F. The dispersibility and stability of coal particles in hydrocarbon media with a polyisobutene succinamide dispersing agent. Colloids and surfaces. 1984;11(3-4):423-7.

[111] Heavens S. Electrophoretic deposition as a processing route for ceramics. Noyes Publications, Advanced Ceramic Processing and Technology. 1990;1:255-83.

[112] Besra L, Liu M. A review on fundamentals and applications of electrophoretic deposition (EPD). Progress in materials science. 2007;52(1):1-61.

[113] Taylor SE. The electrodeposition of asphaltenes and implications for asphaltene structure and stability in crude and residual oils. Fuel. 1998;77(8):821-8.

[114] Khvostichenko DS, Andersen SI. Electrodeposition of asphaltenes. 1. Preliminary studies on electrodeposition from oil− heptane mixtures. Energy & fuels. 2009;23(2):811-9.

[115] Krylova I. Painting by electrodeposition on the eve of the 21st century. Progress in Organic Coatings. 2001;42(3-4):119-31.

[116] Gurrappa I, Binder L. Electrodeposition of nanostructured coatings and their characterization—a review. Science and Technology of Advanced Materials. 2008.

[117] Hasegawa K, Kunugi S, Tatsumisago M, Minami T. Preparation of thick films by electrophoretic deposition using surface modified silica particles derived from sol-gel method. Journal of sol-gel science and technology. 1999;15(3):243-9.

[118] Du C, Heldbrant D, Pan N. Preparation and preliminary property study of carbon

nanotubes films by electrophoretic deposition. Materials Letters. 2002;57(2):434-8.

[119] Shan W, Zhang Y, Yang W, Ke C, Gao Z, Ye Y, et al. Electrophoretic deposition of nanosized zeolites in non-aqueous medium and its application in fabricating thin zeolite membranes. Microporous and Mesoporous Materials. 2004;69(1-2):35-42.

[120] Yum J-h, Seo S-Y, Lee S, Sung Y-E. Y 3Al5 O 12: Ce0. 05 phosphor coatings on gallium nitride for white light emitting diodes. Journal of the Electrochemical Society. 2003;150(2):H47.

[121] Shane MJ, Talbot JB, Kinney BG, Sluzky E, Hesse K. Electrophoretic deposition of phosphors: II. Deposition experiments and analysis. Journal of colloid and interface science. 1994;165(2):334-40.

[122] Shane MJ, Talbot JB, Schreiber RD, Ross CL, Sluzky E, Hesse K. Electrophoretic deposition of phosphors: I. Conductivity and zeta potential measurements. Journal of colloid and interface science. 1994;165(2):325-33.

[123] Hayashi K, Furuya N. Preparation of gas diffusion electrodes by electrophoretic deposition. Journal of the Electrochemical Society. 2004;151(3):A354.

[124] Maiti HS, Datta S, Basu RN. High-Tc Superconductor Coating on Metal Substrates by an Electrophoretic Technique. Journal of the American Ceramic Society. 1989;72(9):1733-5.

[125] Yau J, Sorrell C. High-Jc (Bi, Pb) 2Sr2Ca2Cu3O10+ x tapes fabricated by electrophoretic deposition. Physica C: Superconductivity and its applications. 1997;282:2563-4.

[126] Wei M, Ruys A, Milthorpe B, Sorrell C, Evans J. Electrophoretic deposition of hydroxyapatite coatings on metal substrates: a nanoparticulate dual-coating approach. Journal of Sol-Gel Science and Technology. 2001;21(1):39-48.

[127] Sridhar T, Mudali UK. Development of bioactive hydroxyapatite coatings on Type 316L stainless steel by electrophoretic deposition for orthopaedic applications. Transactions of the Indian Institute of Metals. 2003;56(3):221-30.

[128] Poortinga AT, Bos R, Busscher HJ. Controlled electrophoretic deposition of bacteria to surfaces for the design of biofilms. Biotechnology and bioengineering. 2000;67(1):117-20.

[129] Lovsky Y, Lewis A, Sukenik C, Grushka E. Atomic-force-controlled capillary electrophoretic nanoprinting of proteins. Analytical and bioanalytical chemistry. 2010;396(1):133-8.

[130] Boccaccini A, Keim S, Ma R, Li Y, Zhitomirsky I. Electrophoretic deposition of biomaterials. Journal of the Royal Society Interface. 2010;7(suppl_5):S581-S613.

[131] Chen Q, Xu S, Liu Q, Masliyah J, Xu Z. QCM-D study of nanoparticle interactions. Advances in colloid and interface science. 2016;233:94-114.

[132] Jaiswal A, Smoukov S, Poggi M, Grzybowski B, editors. Quartz crystal microbalance with dissipation monitoring (QCM-D): real-time characterization of nano-scale interactions at surfaces. Proceedings of the 2008 NSTI Nanotechnology Conference and Trade, Bosten; 2008.

[133] Irwin E, Ho J, Kane S, Healy K. Analysis of interpenetrating polymer networks via quartz crystal microbalance with dissipation monitoring. Langmuir. 2005;21(12):5529-36.

[134] Olanya G, Iruthayaraj J, Poptoshev E, Makuska R, Vareikis A, Claesson PM. Adsorption characteristics of bottle-brush polymers on silica: Effect of side chain and charge density. Langmuir. 2008;24(10):5341-9.

[135] Nguyen TH, Elimelech M. Adsorption of plasmid DNA to a natural organic matter-coated silica surface: kinetics, conformation, and reversibility. Langmuir. 2007;23(6):3273-9.

[136] Guzman E, Ortega F, Baghdadli N, Cazeneuve C, Luengo GS, Rubio RG. Adsorption of conditioning polymers on solid substrates with different charge density. ACS applied materials & interfaces. 2011;3(8):3181-8.

[137] Wayment-Steele HK, Johnson LE, Tian F, Dixon MC, Benz L, Johal MS. Monitoring N3 dye adsorption and desorption on TiO2 surfaces: a combined QCM-D and XPS study. ACS Applied Materials & Interfaces. 2014;6(12):9093-9.

[138] Ekholm P, Blomberg E, Claesson P, Auflem IH, Sjöblom J, Kornfeldt A. A quartz crystal microbalance study of the adsorption of asphaltenes and resins onto a hydrophilic surface. Journal of colloid and interface science. 2002;247(2):342-50.

[139] Abudu A, Goual L. Adsorption of crude oil on surfaces using quartz crystal microbalance with dissipation (QCM-D) under flow conditions. Energy & Fuels.

2009;23(3):1237-48.

[140] Xiang B, Truong NTV, Feng L, Bai T, Qi C, Liu Q. Study of the role of sodium citrate in bitumen liberation. Energy & Fuels. 2019;33(9):8271-8.

Chapter 3 Electrophoretic Deposition of Bitumen-, Asphaltene-, or Maltene-Coated Kaolinite from Cyclohexane Suspensions

3.1 Introduction

Kaolinite is the most abundant clay mineral in the oil sands deposits of Alberta, Canada [1]. Kaolinite is difficult to remove from oil sands bitumen products because its small size, especially bitumen products generated from a non-aqueous extraction (NAE) process. The NAE process was first explored in the 1960s [2] as an alternative to the Clark hot water extraction process (CHWE) with the aim of replacing the latter thus eliminating the latter's environmental issues, such as high fresh water and energy consumptions, high greenhouse gas emissions, and the accumulation of tailings ponds[3]. Extensive research efforts have been devoted to improving the NAE process performance and many modifications have been proposed to the original NAE process over the past several decades [4, 5]. However, the difficulty of removing fine mineral solids from the bitumen product remains one of the major issues that prevent the NAE process from being commercially viable [6].

The fine mineral solids in NAE bitumen products are mostly coated by organic matters (bitumen or bitumen subfractions) and dispersed in organic solvents that are "good solvents" for the bitumen and bitumen subfractions [7]. The coating has been identified as one of the reasons why they are difficult to remove [8]. Various methods have been investigated to remove the fine mineral solids from NAE bitumen products [9-12]. Among them, using an electrostatic field to enhance fine mineral solids removal from NAE bitumen is a novel concept where reported work is scarce. Fundamental questions such as whether the mineral particles are charged when they are coated by organic matters and dispersed in NAE bitumen product in an organic solvent, and the associated charging

characteristics and influencing factors have not been studied, much less clearly-understood.

In this study, the charging characteristics of kaolinite coated by bitumen and bitumen sub-fractions (asphaltene and maltene) suspended in cyclohexane were studied to understand its charge in the NAE bitumen product. Cyclohexane was reported as the most promising solvent for NAE process because of its high efficiency in both bitumen and solvent recovery and in the quality of the extracted bitumen product [6]. It is well known that particles acquire surface charges in an aqueous suspension by unequal dissolution of lattice ions, hydrolysis of surface functional groups, adsorption from aqueous solutions, and isomorphic substitution in the crystal lattice (mostly for clays) [13]. All of the above cause a distribution of counterions around the particle and form the so-called electrical double layer in aqueous suspensions. Colloidal particles in nonpolar solvents, on the other hand, are thought to be difficult to acquire charges due to the low dielectric permittivity of nonpolar solvents [14]. This can be understood by calculating the Bjerrum length λ_B. The Bjerrum length is the distance at which the attractive electrostatic interaction between two elementary charges is balanced by thermal energy ($\kappa_B T$). If the distance between two opposite elementary charges is less than the Bjerrum length, the thermal energy would not be sufficient to prevent the charges from associating with each other to form a neutral entity under the electrostatic attraction. Therefore, the distance between two opposite elementary charges must always be maintained at larger than the Bjerrum length to allow them to remain charged. The Bjerrum length is given by $\lambda_B = e^2/(4\pi\varepsilon_r\varepsilon_0\kappa_B T)$, where ε_r is the relative dielectric permittivity of the medium, T is the absolute temperature, and the other parameters are all constant: e the elementary charge ($\approx 1.602\times10^{-19}$ C), ε_0 the vacuum permittivity ($\approx 8.85\times10^{-12}$ F·m^{-1}), and κ_B the Boltzmann constant ($\approx 1.38\times10^{-23}$ J·K^{-1}) [15].

Assuming T = 300 K, the Bjerrum length λ_B in water ($\varepsilon_r \approx 80$) is about 0.7 nm, a distance that can be easily achieved by the hydration shell of monovalent ions. In comparison, the Bjerrum length in an organic medium such as cyclohexane ($\varepsilon_r \approx 2$) is about 28 nm. It would be difficult to maintain such large distances between two oppositely charged ions in cyclohexane. Therefore, particles would normally not carry net charges in nonpolar solvents unless the charges are housed within supramolecular structures. Studies suggested that such supramolecular structures can be reverse micelles for instance, which can keep the charges separate beyond the Bjerrum length, so that the charges are stable in nonpolar solvents [14, 16, 17]. Particles can be charged in an organic solvent in this case by the interactions between the surfactants and the functional groups or ionic species on the particle surface, preferential adsorption of the micellar ions, ionization of the surface functional groups, or the combination and interplay of those mechanisms [14, 17-20]. The system of kaolinite coated by bitumen and/or bitumen subfractions dispersed in cyclohexane is different from the systems studied and reported in the literature. In the cyclohexane suspensions of bitumen-coated kaolinite system, no surfactant was added. Although bitumen is known to release surfactants in the warm water extraction process, whether it releases surfactants in an organic media such as cyclohexane is largely unknown. Even if it does, the critical micelle concentration (CMC) would be difficult to reach based on the small amount that may be dissolved from the coating layer. Therefore, reverse micelles may not have played a role in particle charge in such a system.

In this work, the charges carried by coated kaolinite in cyclohexane were investigated through electrophoretic deposition, and the deposited films were characterized by

analytical methods such as Fourier transform infrared (FTIR) spectroscopy and X-ray photoelectron spectroscopy (XPS) to decipher the chemistry basis of the charges.

3.2 Materials and Methods

3.2.1 Materials

The bitumen sample used in this work was collected from an oil sands operator in the Fort McMurray region in northern Alberta, Canada. A high purity ASP 600 kaolinite sample with a vendor specified brightness of 85% and average particle size of 0.6 μm was purchased from BASF. The chemical composition of the kaolinite was analyzed by a Bruker CTX800 X-ray fluorescence analyzer (XRF) and given in **Table 3.1**. X-ray diffraction analysis of the ASP 600 kaolinite sample was previously carried out by other researchers in our group and it showed the sample to be high purity kaolinite with minor amount of quartz. Organic solvents including cyclohexane (> 99%), toluene (> 99.9%), and n-heptane (> 95%) were purchased from Fisher Scientific. All solvents were used as received without further purification.

Table 3.1 Chemical composition of kaolinite sample measured by a Bruker CTX800 X-ray fluorescence analyzer.

Chemical composition	**Weight (%)**
SiO_2	45.56
Al_2O_3	32.86
MgO	0.82
K_2O	0.14
Ti	0.91
Fe	0.52
Ca	0.04
Cr	0.02
P	0.02
Zn	0.01

3.2.2 Preparation of solids-free-bitumen subfractions

The as-received bitumen sample was purified to remove any contained fine mineral solids that could interfere with the study. To purify the bitumen sample, toluene was used to dilute the as-received bitumen at a 1:1 weight ratio. The diluted bitumen was centrifuged at 13,000 RCF for 1 h. The solids-free-bitumen was obtained by collecting the supernatant and evaporating toluene by a rotary evaporator. Asphaltene and maltene were extracted from the solids-free-bitumen by the following process: (i) The solids-free-bitumen was mixed with n-heptane at a 1:40 volume ratio with magnetic stirring (2 h) and ultrasonic treatment (45 min). The mixture was left to stand for 24 h to allow asphaltene to precipitate. (ii) The precipitated asphaltene was separated from the maltene by vacuum filtration using a 0.22 μm pore size PVDF membrane filter. (iii) The separated asphaltene was washed repeatedly with n-heptane and then collected after air drying in a fume hood. (iv) The maltene was obtained by removing n-heptane from the filtrate using a rotary evaporator. The elemental compositions of the bitumen, asphaltene, and maltene samples were measured by a Flash 2000 CHNS/ O elemental analyzer and the results are shown in **Table 3.2**.

Table 3.2 Elemental compositions of bitumen, asphaltene, and maltene samples measured by Flash 2000 CHNS/O Elemental Analyzer.

Sample	C (wt.%)	H (wt.%)	O (wt.%)	N (wt.%)	S (wt.%)
Bitumen	80.92	9.92	1.18	0.72	5.44
Asphaltene	79.46	7.96	1.96	1.25	8.29
Maltene	82.45	11.12	0.71	0.41	4.44

3.2.3 Preparation of organic-coated kaolinite

Kaolinite samples were first heated at 400℃ for 6 h to remove free water in a muffle furnace. The dry kaolinite sample was cooled to room temperature and stored in a drying desiccator for later use. Bitumen, asphaltene, and maltene samples were each diluted in toluene at a 1:3 mass ratio and used to treat the kaolinite. Bitumen-coated kaolinite (BCK) was prepared by mixing 5 g dry kaolinite with 100 mL toluene-diluted bitumen and stirred for 24 h. Four times ultrasonic treatments (1 min each) were performed during the stirring. The treated kaolinite was collected by filtration and washed repeatedly by toluene until the filtrate was colorless. The obtained BCK sample was dispersed in cyclohexane for later use. Asphaltene-coated kaolinite (ACK) and maltene-coated kaolinite (MCK) were prepared by the same process except that bitumen was replaced by asphaltene and maltene, respectively. The particle size distribution of these three organic-coated kaolinite was measured by a Malvern Mastersizer 3000 particle size analyzer and given in **Table 3.3**. The zeta potentials of BCK, ACK, and MCK suspensions in cyclohexane were measured by phase analysis light scattering (PALS) using a Brookhaven ZetaPALS zeta potential analyzer. The concentration of each sample in cyclohexane for zeta potential measurement was 100 mg/L. To avoid electric field-induced charging effects, the measurements were made at several applied voltages and the mobility was extrapolated to zero field strength [21]. After concluding that charging effects were not significant for these samples under the measurement conditions, each measurement was performed with an applied sinusoidal voltage of 130 V and a frequency of 10 Hz.

Table 3.3. Particle size distribution of BCK, ACK, and MCK measured by a Malvern Mastersizer 3000 particle size analyzer.

Sample	D_X (10) (μm)	D_X (50) (μm)	D_X (90) (μm)
BCK	0.44	0.84	1.81
ACK	0.47	0.91	2.02
MCK	0.46	0.84	1.80

3.2.4 Electrophoretic deposition experiments

The electrophoretic deposition experiments were carried out in a 10×40×40 mm^3 rectangular cell (16 mL volume). Two 40×40 mm^2 copper foils, 25 μm in thickness, that functioned as electrodes were placed parallel in the cell and the distance between the surfaces of the copper sheets was 10 mm. A 1500 V direct current (DC) voltage was applied between the copper electrodes by a Thermo EC 3000 XL power supply during electrophoretic deposition experiments. Two series of electrophoretic deposition experiments were performed. In the first series, cyclohexane suspension of kaolinite as well as solutions of bitumen, asphaltene, and maltene in cyclohexane were prepared at a concentration of 2 g/L, treated in an ultrasonic bath, and added to the cell for electrophoretic deposition. The duration of each deposition was 2 min. As control blank tests, the samples (kaolinite, bitumen, asphaltene, and maltene) were suspended or dissolved in cyclohexane and added to the cell but without applying voltage. The resulting electrodes were observed and photographed to judge the charges carried by the kaolinite, bitumen, asphaltene, and maltene samples. The second series of experiments were carried out to investigate the influence of sample concentration and electrophoretic deposition duration on the amount of the material electrodeposited on the electrodes from BCK, ACK,

and MCK suspensions in cyclohexane. The samples were dispersed in cyclohexane at concentrations of 1 g/L, 2 g/L, and 4 g/L. After 5 min ultrasonic treatment and 15 min standing, a 4 mL sample was added to the cell and electrophoretic deposited at the 1500 V DC electric field for different time periods (30 s, 1 min, 2 min, 3 min, 5 min, and 10 min) for each test. The deposited mass of each test was measured by an analytical balance with a capacity of 220 g and a readability of 0.1 mg. The electrodes after 2 min electrophoretic deposition of the three samples with 2 g/L particle concentration were also photographed. As control blank tests, the copper electrodes were also photographed after they were contacted with the 2 g/L organic-coated kaolinite samples in the cell for 2 min but without applying a voltage.

3.2.5 Fourier transform infrared (FTIR) spectroscopy

FTIR spectra of BCK, ACK, and MCK that were deposited on the anode and cathode were acquired using a Bruker Alpha FTIR spectrometer. The deposited samples for FTIR analyses were from the 2 min electrophoretic deposition tests with a particle concentration of 2 g/L in the deposition cell. The sample that was deposited on the 25 μm thick copper foil was measured directly by pressing the foil against an ATR crystal made of diamond crystal that was brazed into tungsten carbide. The high mechanical strength of the crystal allowed the application of a high pressure on the sample and therefore making a tight contact between the copper foil (thus the deposited sample) and the ATR crystal. Every sample was given 128 scans at a resolution of 4 cm^{-1}. To highlight the organic components that adsorbed on the kaolinite, the peaks of kaolinite were subtracted by spectrum subtraction. The spectrum subtraction was performed by $S = A - kB$, where S is the result of spectrum subtraction, A the spectrum of the samples, k a multiplier for spectrum

subtraction, and *B* the spectrum of kaolinite. Different multipliers (*k*) were used for different regions of interest (4000-3500, 3500-1300, and 1300-750 cm^{-1}).

3.2.6 X-ray photoelectron spectroscopy (XPS)

XPS analyses of kaolinite, BCK, ACK, and MCK particle samples as well as electrophoretic deposited films from cyclohexane suspensions of the three organic-coated samples were performed using a Kratos Axis (Ultra) XPS spectrometer with monochromatized Al Kα X-ray. The samples electrophoretic deposited on the copper electrodes were measured directly and the powder samples (kaolinite, BCK, ACK, and MCK) were glued to Al foils for measurement. The spectrometer was calibrated by the binding energy of Au 4f7/2 (84.0 eV) with reference to Fermi level. The pressure of the analysis chamber during measurements was lower than 5×10^{-10} Torr. Survey spectra of samples were collected at an analyzer pass energy of 160 eV within a binding energy range from 0 to 1100 eV while high-resolution peaks of C 1s, O 1s, N 1s, and S 2p were measured at the pass energy of 20 eV to investigate chemical bonding from their core electron-binding energies. XPS scans were performed on a sample area of 2 mm by 1 mm. Since the particle size of the kaolinite was less than 2 μm, the collected data was considered statistically representative.

3.3 Results and Discussion

3.3.1 Images of deposited films of kaolinite, bitumen, asphaltene, and maltene

Electrophoretic deposition experiments and control experiments of kaolinite, bitumen, asphaltene, and maltene samples in cyclohexane (the first series of electrophoretic deposition experiments) were conducted and the images of the electrodes after deposition

are shown in **Figure 3.1**. As can be seen, kaolinite generally did not deposit on the electrodes with or without applied voltage and if anything, there were probably some very sporadic deposits on the anode when voltage was applied. The subtle difference between deposition with or without voltage suggests that although kaolinite particles may be negatively charged due to isomorphic substitution in the crystal lattice, in this system, there were no supramolecular structures in the suspension to maintain the distance between the negatively charged kaolinite and positively charged counterions at longer than the Bjerrum length in cyclohexane (~28 nm at 300 K). Therefore, kaolinite particles in cyclohexane were almost electrical-neutral. Asphaltene showed significantly different deposition behaviors with or without applied voltage. No asphaltene was found to deposit on either electrode when no voltage was applied. After electrophoretic deposition in cyclohexane under a 1500 V electric field, asphaltene was found to be deposited on the cathode, which indicates that the asphaltene supramolecules that dissolved in cyclohexane were ionized and mainly carried positive charges. In contrast, the application of voltage did not appear to significantly increase the amount of bitumen and maltene deposited on either electrode. Just slightly more intense coloration on both anode and cathode was observed when the 1500 V voltage was applied (comparing **Figures 3.1(b)** with **3.1(f)**, and **Figures 3.1(d)** with **3.1(h)**). This indicates that bitumen and maltene in cyclohexane may contain a very small amount of charge carriers. Overall, it appeared that in the cyclohexane solutions of bitumen, asphaltene, and maltene, supramolecular structures may exist that were able to give the charged species the required distances to exceed the Bjerrum length in cyclohexane. But the quantity of such charged entities was very small.

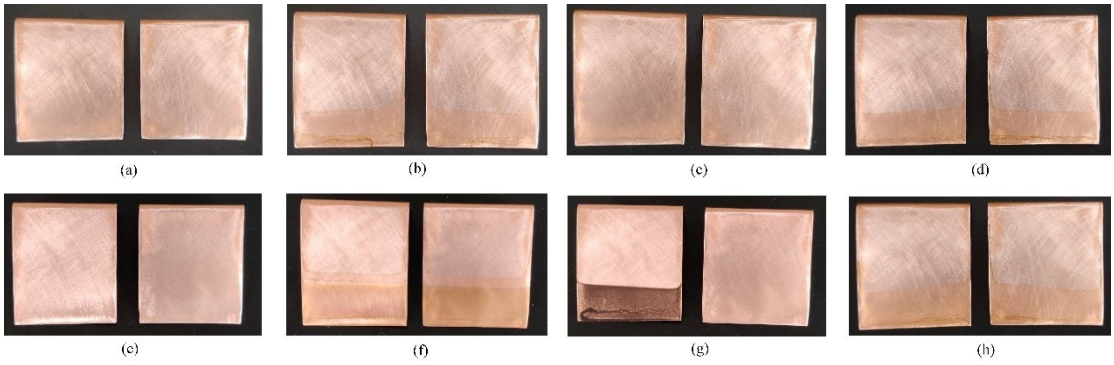

Figure 3.1 Photographs of electrodes after 2 min deposition/electrophoretic deposition. The upper panel shows the electrodes submerged in cyclohexane suspensions of (a) kaolinite, (b) bitumen, (c) asphaltene, and (d) maltene without applied voltage. The bottom panel shows the electrophoretic deposition from cyclohexane suspensions of (e) kaolinite, (f) bitumen, (g) asphaltene, and (h) maltene under 1500 V DC electric field. In each image panel, the cathode (-) is on the left and the anode (+) is on the right. The test cell was filled to about one-third of the depth so the deposition only occurred at the bottom portion of the electrodes.

3.3.2 Fraction of surface coverage and zeta potential of the organic-coated kaolinite

For the BCK, ACK, and MCK samples, the fraction of surface coverage θ of bitumen, asphaltene, and maltene on the kaolinite surface was estimated according to Eq. (3.1) [22]:

$$\theta = \frac{C_{coated} - C_0}{C_{bulk} - C_0} \tag{3.1}$$

where C_{coated} is the atomic concentration of carbon on the surface of samples BCK, ACK, or MCK measured by XPS; C_0 is the atomic concentration of carbon on kaolinite surface (XPS measurement showed that the kaolinite sample contained 3.68 at.% C on the surface,

which may be contamination from atmosphere.); C_{bulk} is the carbon atomic concentration of bitumen, asphaltene, or maltene calculated from the composition data in **Table 3.2**.

The measured surface coverage of organic matter and the zeta potential of BCK, ACK, and MCK in cyclohexane are shown in **Table 3.4**. As can be seen, kaolinite surface was not completely coated by bitumen and bitumen subfractions. Compared with bitumen and maltene, asphaltene had a slightly higher surface coverage on the kaolinite. All three coated kaolinite samples showed negative zeta potentials in cyclohexane, indicating that the kaolinite coated by bitumen, asphaltene, or maltene was negatively charged in cyclohexane. The reason may be that the adsorbed organic layer could keep the charged kaolinite particles apart at a distance larger than the Bjerrum lengths [8, 23]. At the same time, part of the coating layer may dissolve or dislodge from the surface and form supramolecular structures that could "sequester" the balancing counterions from the inherently negatively charged kaolinite. The magnitude of zeta potentials followed the order MCK > BCK > ACK, suggesting that, within the tested range, the degree of surface coverage was not directly correlated to the charges of coated kaolinite in cyclohexane, and the main influencing factor was the type of organic coating.

Table 3.4 Surface coverage of bitumen, asphaltene, or maltene on kaolinite (BCK, ACK, and MCK) and the corresponding zeta potentials of the coated kaolinite.

Sample	Surface coverage (%)	Zeta potential (mV)
BCK	35.0	-20.1
ACK	41.2	-12.4
MCK	34.5	-28.1
Un-coated kaolinite	0	0

3.3.3 Electrophoretic deposition of the organic-coated kaolinite samples

Figure 3.2 shows photographs of copper electrodes after deposition in cyclohexane suspensions of BCK, ACK, and MCK with or without the application of a 1500 V DC electric field. As can be seen from **Figures 3.2(a-c)**, the organic-coated kaolinite particles were not deposited on the copper electrodes without the application of the voltage. Therefore, the deposits collected on the electrodes with the application of the voltage should be due to the electrophoretic deposition rather than natural adsorption at this particle concentration (2 g/L). In addition, photographs of electrodes after electrophoretic deposition (**Figures 3.2(d-f)**) show that BCK and MCK particles were mainly electrophoretic deposited on the anode and only a very small amount of particles were electrophoretic deposited on the cathode, indicating that BCK and MCK particles were mainly negatively charged in cyclohexane. ACK particles, on the other hand, were electrophoretic deposited on both anode and cathode with similar amount as shown in **Figure 3.2(e)**. This indicated that some ACK particles dispersed in cyclohexane were positively charged while others were negatively charged. According to the zeta potential data shown in **Table 3.4**, the deposition amount on the anode should be higher, but an accurate comparison could not be made with the information from the photograph.

Figure 3.3 shows the influence of particle concentration and electrophoretic deposition time on electrophoretic deposition amount of BCK, MCK on the anode and the amount of ACK on both anode and cathode. The electrophoretic deposition amount of BCK and MCK on the cathode were not presented by **Figure 3.3** due to the very low value as can be seen in **Figures 3.2(d) and (f)**. It can be clearly seen from **Figure 3.3** that the deposition amount of ACK on the anode was larger than on the cathode. Therefore, consistent with

the zeta potential data, the particles of these three samples dispersed in cyclohexane were mainly negatively charged, and the deposited amounts on the anodes followed the same order as the magnitude of zeta potential, MCK > BCK > ACK. **Figure 3.3** also indicates that the mass of deposits increased with the increase of the concentration of the particles and the electrophoretic deposition time. The mass of the deposits seemed to reach a maximum after around 5 min of electrophoretic deposition. This was true for all three samples. The reason why the deposit mass did not further increase after about 5 min was not the deposited film stopped more kaolinite from depositing. The reason the deposition stopped was because the charge kaolinite was exhausted. Otherwise, the maximum deposition amounts of the three samples should be close, not the observed MCK > BCK >ACK. In addition, since 4 mL of particle suspensions were added to the cell for each test, there were 16 mg, 8 mg, and 4 mg kaolinite particles in suspensions at the concentrations of 4 g/L, 2 g/L, and 1 g/L, respectively. Not all particles were deposited under the test conditions even with extended deposition time. It is possible that not all the particles were charged, and the deposited amount was limited by the available amount of charged particles but not by the surface area of the electrodes.

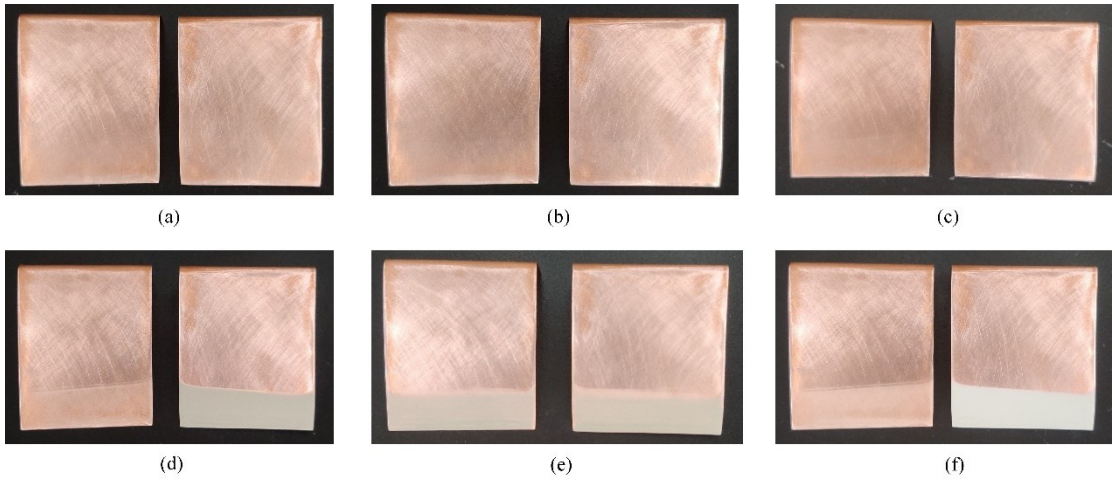

Figure 3.2 Photographs of electrodes after 2 min deposition/electrophoretic deposition experiments of organic-coated kaolinite suspended in cyclohexane with a concentration of 2 g/L. The upper panel shows the deposition from cyclohexane suspensions of (a) BCK, (b) ACK, and (c) MCK without applied voltage. The lower panel shows the electrophoretic deposition from cyclohexane suspensions of (d) BCK, (e) ACK, and (f) MCK under a 1500 V DC electric field. In each image panel, the cathode (-) is on the left and the anode (+) is on the right. The test cell was filled to about one-third of the depth so the deposition only occurred at the bottom portion of the electrodes.

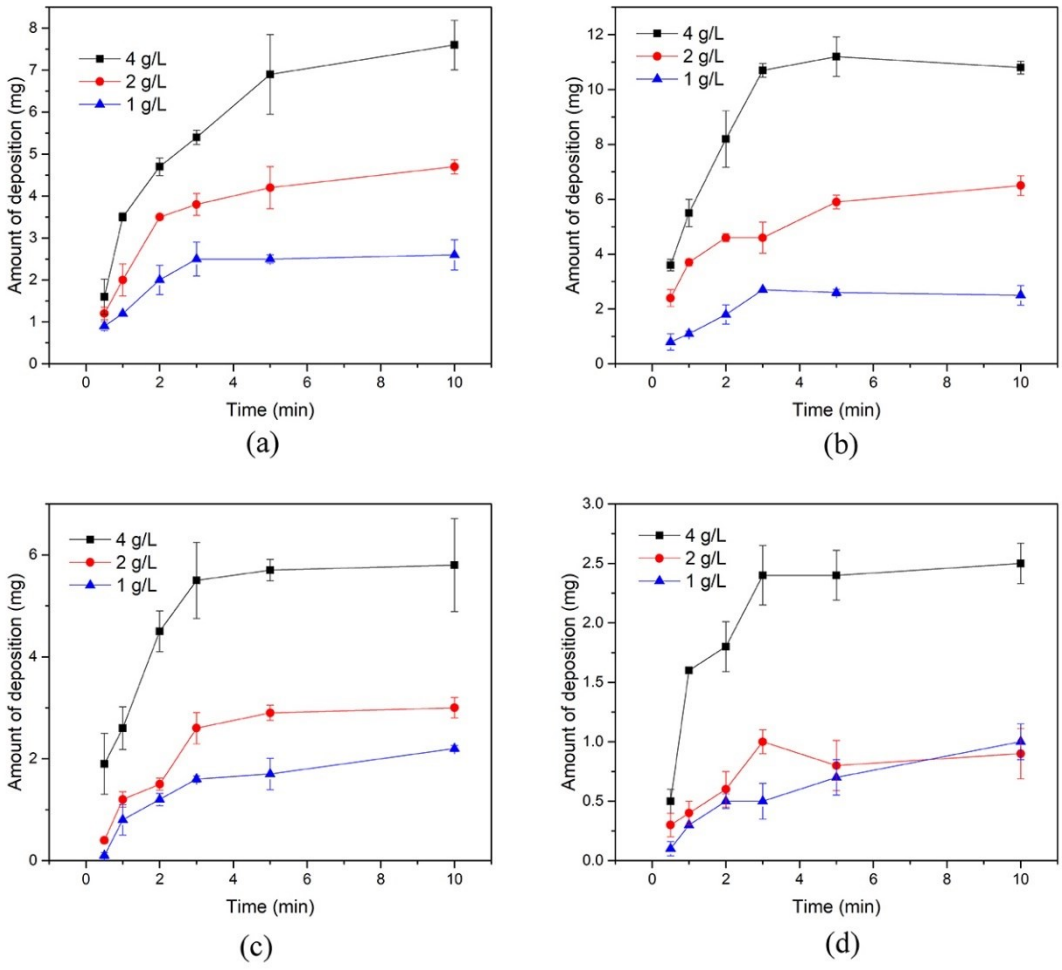

Figure 3.3 The amount of organic-coated kaolinite deposited from cyclohexane suspensions at 1500 V DC electric field at different particle concentrations and electrophoretic deposition time. (a) BCK on the anode, (b) MCK on the anode, (c) ACK on the anode, (d) ACK on the cathode. The deposited amounts on the cathode from BCK and MCK were not shown here due to the very low value as can be seen in **Figure 3.2**. Error bars represent standard deviations of three repeat tests under the same conditions.

3.3.4 Elemental composition of the electrophoretic deposited films

Table 3.5 shows the atomic concentration of C, O, N, S, Al, and Si of the anode and cathode films electrophoretic deposited from BCK, ACK, and MCK suspensions. The data

were obtained through XPS measurement. For all the samples, the atomic concentrations of Si were higher in the anode films and the atomic concentrations of Al were higher in the cathode films. This may be caused by the impurity minerals in the kaolinite sample, and indicated that the Si component tends to be negatively charged in cyclohexane, while the Al component tends to be positively charged in cyclohexane. It is reported that SiO_2 has a much stronger Lewis acidity than Al_2O_3 [24]. When minerals were dispersed in aprotic liquid cyclohexane, it is possible that Lewis acid-base interactions happened between SiO_2, cyclohexane, and Al_2O_3 which led to charge transfer. The Si component accepted electrons and became negatively charged, while Al component was positively charged after donating electrons. It is important to emphasize that XPS measurement retrieved data from a depth of only a few nanometers beneath the surface. The presence of Si and Al in the XPS results suggested that the coating was patchy and discontinuous.

Although BCK, ACK, and MCK samples in cyclohexane were all negatively charged as shown by zeta potential data (**Table 3.4**), their deposits on the cathode may include not only "positively charged counterions" that were dislodged from the coating layer, but also positively charged coated kaolinite particles. Based on the fact that the atomic concentration of elements measured by XPS has an accuracy of about 0.1 %, it can be seen that the ACK particles deposited on the anode and cathode have similar heteroatom content, while for BCK and MCK particles, the deposited anode films were high in sulfur and the very thin cathode films were high in nitrogen. Therefore, Nitrogen-containing components may be mainly positively charged, and sulfur-containing components mostly negatively charged. More sulfur was electrophoretic deposited on both anode and cathode from ACK than from MCK. This trend was consistent with data in **Table 3.2** that shows that

asphaltene contained more sulfur than maltene. The heteroatom content data here, combined with the surface coverage data and elemental analysis of bitumen, asphaltene, and maltene, seemed to indicate that the asphaltene coating on kaolinite (ACK) was more difficult to dislodge from the surface than kaolinites that were coated by bitumen (BCK) and maltene (MCK). Indeed, asphaltene has been reported to possess larger molecular weights and higher polarity than maltene and bitumen, leading to stronger affinity with kaolinite surface through polar and chemical interactions [25, 26].

Table 3.5 The elemental concentration of electrophoretic deposited films on anode and cathode from cyclohexane suspensions of BCK, ACK, and MCK samples obtained from 2 min electrophoretic deposition with 2 g/L particle concentration.

Elements	**BCK (atomic %)**		**ACK (atomic %)**		**MCK (atomic %)**	
	Anode	Cathode	Anode	Cathode	Anode	Cathode
C	34.92	36.54	57.69	57.09	34.36	27.72
O	46.03	44.05	27.86	27.26	43.63	49.28
N	0.58	0.96	0.73	0.71	0.29	0.49
S	0.87	0.72	1.39	1.46	0.36	~ 0
Al	7.07	8.12	5.25	7.91	8.81	14.03
Si	10.52	9.61	7.08	5.56	12.55	8.48

3.3.5 FTIR spectra of the electrophoretic deposition films

Figure 3.4 shows the FTIR spectra of the electrophoretic deposited films from cyclohexane suspensions of BCK. The deposited films on both anodes and cathodes showed the presence of complex functional groups. Peaks in the wavenumber range between 2500 cm^{-1} and 2000 cm^{-1}, which corresponded to the stretching of triple bonds and/or consecutive double bonds, were observed in the spectra on both electrodes. This possibly indicated that alkyne, cyanide, and cumulene may be contained in the BCK

deposited films. Alkyne, cyanide, and cumulene were reported to be present in the Alberta oil sands bitumen [27]. Many spectrum features representing aromatic hydrocarbons were observed in the spectra. These included the peak at 3030 cm^{-1} representing =CH stretching in aromatics, and the peaks between 1600 cm^{-1} and 1500 cm^{-1} showing C=C vibration in aromatics. This indicated that there were certain amounts of aromatic hydrocarbons in the deposited films on both anode and cathode. In contrast, the content of carboxyl groups showed obvious difference between the films on anode and cathode. More specifically, peaks around 1750 cm^{-1} showed C=O stretching and its shifted positions implied different attributions (1820-1720 cm^{-1} for ester, 1740-1650 cm^{-1} for carboxyl, and 1700-1630 cm^{-1} for ketone). The -OH in-plane (~1430 cm^{-1}) and out-of-plane (950-900 cm^{-1}) bending vibrations together with peaks around 1750 cm^{-1} described the presence of carboxyl groups in the deposited films. These peaks were much stronger on the anode films than on the cathode films, clearly due to the anionic nature of the carboxyl groups. The spectra also reveal some heteroatom groups such as S=O and C-N as marked in the graph.

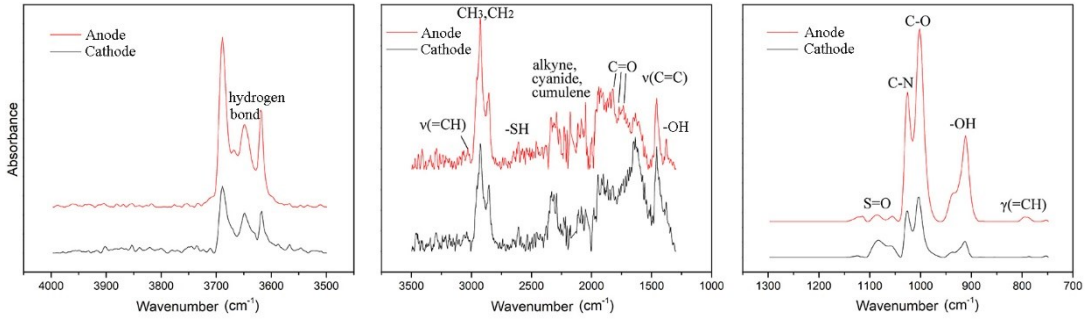

Figure 3.4 FTIR spectra of the electrophoretic deposited films on both anodes and cathodes from cyclohexane suspensions of BCK obtained from 2 min electrophoretic deposition with 2 g/L particle concentration.

Figure 3.5 presents the FTIR spectra of the electrophoretic deposited films from cyclohexane suspensions of ACK. Similar to BCK, the FTIR spectra also suggested the presence of triple bonds and consecutive double bonds moieties in the ACK films. The content of aromatic hydrocarbons seemed to be lower in ACK films than in BCK films. The content of carboxyl group suggested by the combination of C=O stretching vibration, -OH in-plane and out-of-plane bending vibration was significantly lower in ACK films than BCK films. Since ACK particles suspended in cyclohexane had a lower measured zeta potential and a lower electrophoretic deposition amount than the other two organic-coated particle samples, it can be concluded that the anionic carboxyl groups were important negative charge carriers and primary contributors to the charges of the organic-coated kaolinite suspended in cyclohexane. The lack of (anionic) carboxyl groups in asphaltene was one of the reasons why asphaltene deposited readily on the cathodes (**Figure 3.1 (g)**). In addition, the S=O peak in ACK was significantly stronger than in BCK films, which is consistent with the analysis of element concentrations in the deposited films determined by XPS.

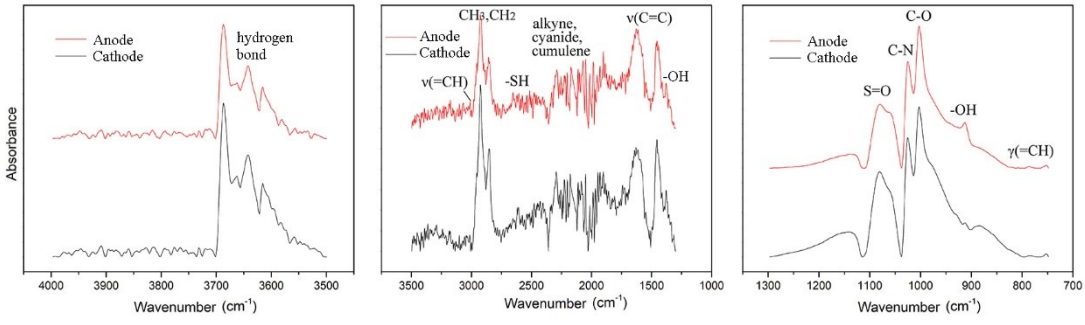

Figure 3.5 FTIR spectra of the electrophoretic deposited films on both anodes and cathodes from cyclohexane suspensions of ACK obtained from 2 min electrophoretic deposition with 2 g/L particle concentration.

Figure 3.6 shows the FTIR spectra of the electrophoretic deposited films from cyclohexane suspensions of MCK. The MCK spectra were similar to the BCK spectra, with more aromatic hydrocarbons and carboxyl groups and much less S=O groups than ACK films. The carboxyl contents were also much higher in the electrophoretic deposition films on the anode than on the cathode. Regarding the aromatics, the splitting of peaks between 1600 cm^{-1} and 1500 cm^{-1} indicated that the aromatic rings may be conjugated with C=O, C=C, NO_2, or S. This splitting was most evident in MCK spectra, since the lack of heteroatoms compared with the ACK and BCK particles, the aromatics in deposited films form cyclohexane suspensions of MCK should be mainly conjugated with C=O and C=C.

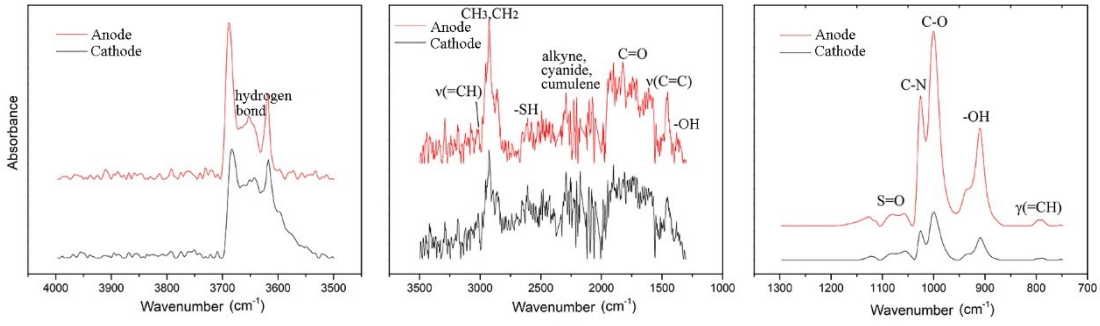

Figure 3.6 FTIR spectra of the electrophoretic deposited films on both anodes and cathodes from cyclohexane suspensions of MCK obtained from 2 min electrophoretic deposition with 2 g/L particle concentration.

Overall, the FTIR spectra of the electrophoretic deposited films from cyclohexane suspensions of these three coated kaolinite samples indicated that all three samples had complex functional group composition, and the films deposited on both anode and cathode appeared to be composed of similar functional groups, although variations existed in the quantity of the same functional groups and between different coated-kaolinite samples.

ACK had more heteroatoms and less aromatics than the other two samples, and particularly, carboxyl content in ACK deposited films was much lower than in BCK and MCK deposited films. Carboxyl groups were found to be an important factor that contributed to the negative charges when combining the FTIR data and previous results (zeta potential and deposition amount).

3.3.6 XPS spectra of the electrophoretic deposited films

Figures 3.7, 3.8, and 3.9 show the C, O, N, and S high-resolution XPS raw and deconvoluted spectra of electrophoretic deposited anode and cathode films from BCK, ACK, and MCK cyclohexane suspensions. For films deposited from BCK sample (**Figure 3.7**), the C and O elements on both anode and cathode films had relevant simple chemical states. Among them the C=O double bond was found in the cathode film but absent in the anode film. The spectrum of N 1s electron in the cathode film was deconvoluted into two peaks representing -N-O and -C-N bonds, while the spectrum of N 1s in the anode film mainly showed -C-N bond (**Figure 3.7**). This indicates that besides the higher concentration of N in the cathode film, the N-bearing species in the cathode film were more complex compared with that of the anode film. In contrast, the S in the deposits on the two electrodes showed the opposite trend. As can be seen from **Figure 3.7**, the spectrum of S 2s electron of the anode film was deconvoluted into -S-H and -C-S-C- bonds, while that of the cathode film was mainly -S-H.

For films deposited from ACK sample suspended in cyclohexane, the nature of O and N elements in both the anode and cathode films were similar (**Figure 3.8**). However, both the C and S elements in the anode film showed more chemical states than those in the

cathode film. More specifically, the C and S in the anode film clearly showed a higher degree of association with oxygen, such as ether oxygen -C-O-C-, alcohol -C-OH, and sulfoxy -SO (**Figure 3.8**), despite the lower carboxyl contents revealed from the FTIR spectra in ACK (**Figure 3.5**).

For films deposited from MCK sample suspended in cyclohexane (**Figure 3.9**), the contents of N and S were clearly much lower than those from the films deposited from BCK and ACK. There was in fact no detectable S element in the cathode film, and barely any N in the anode film. The spectra of S 2p electron in the anode film and the N 1s electron in the cathode film both showed that they existed in a single chemical state, as -S-H and -C-N. In addition, the chemical states of the C and O elements in both the anode and cathode films were essentially the same (**Figure 3.9**) and if anything, the C in the anode showed one more chemical state (O-C=O).

In summary, the organic-coated kaolinite particles that deposited on the anode had lower concentration of N than the particles deposited on the cathode. The N-bearing species were more complex in the cathode films while the S-bearing species were more complex in the anode films. The anode films showed C and S species with higher oxidation states that were associated with oxygen. Besides, Na Auger peaks were found from the deposited films of BCK and MCK. In addition, maltene contained more chemical species that are readily soluble in cyclohexane than asphaltene. We speculate that more maltene might be desorbed from the MCK particle surface when they were suspended in cyclohexane, and the dissolved maltene would be more likely to act as charge-stabilizing supramolecular entities, contributing to the deposition on both anode and cathode with essentially similar organic compositions.

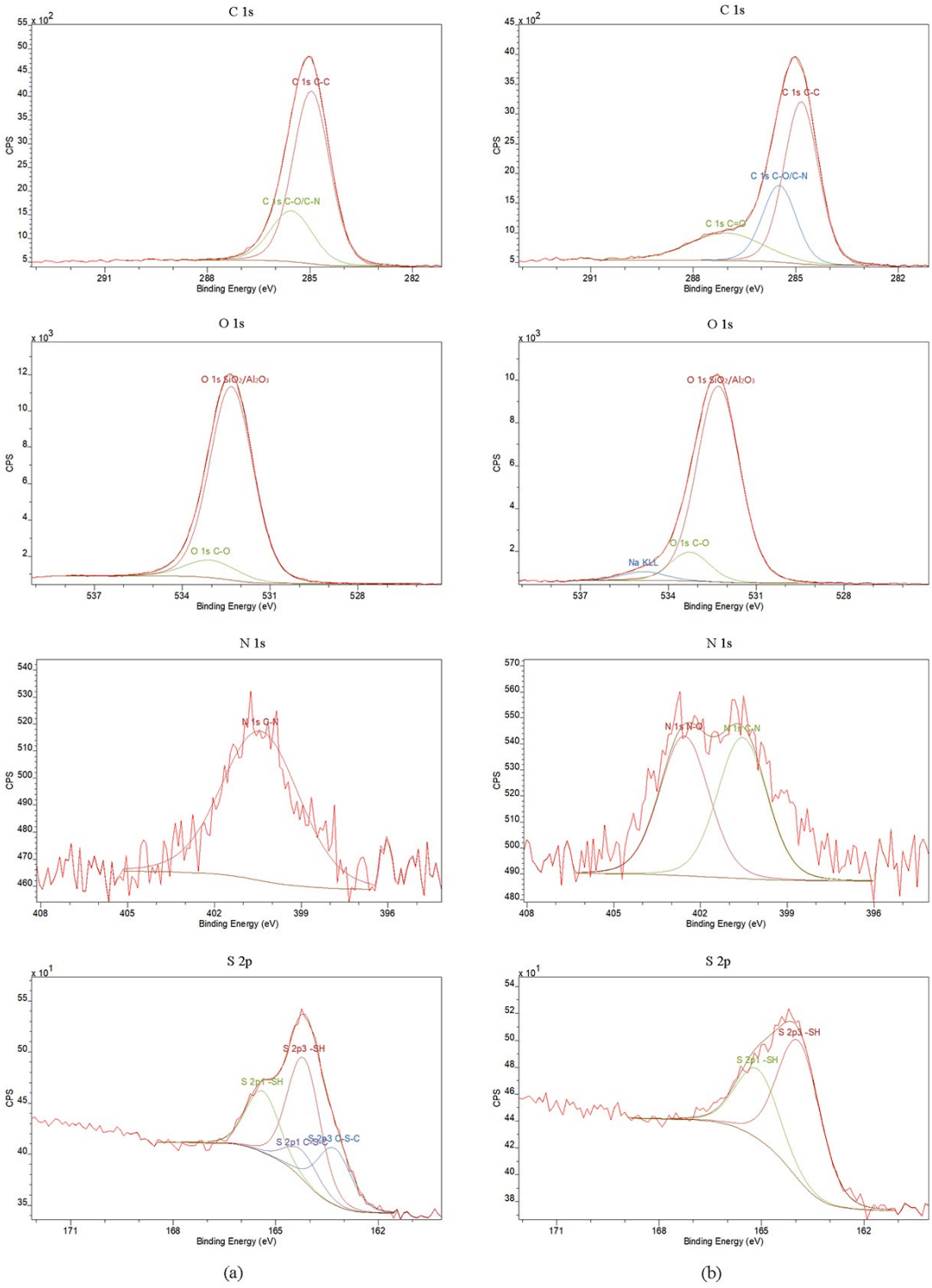

Figure 3.7 XPS high-resolution spectra of C 1s, O 1s, N 1s, and S 2p binding energies with deconvoluted peaks for films deposited from BCK sample on (a) anode, and (b) cathode obtained from 2 min electrophoretic deposition with 2 g/L particle concentration.

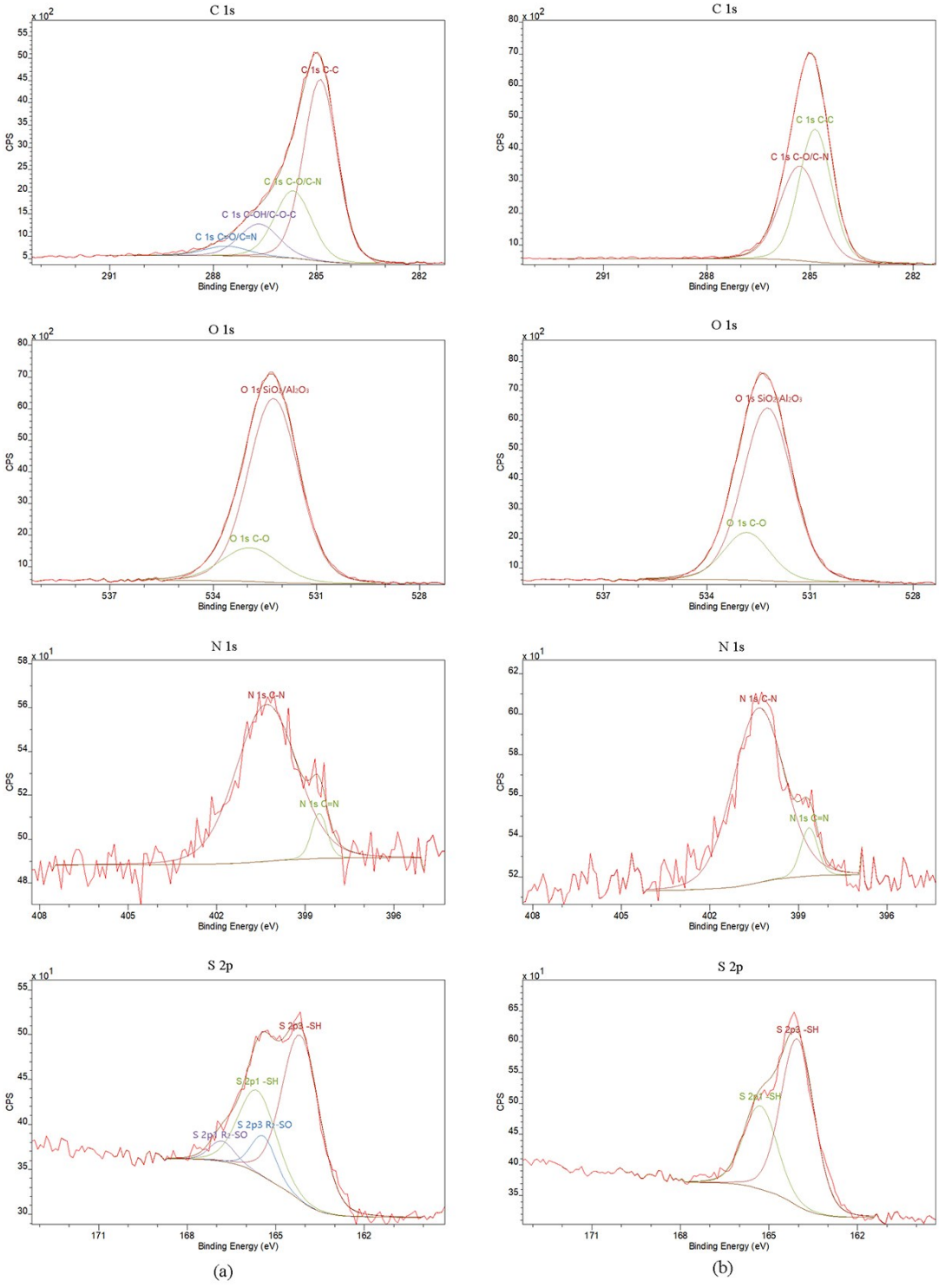

Figure 3.8 XPS high-resolution spectra of C 1s, O 1s, N 1s, and S 2p binding energies with deconvoluted peaks for films deposited from ACK sample on (a) anode, and (b) cathode obtained from 2 min electrophoretic deposition with 2 g/L particle concentration.

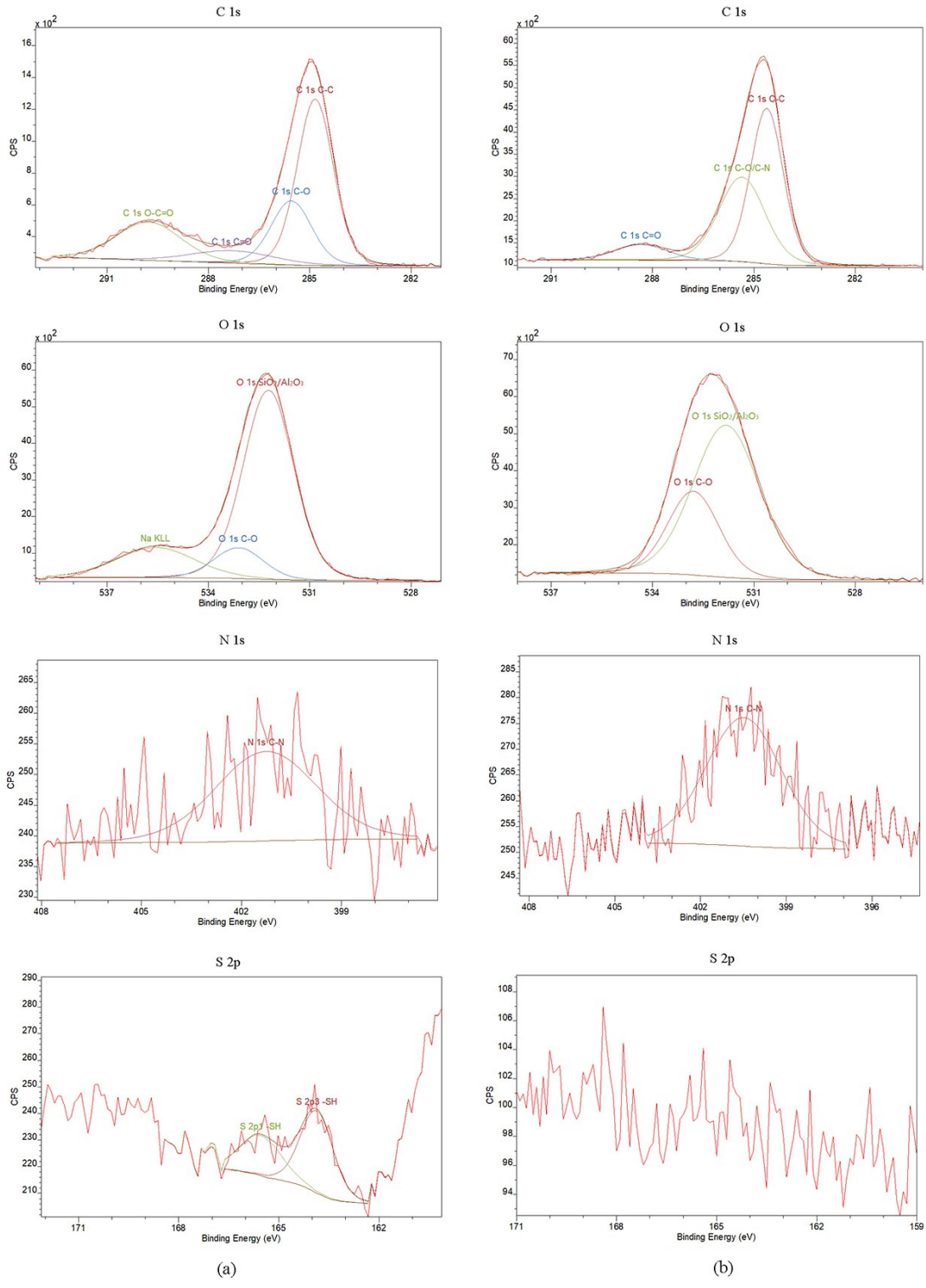

Figure 3.9 XPS high-resolution spectra of C 1s, O 1s, N 1s, and S 2p binding energies with deconvoluted peaks for films deposited from MCK sample on (a) anode, and (b) cathode obtained from 2 min electrophoretic deposition with 2 g/L particle conc5entration.

3.4 Conclusions

The charges carried by kaolinite particles, with or without an organic coating of bitumen, asphaltene, or maltene, suspended in an organic solvent, cyclohexane, were studied in this work by electrophoretic deposition at an applied voltage of 1500 V DC. The electrophoretic deposited films on both anode and cathode were characterized by Fourier transform infrared spectroscopy (FTIR) and X-ray photoelectron spectroscopy (XPS) analyses, in addition to the determination of the influence of particle concentration and electrophoretic deposition time on deposition amount. The major observations and conclusions are:

1). Bare kaolinite particles did not carry a net charge in cyclohexane as they did not deposit on either anode or cathode under the 1500 V DC electric field. This was probably due to the instability of any charges that may develop. In the absence of dissolved species in cyclohexane, there were no supramolecular structures in the suspension to keep the charge carriers at a distance larger than the required Bjerrum lengths in cyclohexane. Thus, any developed net charges would have likely associated into neutral species.

2). The kaolinite sample was coated by hydrocarbon compounds through treatment in a toluene solution with dissolved bitumen, asphaltene, or maltene. The resulting samples were denoted BCK, ACK, and MCK. XPS surface elemental concentration analysis showed that the treated samples had fractional surface organic coverage, with BCK and MCK both at about 0.35 while ACK at 0.41. Zeta potential measurement in a cyclohexane medium showed zeta potential of -20.1 mV (BCK), -12.4 mV (ACK), -28.1 mV (MCK), and 0 mV (bare kaolinite).

3). BCK and MCK particles mainly deposit on the anode, and ACK deposited on both anode and cathode when their suspensions in cyclohexane were freshly prepared. The deposited amount increased with kaolinite concentration and deposition time and levelled off after 5 min of electrophoretic deposition.

4). FTIR spectra showed that the films electrophoretic deposited on the anode from BCK and MCK contained much higher concentrations of carboxyl groups than the anode films deposited from ACK. The presence of carboxyl groups seemed to be a defining character that contributed to the negative charges. In fact, the carboxyl-group-deficient asphaltene was found to deposit mostly to the cathode when it was dissolved in cyclohexane.

5). XPS electron binding energy spectra and surface elemental concentration analyses of the electrophoretic deposited films on both anodes and cathodes showed that, generally, the cathode films had a higher N content, and the anode films showed C and S species with higher oxidation states that were associated with oxygen.

References

[1] Masliyah JH, Czarnecki J. Xu Z. Oil sands composition: bitumen, mineral solids, and inorganic ions. In: Handbook on theory and practice of bitumen recovery from Athabasca oil sands, volume I: theoretical basis. Kingsley Knowledge Pub; 2011. p. 177-96.

[2] West RC. Non-aqueous process for the recovery of bitumen from tar sands. US Patent 3, 131, 141; 1964.

[3] Hooshiar A, Uhlik P, Liu Q, Etsell TH, Ivey DG. Clay minerals in nonaqueous extraction of bitumen from Alberta oil sands: Part 2. Characterization of clay minerals. Fuel Process Technol 2012; 96: 183-94.

[4] Lin F, Stoyanov SR, Xu Y. Recent advances in nonaqueous extraction of bitumen from mineable oil sands: a review. Org Process Res Dev 2017; 21 (4): 492-510.

[5] Zhang H, Tan X, Liu Q. Fine solids removal from non-aqueous extraction bitumen: A literature review. Fuel 2021; 288: 119727.

[6] Nikakhtari H, Wolf S, Choi P, Liu Q, Gary MR. Migration of fine solids into product bitumen from solvent extraction of Alberta oilsands. Energy Fuels 2014; 28 (5): 2925-32.

[7] Bensebaa F, Kotlyar LS, Sparks BD, Chung KH. Organic coated solids in Athabasca bitumen: Characterization and process implications. Can J Chem Eng 2000; 78 (4): 610-6.

[8] Liu J, Cui X, Huang J, Xie L, Tan X, Liu Q, et al. Understanding the stabilization mechanism of bitumen-coated fine solids in organic media from non-aqueous extraction of oil sands. Fuel 2019; 242: 255-64.

[9] Dixon DV, Stoyanov SR, Xu Y, Zeng H, Soares JB. Challenges in developing polymer flocculants to improve bitumen quality in non-aqueous extraction processes: an experimental study. Pet Sci 2020: 1-11.

[10] Graham R, Helstrom J, Mehlberg R. A solvent extraction process for tar sand. Eastern Oil Shale Symposium 1987: 93-9.

[11] Alquist HE, Ammerman AM. Process for extracting bitumen from tar sands. US Patent 4, 229, 281; 1980.

[12] Cullinane JT, Minhas BS. Electrostatic filtration of fine solids from bitumen. US Patent 9, 752, 079; 2017.

[13] Crittenden JC, Trussell R, Rhodes H, David W, Howe KJ, Tchobanoglous G. Stability of particles in water. In: MWH's water treatment – principles and design (3rd Edition). John Wiley Sons; 2012. p. 546-57.

[14] Lee J, Zhou ZL, Alas G, Behrens SH. Mechanisms of particle charging by surfactants in nonpolar dispersions. Langmuir 2015; 31 (44): 11989-99.

[15] Moritz R, Zardalidis G, Butt HJ, Wagner M, Mullen K, Floudas G. Ion size approaching the Bjerrum length in solvents of low polarity by dendritic encapsulation. Macromolecules 2014; 47 (1): 191-96.

[16] Ponto BS, Berg JC. Clay particle charging in apolar media. Applied Clay Sci 2018; 161: 76-81.

[17] Lee J, Zhou ZL, Behrens SH. Charging mechanism for polymer particles in nonpolar surfactant solutions: influence of polymer type and surface functionality. Langmuir 2016; 32 (19): 4827-36.

[18] Smith GN, Eastoe J. Controlling colloid charge in nonpolar liquids with surfactant. Phys Chem Chem Phys 2013; 15 (2): 424-439.

[19] Smith PG, Patel MN, Kim J, Milner TE, Johnston KP. Effect of surface hydrophilicity on charging mechanism of colloids in low-permittivity solvents. J Phys Chem C 2007; 111 (2): 840-8.

[20] Guo Q, Lee J, Singh V, Behrens SH. Surfactant mediated charging of polymer particles in a nonpolar liquid. J Colloid Interface Sci 2013; 392: 83-9.

[21] Gacek MM, Berg JC. Investigation of surfactant mediated acid-base charging of mineral oxide particles dispersed in apolar systems. Langmuir 2012; 28 (51): 17841-5.

[22] Wang S, Liu Q, Tan X, Xu C, Gray MR. Study of asphaltene adsorption on kaolinite by X-ray photoelectron spectroscopy and time-of-flight secondary ion mass spectroscopy. Energy Fuels 2013; 27 (5): 2465-73.

[23] Jin Y, Liu W, Liu Q, Yeung A. Aggregation of silica particles in non-aqueous media. Fuel. 2011 Aug 1; 90(8): 2592-7.

[24] Rosenholm JB. Evaluation of particle charging in non-aqueous suspensions. Adv Colloid Interface Sci 2018; 259: 21-43.

[25] Li X, Bai Y, Sui H, He L. Understanding desorption of oil fractions from mineral surfaces. Fuel. 2018 Nov 15; 232: 257-66.

[26] Adams JJ. Asphaltene adsorption, a literature review. Energy & Fuels. 2014 May 15; 28(5): 2831-56.

[27] Goual L, Horváth-Szabó G, Masliyah JH, Xu Z. Characterization of the charge carriers in bitumen. Energy Fuels. 2006; 20(5): 2099-108.

Chapter 4 Kaolinite Surface Charges Developed in Cyclohexane Suspensions with Dissolved Span 80 or Bitumen: Electrophoretic Deposition and Adsorption/Desorption Studies

4.1 Introduction

The Canadian oil sands resource in northern Alberta is one of the largest proven crude oil reserves in the world [1, 2]. Bitumen, an extra heavy crude oil, is the hydrocarbon embedded in the oil sands [3]. Currently, a warm-water extraction process is used to recover bitumen from the surface-mined oil sands. The warm-water extraction process has some inherent shortcomings, such as high energy consumption and high greenhouse gas emissions caused by heating fresh river water to around 50℃, and the accumulation of environmentally harmful, slow-settling fluid fine tailings [4, 5].

Non-aqueous extraction (NAE) [6] technology is one of the alternatives to solve the inherent issues of the warm-water extraction process. In an NAE process, bitumen is extracted from oil sands by an organic solvent instead of warm water. Therefore, the NAE technology has the potential to eliminate the use of fresh water in bitumen recovery from oil sands. However, the NAE technology is not commercially viable currently. One of the major technological hurdles is the high mineral solids content in the bitumen products [7, 8]. These fine solids are difficult to remove, lowering the quality of bitumen and preventing it from being directly used as a feed to high-conversion refineries. Sending the NAE bitumen to an upgrader prior to high-conversion refineries is out of the question due to the high capital investment and energy consumption of the upgrader. The challenge is therefore to develop an effective, economic and environmentally-friendly technique to remove the fine mineral solids from NAE bitumen.

It is reported that an external electric field can enhance fine mineral solids removal from NAE bitumen [9]. Nevertheless, how the fine mineral solids acquire a charge in a nonpolar liquid such as NAE bitumen is poorly understood. Most studies on particle charging in a nonpolar organic liquid attribute the charges to the added surfactants through a reverse-micelle-charge-stabilization mechanism [10-15], which acts like hydrated counter ions to electrical double layer in an aqueous suspension. However, particle charging in a nonpolar organic medium in the presence of bitumen is understandably more complex. In the previous chapter, we reported the charging behaviors of kaolinite that was previously-coated by bitumen or bitumen subfractions (asphaltene or maltene) and then suspended in cyclohexane through electrophoretic deposition experiments [16]. We found that the pristine kaolinite particles were electrical-neutral in cyclohexane, but they carried a charge when previously coated by bitumen or bitumen subfractions and then suspended in cyclohexane. During electrophoretic deposition, most of the bitumen- or bitumen-subfraction-coated kaolinite particles deposited on the anode and only a small portion of the particles deposited on the cathode [16]. Higher carboxyl group contents were observed on particles that were deposited on the anode, while particles deposited on the cathode had higher N content [16]. In the previous chapter, the kaolinite was coated with bitumen or bitumen subfractions, followed by drying and re-suspension in clean cyclohexane. There was therefore a very limited amount of dissolved organic species in cyclohexane. In this chapter, the charging mechanism of pristine kaolinite in cyclohexane with dissolved bitumen was studied through electrophoretic deposition and instrumental analysis. To further elucidate the charging mechanisms of kaolinite in cyclohexane influenced by bitumen, a common surfactant, sorbitan monooleate (Span 80), which is widely used as an

adjuvant in the analysis of particle charging in nonpolar media, was also introduced to better understand the charging mechanism. The effects of bitumen on kaolinite charging in cyclohexane were compared with those of Span 80.

4.2 Materials and Methods

4.2.1 Materials

The kaolinite sample used in this work was ASP 600 kaolinite obtained from BASF, which had a median particle size of 0.6 μm. The chemical composition of the kaolinite sample was determined by a Bruker CTX800 X-ray fluorescence analyzer (XRF) and the result has been given in **Table 3.1** (Chapter 3). The bitumen sample was obtained from an oil sands operator in the Fort McMurray region in Alberta, Canada. The as-received bitumen sample contained fine mineral solids that may interfere with the study. Therefore, a Beckman Avanti J-301 high speed centrifuge was used to remove the fine mineral solids from the bitumen sample. The as-received bitumen sample was first diluted in toluene at a 1:1 mass ratio. The diluted bitumen was then centrifuged at 13000 RCF for 1 h. The solids-free-bitumen was obtained by collecting the supernatant and evaporating toluene by a rotary evaporator. The solvents used in this work, including cyclohexane (purity > 99%), toluene (purity > 99.9 %), and n-pentane (purity > 99.5), were purchased from Fisher Scientific Canada. The surfactant Span 80 used in this work was purchased from Sigma Aldrich with a product number of S6760, whose molecular structure is shown in **Figure 4.1**. It has a vendor-specified purity of 60% based on the content of oleic acid measured by gas chromatography. Other ingredients in this Span 80 sample mainly include linoleic, linolenic, and palmitic acids.

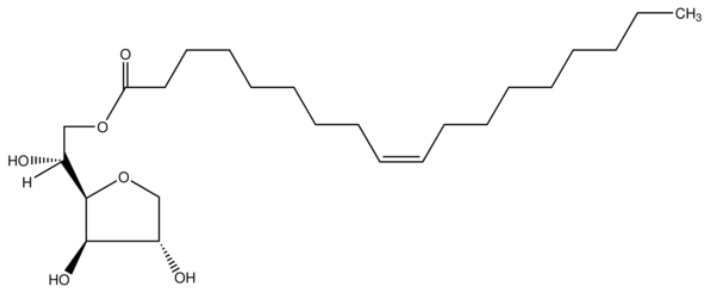

Figure 4.1. The molecular structure of Span 80 from Sigma Aldrich (product number S6760).

4.2.2 Electrophoretic deposition

A rectangular cell with an inner dimension of 10×40×40 mm^3 was used to perform the electrophoretic deposition. The schematic of the cell and electrode set up is shown in **Figure 4.2**. Two copper electrodes were placed against the two walls (40×40 mm^2) of the cell, so the electrodes were parallel and about 10 mm apart. During electrophoretic deposition, 1500 V direct current (DC) voltage was applied using a Thermo EC 3000 XL power supply, and 4 mL sample was used for each test.

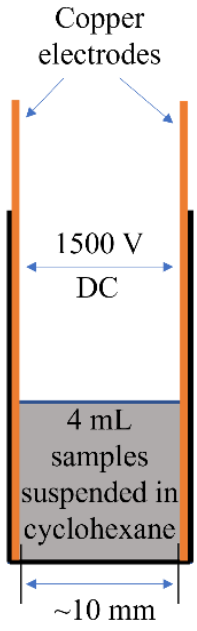

Figure 4.2. Schematic representation of the electrophoretic deposition cell.

The electrophoretic deposition study was designed to investigate the effects of Span 80 or bitumen on the charging states of kaolinite suspended in cyclohexane. First, kaolinite was electrodeposited without any additive, i.e., 4 mL of a 2 g/L kaolinite-cyclohexane suspension was electrodeposited for 5 min at 1500 V DC, which served as control. To study the effects of Span 80 or bitumen, 0.1 mL of a cyclohexane solution of Span 80 or bitumen was added to the 4 mL 2 g/L kaolinite-cyclohexane suspension, and the mixture was then electrodeposited under the same condition (5 min at 1500 V DC). The concentrations of the 0.1 mL additive-cyclohexane solutions varied at 0.01, 0.1, 1, 10, and 100 g/L, to set the amount of the Span 80 or bitumen in the kaolinite-cyclohexane suspension at 2.5×10^{-4}, 2.5×10^{-3}, 2.5×10^{-2}, 0.25, and 2.5 g/L, respectively because of the 40 times dilution. After electrophoretic deposition, the electrodes were photographed, and the deposited masses were weighed by an analytical balance with a resolution of 0.1 mg. As control blank tests, these slurry samples were also added to the cell for 5 min without

applying a voltage to see if they could naturally deposit on the electrodes without an external electrical field.

In order to determine whether the charges on kaolinite were due to Span 80 or bitumen solubilized in cyclohexane or due to the additives that were adsorbed on the kaolinite surface, the 4 mL 2 g/L kaolinite-cyclohexane suspension that was treated with the presence of 0.25 g/L bitumen, or 0.25 g/L Span 80 was filtered, and the filter cake (kaolinite) was washed repeatedly with cyclohexane until the filtrate was colorless (the same number of washing steps was used for the case of Span 80). The obtained filter cakes were referred to as KB and KS, representing kaolinite that was treated with bitumen or Span 80, respectively. The filter cake was re-dispersed in fresh cyclohexane at a concentration of 2 g/L (several batches of filtration were performed in order to obtain sufficient quantity of the filter cakes to make a new 4-mL 2 g/L suspension). After re-dispersion, 4 mL of the KB or KS suspensions were electrodeposited for 5 min under 1500 V DC. The KB particles were also re-dispersed in *n*-pentane and toluene to make 4-mL 2 g/L suspensions for the electrophoretic deposition tests at the same condition. The weights of the deposits on the electrodes were measured using the analytical balance. The deposits were also scraped off, dried and analyzed for CHNS elemental compositions.

In order to determine if any residual bitumen or Span 80 were present in the re-suspended KB or KS, the re-dispersed cyclohexane suspension of KB or KS was also filtered. The filtrate was analyzed by a UV-Vis spectrophotometer. The filter cake was subjected to CHNS elemental analysis, and the results were compared with CHNS elemental composition of the deposited particles scraped off from electrodes, if any. In addition, zeta potentials of kaolinite suspended in cyclohexane with different concentrations of Span 80

were measured and correlated to electrophoretic deposition. The isoelectric point (IEP) of kaolinite in aqueous suspension was determined by measuring the zeta potentials of kaolinite in aqueous suspensions at different pH value.

4.2.3 Analytical methods

The filtrates of KB and KS suspensions in cyclohexane were analyzed by a Perkin-Elmer Lambda 365 UV-Vis spectrophotometer. Standard calibration curves were obtained by measuring the absorbance of cyclohexane solution of bitumen or Span 80 with concentrations of 0.001, 0.005, and 0.01 g/L. The wavelength range was 300-700 nm when measuring the filtrates of KB suspension in cyclohexane and 200-700 nm when measuring KS filtrate. The resolution of the UV-Vis spectrophotometer was 1 nm.

A Brookhaven ZetaPALS zeta potential analyzer was used to measure the zeta potential of kaolinite in cyclohexane at different Span 80 concentrations, or in water as a function of pH. The concentrations of Span 80 in cyclohexane were varied at 2.5×10^{-4}, 2.5×10^{-3}, 2.5×10^{-2}, 0.25, and 2.5 g/L, corresponding to the electrophoretic deposition experiments. Phase analysis light scattering (PALS) was used to measure the zeta potential of kaolinite in nonpolar system (cyclohexane) and the Hückel equation was used to convert electrophoretic mobility to zeta potential. The concentration of kaolinite in cyclohexane was 0.1 g/L in zeta potential measurement rather than 2 g/L as used in electrophoretic deposition because the measurement would be inaccurate if the concentration was too high. Four different voltages (70 V, 100 V, 130 V, and 160 V) were initially tested for the zeta potential measurement with the purpose to extrapolate the field-dependent electrophoretic mobility to zero field strength. However, the results did not show a specific effect of

voltage on the measured zeta potential. Therefore, the subsequent zeta potential measurements for kaolinite in cyclohexane were all performed with an applied sinusoidal voltage of 130 V and a frequency of 10 Hz as in a previous work (16). For the zeta potential measurements in water, Smoluchouski's equation was used to convert electrophoretic mobility to zeta potential. Kaolinite was dispersed in water at a concentration of 0.25 g/L with 1 mM KCl as supporting electrolyte. The pH was adjusted by KOH and HCl. The measurements in aqueous system were preformed with automatic voltage and frequency.

A Flash 2000 CHNS/O Elemental Analyzer was used to determine the CHNS elemental compositions of the filter cakes from the cyclohexane suspensions of KB, and the deposits obtained from the KB cyclohexane suspensions. Kaolinite sample, i.e., dried filter cake from kaolinite-cyclohexane suspension, was used as control in the CHNS elemental composition analyses.

4.2.4 Real-time monitoring bitumen desorption from kaolinite surfaces under applied electric fields

A Q-sense E4 Quartz Crystal Microbalance with Dissipation (QCM-D, Biolin Scientific, Sweden) was used and paired with the QEM 401 chamber to monitor the adsorption of bitumen on kaolinite surface and the desorption of bitumen from the surface under applied electric field in real-time. The At-cut quartz crystal sensor with kaolinite coating on the top surface (referred to as kaolinite sensor) was custom-made by nanoScience Instruments. Using the piezoelectric property of quartz, the QCM-D device can detect the sensor's oscillation when an alternating electric potential is applied. The change in frequency and dissipation of the sensor oscillation can be utilized to calculate the mass variation on the

kaolinite sensor surface. The frequency decrease is caused by adsorption and increase by desorption. The dissipation of the adsorbed film reflects its viscoelastic property [17]. Typically, in the case of a rigid and uniformly adsorbed layer, the mass change (Δm) on the sensor surface can be calculated from frequency shift (Δf) using the Sauerbrey model. In the case of loose and soft coating layer, the dissipation change ΔD is larger than 10^{-6} for a 10 Hz frequency, and viscoelastic model is commonly used to estimate the mass change [17-19].

An electrochemical workstation (Metrohm Autolab, Netherlands) was used to provide external electric field by connecting the QCM-D chamber in the form of a three-electrode cell, and the voltage between the working electrode (gold sensor with coated kaolinite) and counter electrode (platinum) was controlled by the electrochemical workstation. Before each measurement, any possible contaminants on the kaolinite sensor were removed by rinsing with toluene and acetone and then exposure to UV-Ozone for 10 minutes. After rinsing with Milli-Q water and drying under purified nitrogen gas, the sensor was exposed to UV-Ozone for 10 minutes again. A two-step QCM-D experiment was designed to investigate the effect of the applied electric field on desorbing bitumen from kaolinite surface. In the first stage, a cyclohexane solution of bitumen was used to deposit a bitumen film on the kaolinite surface. After introducing cyclohexane into the QCM-D chamber to establish a baseline, 0.1 g/L bitumen-in-cyclohexane solution was injected till the adsorption of bitumen on kaolinite sensor surface reached equilibrium. Afterwards, cyclohexane was re-introduced to the chamber to “wash” the loosely-held bitumen from kaolinite surface. A DC electric field (5 and 10 V) was then applied in sequence and the mass change of the kaolinite sensor in real-time was analyzed.

4.3 Results and Discussion

4.3.1 Electrophoretic deposition of kaolinite with the addition of bitumen or Span 80

Figure 4.3 shows the photographs of electrodes obtained from the first series of electrophoretic deposition and the control blank tests (the concentration of bitumen or Span 80 in the kaolinite-cyclohexane suspension was 0.25 g/L). As can be seen from the top panels (a), (b), and (c), no particles were deposited on the copper electrodes without an applied electric field. The bottom panels (d), (e), and (f) show the image of the electrodes when 1500 V DC was applied. Since the cell was not fully filled by the slurry sample, any deposits were only visible at the bottom portion of the electrodes. Image (d) in **Figure 4.3** shows that no deposits were visible from kaolinite-cyclohexane suspension on either electrode, indicating that kaolinite did not carry a net electrical charge. However, when bitumen or Span 80 was added to the kaolinite-cyclohexane suspension, deposits were observed on some electrodes as shown in panels (e) and (f) in **Figure 4.3**, respectively. With the addition of bitumen, image (e) shows that deposits were mainly observed on the anode, there were almost no deposits on the cathode, indicating that kaolinite carried negative charges in cyclohexane with added bitumen. With the addition of Span 80, on the other hand, image (f) shows that the particles were mainly electrodeposited on the cathode and only a very small amount of particles were electrodeposited on the anode, indicating that the addition of Span 80 made kaolinite particles positively charged in cyclohexane.

The images in **Figure 4.3** show that the presence of bitumen or the surfactant Span 80 could make kaolinite particles to carry a net charge in cyclohexane. The amounts of the deposits were weighed at different additive concentrations and the weights are plotted as a function of the concentration of the bitumen or Span 80 in **Figure 4.4**. From **Figure**

4.4(a), it can be seen that only a small amount of particles were deposited on both anode and cathode when the bitumen concentration was lower than 2.5×10^{-2} g/L. At higher bitumen concentrations (i.e., 0.25 g/L and 2.5 g/L), no particles were deposited on the cathode, but the deposited amount on the anode increased significantly, from around 0.8 mg to 5.5 mg when the concentration of bitumen increased from 2.5×10^{-3} to 0.25 g/L. Another 10-fold increase in bitumen concentration (to 2.5 g/L) did not significantly increase the deposited amount further on the anode. Since the total amount of kaolinite in the 4 mL of 2 g/L suspension was about 8 mg, it can be seen that the majority of the kaolinite (about 70%) was deposited at the two highest bitumen concentrations. Therefore, 1 mg bitumen (4 mL of 0.25 g/L bitumen) could make about 5.5 mg kaolinite to carry sufficient negative surface charges in cyclohexane to be driven under a 1500 V/cm voltage gradient.

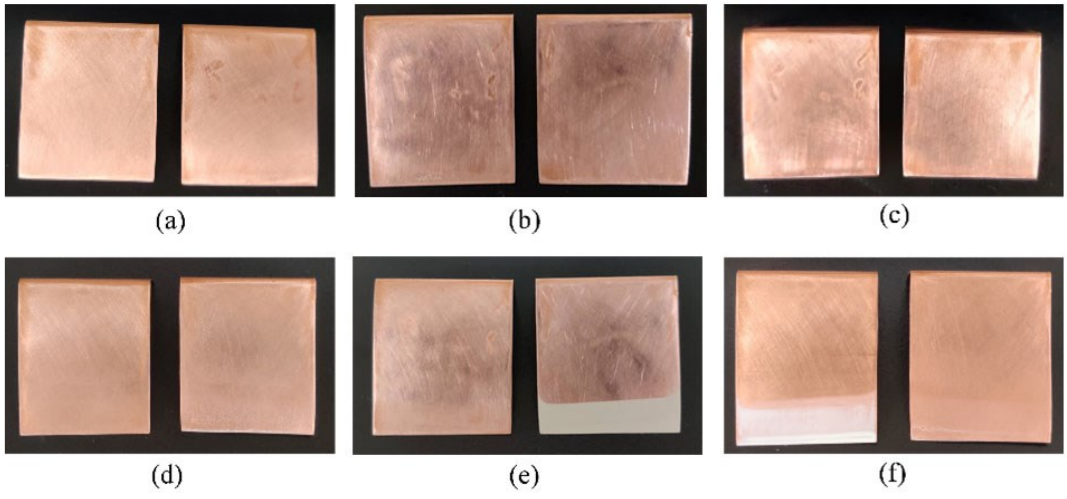

Figure 4.3. Photographs of electrodes after 5 min deposition/electrophoretic deposition from cyclohexane suspensions of kaolinite with and without 0.25 g/L bitumen or Span 80. Upper panel: no electric field. Bottom panel: 1500 V DC. (a) and (d): kaolinite in

cyclohexane. (b) and (e) kaolinite in cyclohexane with added bitumen. (c) and (f): kaolinite in cyclohexane with added Span 80. In each image, cathode (-) is on the left and anode (+) is on the right.

When Span 80 was added to the kaolinite-cyclohexane suspension, **Figure 4.4(b)** shows that kaolinite particles were not electrodeposited when the amount of additive was low (2.5×10^{-4} g/L). When the Span 80 concentration was 2.5×10^{-3}, 2.5×10^{-2}, and 0.25 g/L, particles were found to electrodeposit on the cathode and the deposited amount increased from about 1 mg to more than 5.5 mg. Interestingly, another 10-fold increase in Span 80 concentration, to 2.5 g/L, caused the amount of electrodeposited kaolinite on the cathode to drop to zero. At all Span 80 concentrations, the deposited amount of kaolinite on the anode was very low or zero. This indicated that the addition of an appropriate amount of surfactant Span 80 made kaolinite primarily carry positive charges.

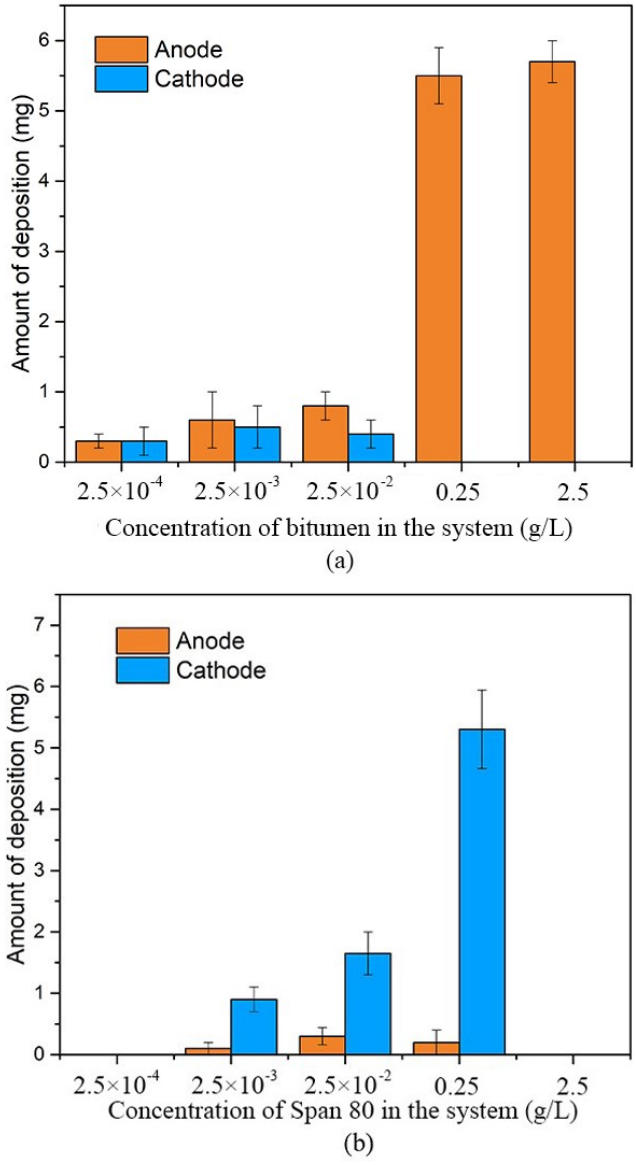

Figure 4.4. The amount of kaolinite electrophoretic deposited from 4 mL 2 g/L kaolinite-cyclohexane suspensions after adding cyclohexane solutions to give different concentrations of (a) bitumen, and (b) Span 80. The concentrations shown in the figures was the actual concentration of bitumen or Span 80 in the electrophoretic deposition bath rather than the concentration of the stock solution of them. Error bars represent standard deviations of three repeat tests under the same conditions. Electrophoretic deposition at 1500 V DC for 5 min.

4.3.2 Kaolinite charging mechanism in cyclohexane with added Span 80

Reports in the literature [11, 20-23] show that when a surfactant is added to a mineral particle suspension of a nonpolar solvent, the polar head of the surfactant can adsorb to the solid particle surface while the nonpolar tail of the surfactant protrude into the solvent. The adsorbed surfactant molecule may form an acid-base adduct with particle surface functional groups. It is possible for charge transfer to occur between the surfactant molecule and the particle surface when the acid-base adducts separate. The charge transfer direction is dependent on the relative acid-base properties of the surfactant and the particle surface. If the surfactant molecule is more acidic than the particle surface, it tends to carry away negative charges during the acid-base adduct separation. The acid-base property of solid particles can be quantified using their point of zero charge (PZC) or isoelectric point (IEP) in aqueous suspensions. The lower the PZC or IEP, the more acidic the mineral. For surfactant that forms reverse micelles in a nonpolar solvent, such as Span 80, its acid-base property is quantified by the so-called effective pH (pH_{Eff}), which is determined using different types of minerals with different PZCs or IEPs. This is illustrated in **Figure 4.5** [11], where the maximum particle charges in a nonpolar solvent in the presence of a specific surfactant is plotted as a function of the PZC or IEP of the solids. In this case, the maximum particle charges of different solids with known PZC or IEP are measured in the nonpolar solvent in the presence of reverse micelles formed by the specific surfactant. The pH_{Eff} of the surfactant is the PZC or IEP of the mineral whose maximum particle charge is zero. It has been reported that when dispersed in organic media with dielectric constant around 2, the pH_{Eff} of a specific surfactant is unique [24, 25]. Therefore, the acid-base properties of a surfactant and solid particles can be compared using the pH_{Eff} of the

surfactant and solid particle's measured PZC or IEP. The empirical pH_{Eff} value of Span 80 was reported to be approximately 0 [23] according to the method mentioned above, which was lower than the IEP of kaolinite used in this work (about 1.8 as shown in **Figure 4.6**). Therefore, Span 80 is more acidic than kaolinite, so that the kaolinite-Span 80 acid-base interaction and the subsequent adduct separation between kaolinite and Span 80 would see Span 80 carrying away negative charges when its concentration was sufficiently high to form reverse micelles, leaving kaolinite positively charged. This is consistent with the results shown in **Figure 4.4(b)**.

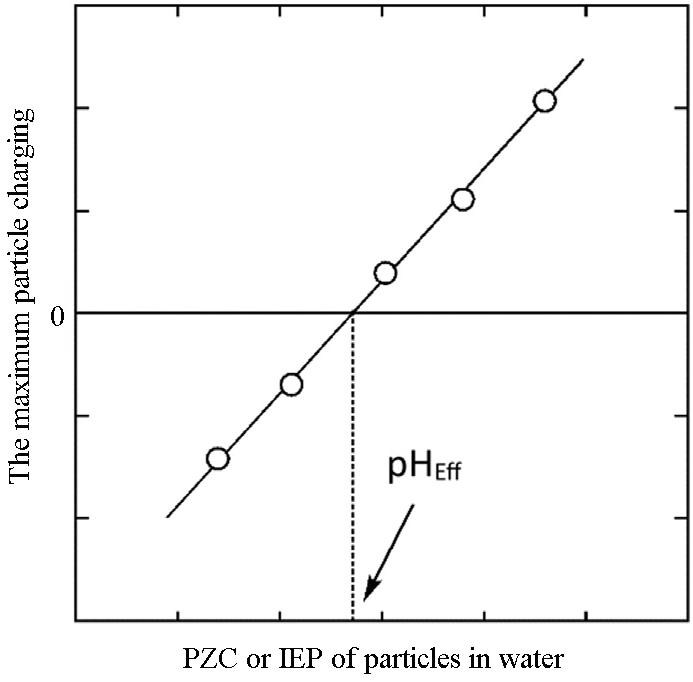

Figure 4.5. Schematic diagram to determine the empirical effective pH (pH_{Eff}) of a surfactant by measuring the maximum particle charges in nonpolar media. The maximum charges of different solids with different PZC or IEP are measured in a nonpolar media in the presence of a specific surfactant. The pH_{Eff} corresponds to the PZC or IEP of the solid in aqueous suspension (adapted from Ponto et al. [11]).

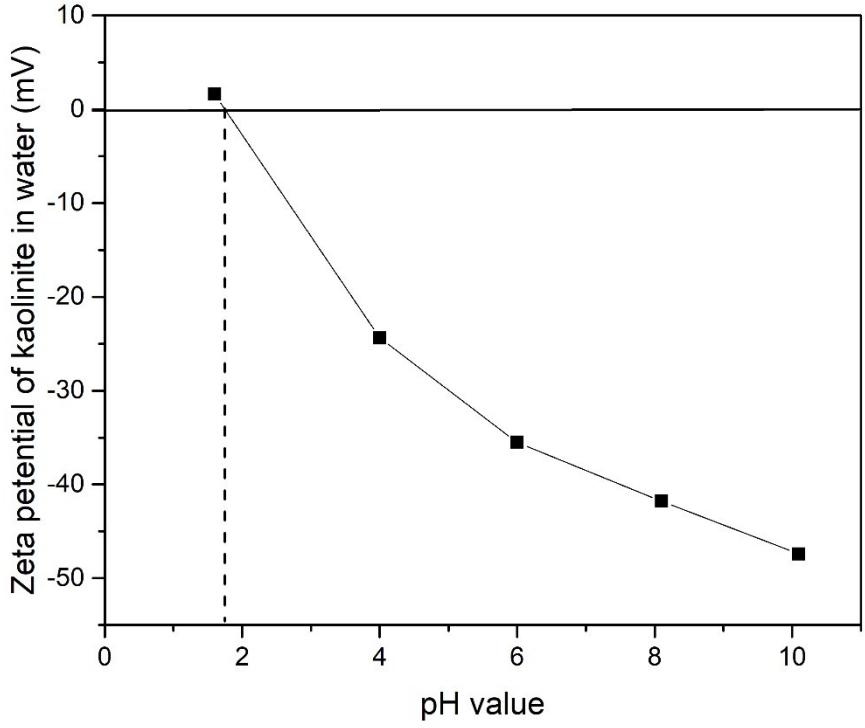

Figure 4.6. Zeta potential of kaolinite in water with different pH value. The pH value at which the zeta potential transitions from positive to negative is the IEP of kaolinite, which is approximately 1.8.

It should be noted that the probabilities for both the separation of acid-base adduct and the charge transfer are usually low, and it should be very infrequent for the charged surfactant molecular ions to escape from the particle surface to the bulk. It has been reported that a charged surfactant molecular ion is far more probable to escape from particle surface if it can be incorporated into a nearby reverse micelle [23]. If a particle is charged in a suspension, there must be counter charges (with opposite signs) in the suspension to maintain electric charge neutrality. The charged particle will attract oppositely charged species to resume electrical neutrality if the distance between them is sufficiently close.

The critical distance for opposite charges to associate with each other can be calculated by Bjerrum length (λ_B) which has been introduced in Chapter 3. The λ_B in cyclohexane is about 28 nm at 300 K. This value is much larger than the λ_B in water, which is 0.7 nm at 300 K, a distance that can be easily surpassed by the hydration shells of the ions. Therefore, oppositely charged ions could easily co-exist in water; but it is more difficult to keep oppositely charged ions apart beyond the Bjerrum length in a nonpolar organic solvent like cyclohexane. For cyclohexane suspension of kaolinite with the addition of Span 80, if the negatively charged Span 80 monomer formed by acid-base interaction with kaolinite surface could be incorporated into a reverse micelle, the reverse micelle would provide steric stabilization of charges with its extended tails.

According to above analysis, kaolinite did not carry charges in cyclohexane (**Figure 4.3 (d)**). With the addition of Span 80, some kaolinite particles acquired positive charges due to the acid-base interaction. The concentration of Span 80 had significant influence on kaolinite surface charges. High concentrations of Span 80 would make it more likely to form reverse micelles and result in an increase in the amount of charged kaolinite particles. This is consistent with the result shown in **Figure 4.3 (b)**. The electrodeposited amount of kaolinite particles on the cathode increased significantly when the Span 80 concentration was increased from 2.5×10^{-4} to 0.25 g/L. However, when the concentration of Span 80 in the electrophoretic deposition experimental system was increased to 2.5 g/L, no kaolinite particles were found to electrodeposit on either electrode (**Figure 4.4(b)**). This was likely due to the screening and/or neutralization effect caused by the presence of excessive amount of charge-carrying reverse micelles [23, 26], akin to the compression of electrical double layer in an aqueous system by counter-ions.

The zeta potential of kaolinite was measured in cyclohexane with the addition of Span 80, at concentrations of 2.5×10^{-4}, 2.5×10^{-3}, 2.5×10^{-2}, 0.25, and 2.5 g/L. The results are shown in **Figure 4.7**. As can be seen, the zeta potential of kaolinite increased from approximately 0 to about 30 mV when the Span 80 concentration was increased from 2.5×10^{-4} to 0.25 g/L. When the concentration of Span 80 was further increased to 2.5 g/L, the zeta potential rapidly decreased to around 0. This is consistent with the trend of the amount of electrodeposited kaolinite particles on the cathode shown in **Figure 4.4(b)**. In addition, the zeta potential of kaolinite was consistently positive when Span 80 concentration was between 2.5×10^{-3} and 0.25 g/L, which was in agreement with the results of the electrophoretic deposition experiments shown in **Figure 4.4(b)**.

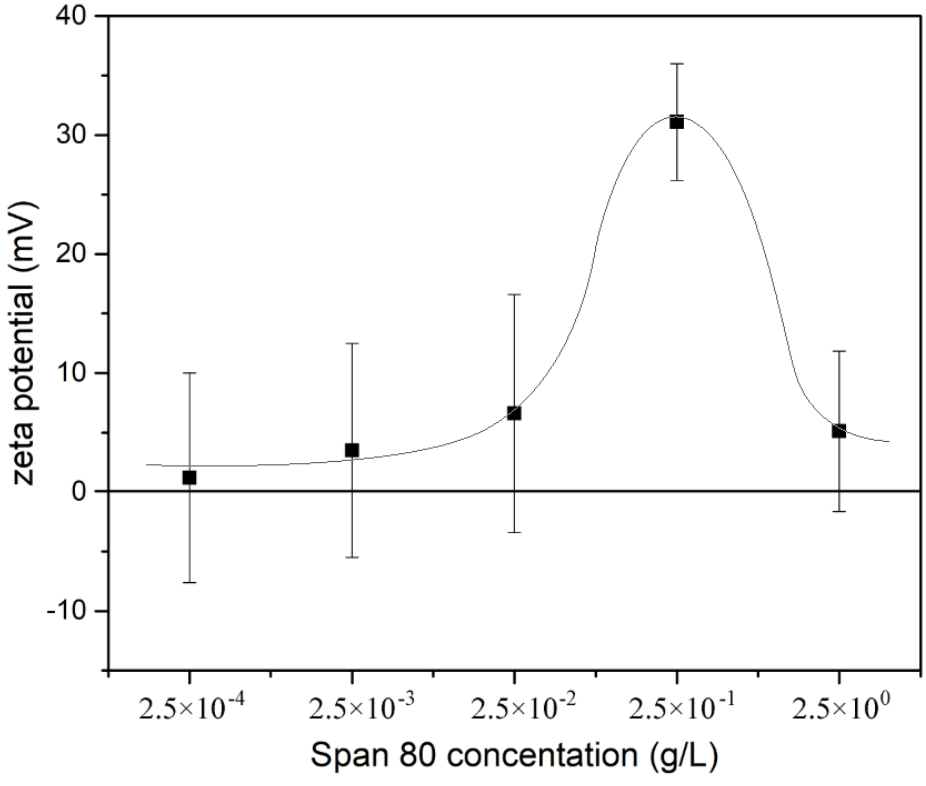

Figure 4.7 Zeta potential of kaolinite in cyclohexane with different concentrations of Span 80.

4.3.3 Kaolinite charging mechanism in cyclohexane with added bitumen

Figure 4.4 shows that the addition of a surfactant (Span 80) or bitumen could make the electrical-neutral kaolinite carry charges in cyclohexane. However, the charges were significantly different depending on which additive was used. The kaolinite charging behavior caused by Span 80 was clearly different from that caused by bitumen. Not only was the sign of the charge different (Span 80 made kaolinite predominantly positively charged whereas bitumen made kaolinite negatively charged), but the effects caused by a change in additive concentration were also different. In the case of Span 80, no deposit was formed on either anode or cathode when its concentration was too low (2.5×10^{-4} g/L) or too high (2.5 g/L). But in the case of bitumen, deposits were formed at all concentrations. Judging from the deposited amounts, Span 80 predominantly made kaolinite positively charged, and the amount of negatively charged kaolinite was very small. However, when bitumen was added, similar amounts of kaolinite were electrodeposited on both the cathode and the anode when the concentrations of the added bitumen were low (2.5×10^{-4} and 2.5×10^{-3} g/L). Only at high concentrations did the bitumen make kaolinite predominantly negatively charged. Therefore, the charging mechanism of kaolinite particles in cyclohexane induced by the addition of bitumen was different from that induced by Span 80. It was possible that factors other than reverse micelles operated in the case of kaolinite particle charging in cyclohexane when bitumen was added. To investigate these phenomena further, we attempted to remove the bitumen or Span 80 from the suspensions (cyclohexane suspensions of kaolinite with the addition of bitumen or Span 80) using filtration. The collected filter cakes were re-dispersed in fresh cyclohexane. The starting suspension was 4 mL 2 g/L kaolinite-in-cyclohexane suspension after the addition

of 0.1 mL cyclohexane solution containing 10 g/L bitumen, or Span 80, respectively (i.e., the actual concentration of these additives in the suspension was 0.25 g/L). It was filtered and repeatedly washed, and the filter cake (labeled as KB, or KS to represent kaolinite that was treated with bitumen or Span 80, respectively) was re-dispersed in fresh cyclohexane at a concentration of 2 g/L and used for electrophoretic deposition at the established conditions (5 min at 1500 V DC). To verify that the re-dispersed cyclohexane suspensions contained minimal amount of bitumen or Span 80, the suspensions were also filtered, and the concentrations of bitumen or Span 80 in the filtrates were measured using UV-Vis spectroscopy. Cyclohexane solutions of bitumen and Span 80 at different concentrations (0.001, 0.005, and 0.01 g/L) were used to obtain calibration spectra for the quantitative UV-Vis spectroscopic analysis. **Figure 4.8** shows the UV-Vis absorbance spectra of both standard solutions and the filtrates from cyclohexane suspensions of KB or KS. As can be seen in **Figure 4.8(a)**, the absorption peaks at the wavelength of around 400 nm can be used to determine the concentration of bitumen in the filtrate collected from a cyclohexane suspension of KB. As can be seen, the absorbance of the filtrate at 400 nm was very close to the absorbance of the 0.001 g/L bitumen-in-cyclohexane standard solution at 400 nm wavelength, suggesting that the bitumen concentration in the filtrate should be very low. Similarly, in **Figure 4.8(b)**, the absorption peaks at around 235 nm can be used to determine the concentration of Span 80 in the filtrate collected from a cyclohexane suspension of KS. As can be seen, the absorbance of the filtrate at 235 nm was lower than that of a 0.001 g/L Span 80-in-cyclohexane standard solution, indicating that there was almost no detectable Span 80 in the filtrate from cyclohexane suspension of KS. In summary, the bitumen or Span 80 from the cyclohexane suspensions of kaolinite could be

effectively eliminated through filtration and repeated washing. Upon re-dispersing the filter cake (kaolinite) in fresh cyclohexane solvent, the amount of bitumen or Span 80 in the suspensions was negligible.

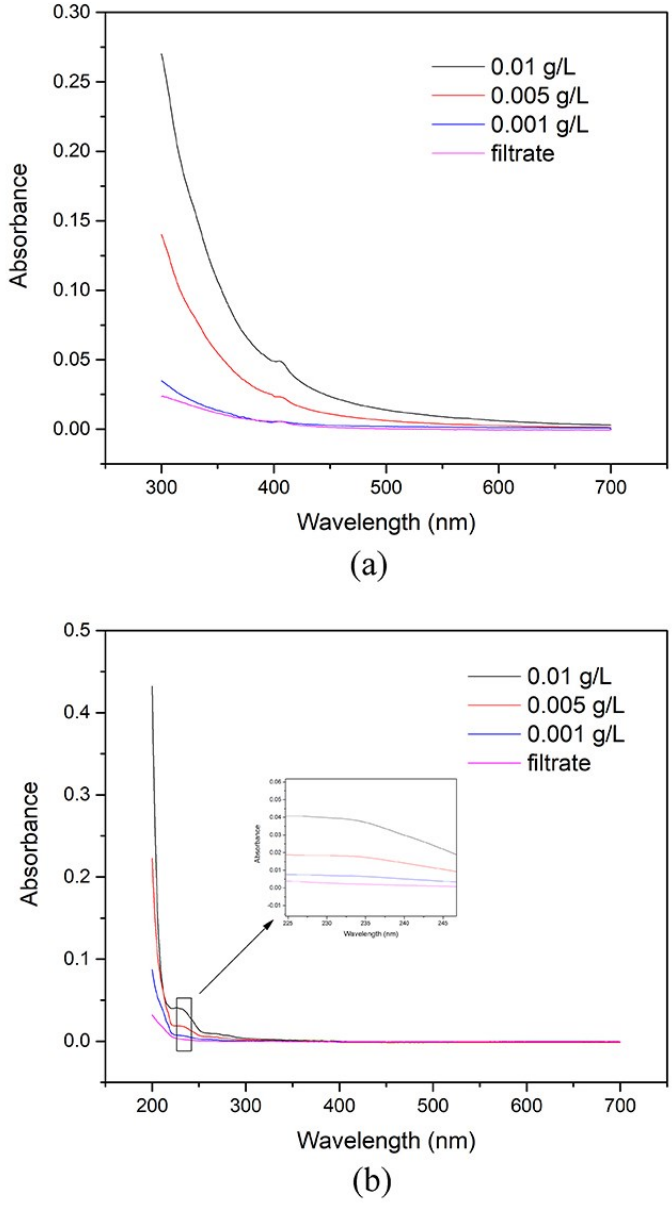

Figure 4.8. The UV-Vis absorbance spectra of (a) bitumen in cyclohexane standard solutions and filtrate from cyclohexane suspension of KB, and (b) Span 80 in cyclohexane standard solutions and cyclohexane suspension of KS.

Figure 4.9 shows the electrophoretic deposited amounts from the cyclohexane suspensions of KB and KS. These results are compared with the electrophoretic deposition results of the original kaolinite-cyclohexane suspensions (with 0.25 g/L bitumen or Span 80) before filtration. As can be seen, when bitumen was added in the original suspension, the deposited amounts from re-dispersed KB-in-cyclohexane suspension was only slightly lower than the amounts deposited from the original suspension. However, when Span 80 was added in the original suspension, the deposited amount from the re-dispersed KS-in-cyclohexane suspension was significantly reduced, to close to zero. The major difference between the cyclohexane suspensions of kaolinite-Span 80 mixture and KS was that the suspension of KS contained almost no free Span 80, whereas Span 80 was present in abundant quantities (i.e., the cyclohexane suspension of kaolinite-Span 80 mixture) before filtration. This indicates that Span 80 (and its reverse micelles) was important for the charging of kaolinite particles in cyclohexane. When the Span 80 was removed by filtration and repeated washing, the kaolinite particles were unable to acquire net charges, resulting in a significantly reduced electrodeposited amount. However, even after removing almost all the free bitumen, the majority of the KB that was re-dispersed in cyclohexane seemed to have largely retained the net charges. Therefore, the reasons why kaolinite particles carried net charges in cyclohexane after adding bitumen did not appear to be the same as adding Span 80. In the case of Span 80, it was likely the reverse micelles of Span 80 in cyclohexane stabilized opposite charges to enable a net surface charge of kaolinite. We hypothesize that in the case of adding bitumen, it was the adsorbed bitumen on the kaolinite surface that was responsible for the net charges of kaolinite in cyclohexane.

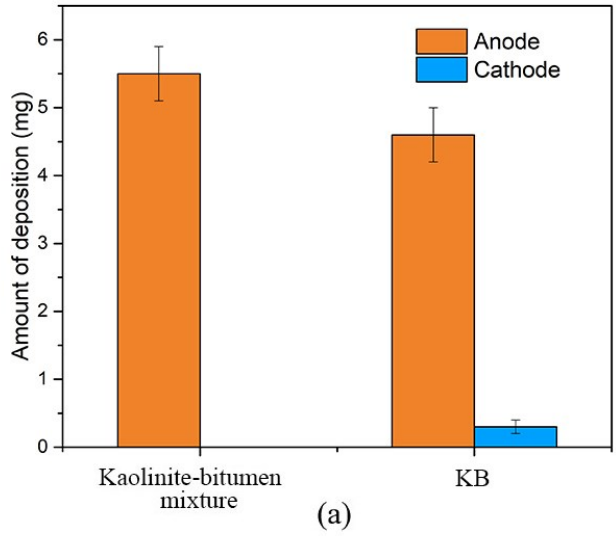

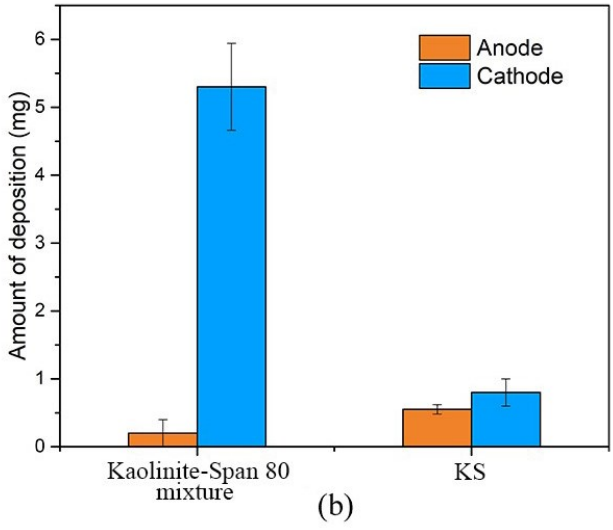

Figure 4.9. Comparison of the electrodeposited amounts of kaolinite from cyclohexane suspensions of (a) kaolinite-bitumen mixture, and KB, (b) kaolinite-Span 80 mixture, and KS on the anode (orange bars) and cathode (blue bars). Error bars represent standard deviations of three repeat tests under the same conditions. The "kaolinite-bitumen mixture" and "kaolinite-Span 80 mixture" were the original suspensions of kaolinite dispersed in the bitumen and Span 80 solutions. The "KB" and "KS" were suspensions of cyclohexane with the filtered and washed kaolinite that originated from the "kaolinite-bitumen mixture" and "kaolinite-Span 80 mixture", respectively.

The elemental compositions of KB particles before and after electrophoretic deposition were measured, and the carbon contents were used to compare the bitumen content of the KB and the deposited KB particles. The results are shown in **Table 4.1**. The carbon content of the untreated kaolinite was also measured and served as control. As can be seen, the kaolinite sample used in this work contained about 0.03 wt.% carbon. The carbon content of particles from cyclohexane suspension of KB was about 4.43 wt.%. Since KB was obtained by adding bitumen in the cyclohexane suspension of kaolinite followed by filtration, the much higher carbon content (than untreated kaolinite) was clearly due to the adsorption of bitumen. When the KB was re-dispersed in cyclohexane and electrodeposited, the majority of the particles were deposited on the anode, indicating predominantly net negative charges. The carbon content of particles deposited on the anode, as shown in **Table 4.1**, was slightly lower than the carbon content of the KB before re-dispersion in cyclohexane. This indicated that a small fraction of adsorbed bitumen on KB had desorbed from kaolinite particles which led to their electrophoretic deposition to the anode. The desorbed fractions probably carried positive charges, leaving the particles negatively charged.

Table 4.1. The carbon contents of kaolinite, and KB particles from cyclohexane suspensions and from deposited film on the anode. Error ranges represent standard deviations of three repeat tests under the same conditions.

Sample	Carbon content (wt.%)	
	Particles from cyclohexane suspension	Particles deposited on the anode
Kaolinite	0.03±0.002	/
KB	4.43±0.013	4.21±0.009

At this point, there was a question about whether the desorption of positively charged bitumen species from the KB surfaces occurred immediately upon re-suspension in cyclohexane, or whether the desorption only occurred under the influence of an external electrical field. QCM-D measurement was carried out to monitor the possible desorption of bitumen from the surface of kaolinite sensor (At-cut quartz crystal sensor with kaolinite coating on the top surface) under the influence of an external electric field in real-time. **Figure 4.10** shows the change in frequency (Δf) and dissipation (ΔD) with time at 7^{th} overtone during the QCM-D measurement. As can be seen, the dissipation change ΔD was larger than 10^{-6} for a 10 Hz frequency, indicating that the bitumen did not form a homogeneous rigid coating layer on the surface of kaolinite sensor [17, 19, 27, 28]. In this case, the Sauerbrey module would not be valid to estimate the mass change. The mass change was therefore calculated according to the Voigt model using Q-Tools software. The mass of adsorbed bitumen on kaolinite sensor surface at different stages of QCM-D measurement was also illustrated in **Figure 4.10**. As can be seen, after the bitumen was adsorbed on kaolinite sensor by injecting 0.1 g/L bitumen-in-cyclohexane solution through the QCM-D chamber, the mass of bitumen adsorbed on each square centimeter of the kaolinite sensor surface maintained at around 429 ng. With the application of a 5 V external electric field, the value decreased to about 413 ng. When the voltage was increased to 10 V, the mass did not show significant change. This indicated that in cyclohexane suspension, the application of an external electric field can induce the desorption of a small amount of adsorbed bitumen from kaolinite surface. An external electrical voltage of 5 V was sufficient to induce the desorption, and a doubling of the applied voltage did not seem to cause more desorption. Since our electrochemical QCM-D setup could not be ramped to

higher voltages, it was unclear if even higher voltages, such as 1500 V used in the electrophoretic deposition in this work, would desorb more bitumen from the kaolinite surface. However, it was clear that the application of an external electrical field could cause further dissolution of bitumen from bitumen-coated kaolinite surface when it was suspended in cyclohexane.

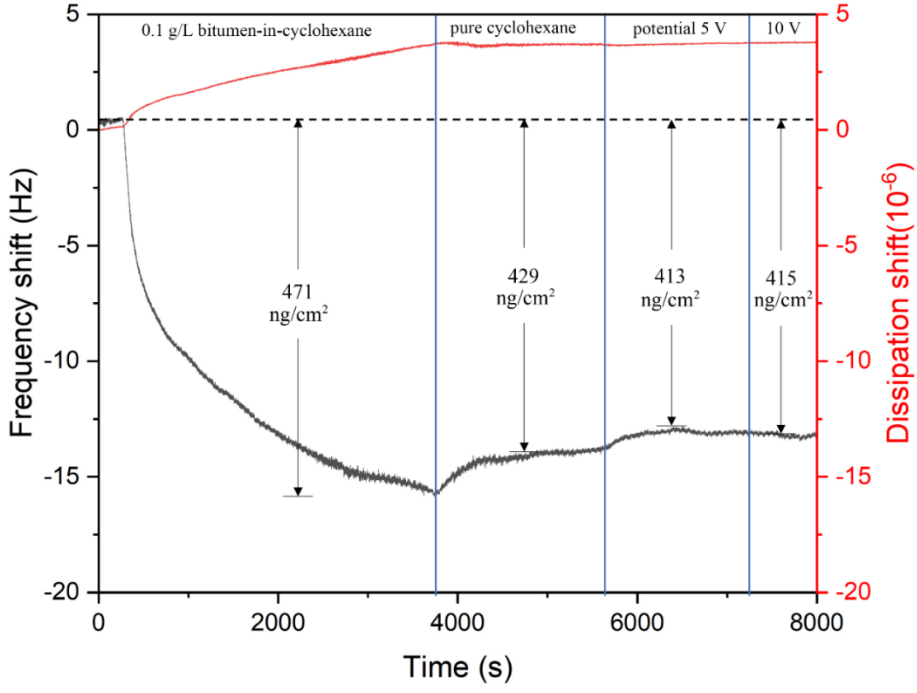

Figure 4.10. Representative frequency and dissipation changes with time (from the 7th overtone measurements) during the QCM-D measurements for the adsorption and desorption of bitumen from 0.1 g/L bitumen-in-cyclohexane solution on kaolinite sensor at different stages: (1) fluid switched to 0.1 g/L bitumen-in-cyclohexane, (2) fluid switched to pure cyclohexane, (3) kept cyclohexane flow and applied 5 V potential, (4) kept cyclohexane flow and applied 10 V potential.

Figure 4.11 shows the amount of electrophoretic deposited KB (i.e., the filter cake obtained from 2 g/L kaolinite-cyclohexane suspension that was treated with 0.25 g/L

bitumen) particles from suspensions of cyclohexane, *n*-pentane, and toluene. As can be seen, when the KB particles were dispersed in cyclohexane, about 4.6 mg kaolinite particles were deposited on the anode and about 0.5 mg particles were deposited on the cathode, suggesting that the KB particles were mainly negatively charged when dispersed in cyclohexane. When the particles were dispersed in *n*-pentane, only about 0.5 mg particles were deposited on the anode and almost no particles were deposited on the cathode. This indicated that the KB particles did not carry net charges or very small fractions may carry negative charges when dispersed in *n*-pentane. KB particle was bitumen-coated kaolinite prepared in cyclohexane, and *n*-pentane is a weaker solvent for bitumen than cyclohexane. If the desorption of the bitumen was responsible for the charging of KB, then it was not surprising to observe almost no electrophoretic deposition of KB in *n*-pentane. When the KB particles were dispersed in a stronger solvent, toluene, it can be seen that the deposited amount on the anode was higher than from cyclohexane. This further supported the hypothesis that the desorption of bitumen from the kaolinite surface was an important cause of bitumen-coated kaolinite charging in nonpolar solvents.

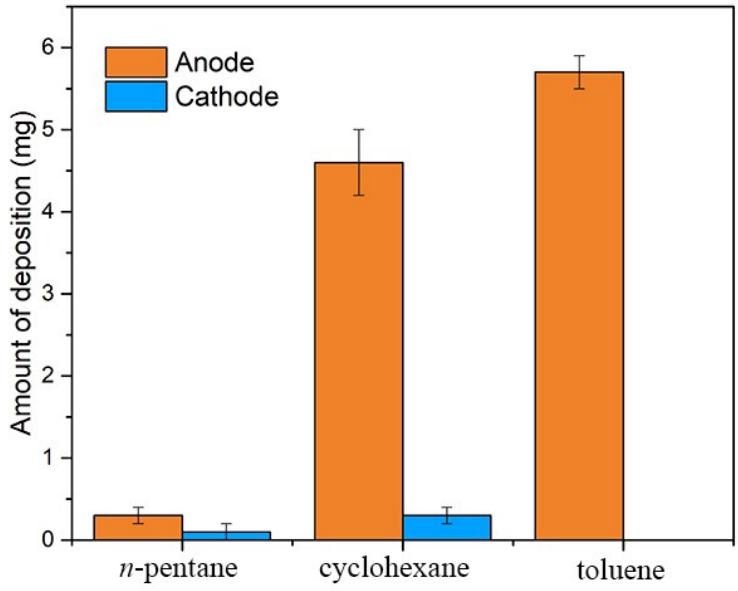

Figure 4.11. The amount of particles electrodeposited from 4 mL 2 g/L *n*-pentane, cyclohexane, and toluene suspensions of KB on the anode (orange bars) and cathode (blue bars). Error bars represent standard deviations of three repeat tests under the same conditions.

4.4 Conclusions

In this study, the development of kaolinite surface charges in cyclohexane with the addition of bitumen was studied by electrophoretic deposition, and the results were contrasted with the addition of a surfactant Span 80. Kaolinite particles were found to carry no net charges in cyclohexane when no bitumen or Span 80 were added, for the kaolinite particles did not electrodeposit on either anode or cathode. The addition of either Span 80 or bitumen made the kaolinite particles charged in cyclohexane, but the mechanism how the charges were developed were different.

With the addition of Span 80, kaolinite particles became positively charged, possibly caused by the acid-base interaction between Span 80 and kaolinite surface which allowed

the Span 80 to sequester anionic species from kaolinite surface and stabilize them by Span 80 reverse micelles in cyclohexane. Both electrophoretic deposition and zeta potential measurements showed that the kaolinite surface charges were significantly influenced by the presence or absence, and the concentration of Span 80. The amount of deposited kaolinite on the cathode increased from 0 to about 5.5 mg when Span 80 concentration was increased form 2.5×10^{-4} to 0.25 g/L, and then decreased to 0 when the concentration of Span 80 was further increased to 2.5 g/L. Similarly, the zeta potential of kaolinite in cyclohexane increased from approximately 0 to about +30 mV when Span 80 concentration was increased from 2.5×10^{-4} to 0.25 g/L. When Span 80 concentration was 2.5 g/L, the zeta potential of kaolinite dropped to around 0. The reason for the initial increase in electrodeposited amount and zeta potential with an increase in Span 80 concentration was likely because higher Span 80 concentration could provide more charge-carrying reverse micelles formed by Span 80. The decrease in the amount of electrodeposited kaolinite and in the kaolinite zeta potential at 2.5 g/L Span 80 was likely due to the screening and/or neutralization effect caused by the presence of high concentrations of the reverse micelles carrying opposite charges, akin to electrical double layer compression by counter-ions in an aqueous suspension.

The development of kaolinite surface charges in cyclohexane in the presence of bitumen was different from that caused by Span 80. At low concentrations of the added bitumen (2.5×10^{-4} and 2.5×10^{-3} g/L), similar low amounts of kaolinite were electrodeposited on both the cathode and the anode. At high concentrations, the added bitumen made kaolinite predominantly negatively charged. When the bitumen concentration increased to 0.25 g/L, no particles were found deposited on the cathode while about 5.5 mg particles deposited

on the anode. A further 10-fold increase in bitumen concentration to 2.5 g/L did not influence the deposition amount significantly, but it did not reduce the deposited amount to zero like Span 80 did.

Removal of the additives (bitumen or Span 80) from the kaolinite-cyclohexane suspension also had significantly different consequences on the charges of kaolinite. The removal of Span 80 by filtration and re-suspension in fresh cyclohexane resulted in a significant decrease in the electrophoretic deposition amount of kaolinite. This was likely caused by the removal of any potentially charge-stabilizing Span 80 reverse micelles. However, removing bitumen by filtration and re-suspension had no significant effect on the electrophoretic deposition amount of kaolinite. CHNS elemental analysis and QCM-D measurements showed that an external electric field could induce the desorption of small amounts of positively charged bitumen species from kaolinite surface, so that the bitumen-coated kaolinite could still be electrodeposited to the anode after filtration and re-suspension in cyclohexane. Indeed, when the bitumen-coated kaolinite was filtered and re-suspended in *n*-pentane, the kaolinite could no longer be electrodeposited, clearly due to the lower dissolving power of the solvent. On the contrary, when the bitumen-coated kaolinite was filtered and re-suspended in toluene, the electrodeposited amount was on par and slightly more than from cyclohexane. This research revealed the charging mechanism for clay particles such as kaolinite in a nonpolar solvent in the presence of bitumen, which was different from the prevailing reverse micelle theory, and the revealed mechanism may have useful implications in removing fine clays from bitumen and other heavy crude by using electrostatic means.

References

[1] Romanova U, Valinasab M, Stasiuk E, Yarranton H, Schramm L, Shelfantook W. The effect of oil sands bitumen extraction conditions on froth treatment performance. Journal of Canadian Petroleum Technology. 2006; 45(09).

[2] Wang D, Tao H, Wang K, Tan X, Liu Q. The filterability of different types of minerals and the role of swelling clays in the filtration of oil sands tailings. Fuel. 2022; 316: 123395.

[3] Berkowitz N, Speight JG. The oil sands of Alberta. Fuel. 1975; 54(3):138-49.

[4] Hooshiar A, Uhlik P, Liu Q, Etsell TH, Ivey DG. Clay minerals in nonaqueous extraction of bitumen from Alberta oil sands: Part 1. Nonaqueous extraction procedure. Fuel processing technology. 2012; 94(1):80-5.

[5] Wu J, Dabros T. Process for solvent extraction of bitumen from oil sand. Energy & fuels. 2012; 26(2):1002-8.

[6] West RC. Non-aqueous process for the recovery of bitumen from tar sands. Google Patents; 1964.

[7] Zhang H, Tan X, Liu Q. Fine solids removal from non-aqueous extraction bitumen: A literature review. Fuel. 2021; 288: 119727.

[8] Nikakhtari H, Wolf S, Choi P, Liu Q, Gray MR. Migration of fine solids into product bitumen from solvent extraction of Alberta oilsands. Energy & fuels. 2014; 28(5):2925-32.

[9] Cullinane JT, Minhas BS. Electrostatic filtration of fine solids from bitumen. Google Patents; 2017.

[10] Lee J, Zhou Z-L, Behrens SH. Charging mechanism for polymer particles in nonpolar surfactant solutions: influence of polymer type and surface functionality. Langmuir. 2016; 32(19):4827-36.

[11] Ponto BS, Berg JC. Clay particle charging in apolar media. Applied Clay Science. 2018; 161: 76-81.

[12] Poovarodom S, Berg JC. Effect of particle and surfactant acid–base properties on charging of colloids in apolar media. Journal of colloid and interface science. 2010; 346(2):370-7.

[13] Ponto BS, Berg JC. Charging of Oxide Nanoparticles in Media of Intermediate Dielectric Constant. Langmuir. 2019; 35(47):15249-56.

[14] Ponto BS. Exploring new avenues of surfactant mediated particle charging in apolar media 2019.

[15] Lee J, Zhou Z-L, Alas G, Behrens SH. Mechanisms of particle charging by surfactants

in nonpolar dispersions. Langmuir. 2015; 31(44):11989-99.

[16] Zhang H, Tan X, Wang K, Liu Q. Electrodeposition of bitumen-, asphaltene-, or maltene-coated kaolinite from cyclohexane suspensions. Fuel. 2022; 311: 122582.

[17] Chen Q, Xu S, Liu Q, Masliyah J, Xu Z. QCM-D study of nanoparticle interactions. Advances in colloid and interface science. 2016; 233: 94-114.

[18] Tamiz Bakhtiari M, Harbottle D, Curran M, Ng S, Spence J, Siy R, et al. Role of caustic addition in bitumen–clay interactions. Energy & Fuels. 2015; 29(1):58-69.

[19] Bai T, Xiang B, Li M, Manica R, Liu Q. Mechanism of modification of bitumen zeta potential by sodium citrate: Interactions between bitumen metal content and ligands. Colloids and Surfaces A: Physicochemical and Engineering Aspects. 2022; 653: 130007.

[20] Pugh RJ, Matsunaga T, Fowkes FM. The dispersibility and stability of carbon black in media of low dielectric constant. 1. Electrostatic and steric contributions to colloidal stability. Colloids and Surfaces. 1983; 7(3):183-207.

[21] Pugh RJ, Fowkes FM. The dispersibility and stability of carbon black in media of low dielectric constant. 2. Sedimentation volume of concentrated dispersions, adsorption and surface calorimetry studies. Colloids and surfaces. 1984; 9(1):33-46.

[22] Smith GN, Eastoe J. Controlling colloid charge in nonpolar liquids with surfactants. Physical Chemistry Chemical Physics. 2013; 15(2):424-39.

[23] Gacek MM, Berg JC. The role of acid–base effects on particle charging in apolar media. Advances in colloid and interface science. 2015; 220: 108-23.

[24] Gacek MM, Berg JC. Investigation of surfactant mediated acid–base charging of mineral oxide particles dispersed in apolar systems. Langmuir. 2012; 28(51):17841-5.

[25] Gacek M, Bergsman D, Michor E, Berg JC. Effects of trace water on charging of silica particles dispersed in a nonpolar medium. Langmuir. 2012; 28(31):11633-8.

[26] Hsu MF, Dufresne ER, Weitz DA. Charge stabilization in nonpolar solvents. Langmuir. 2005; 21(11):4881-7.

[27] Teng F, Liu Q, Zeng H. In situ kinetic study of zinc sulfide activation using a quartz crystal microbalance with dissipation (QCM-D). Journal of colloid and interface science. 2012; 368(1):512-20.

[28] Ekholm P, Blomberg E, Claesson P, Auflem IH, Sjöblom J, Kornfeldt A. A quartz crystal microbalance study of the adsorption of asphaltenes and resins onto a hydrophilic surface. Journal of colloid and interface science. 2002; 247(2):342-50.

Chapter 5 Conclusions, Contributions, and Recommendations

5.1 Summary and Conclusions

In this thesis research, the charging mechanism of kaolinite in cyclohexane was investigated. The driver behind this research was to use an external electric field to assist with the removal of fine mineral particles from nonaqueous extracted (NAE) bitumen from Alberta oil sands. Cyclohexane was used as the organic nonpolar solvent because it had been shown to be one of the most promising solvents for NAE process. Kaolinite was chosen as a representative mineral because it is the dominant clay not only in the oil sands ores but also in NAE bitumen.

Bitumen and bitumen subfractions (asphaltene, maltene) were either added into the cyclohexane suspensions of kaolinite or previously coated onto kaolinite surface to investigate their effects on particle charging. A common surfactant, Span 80, was studied to compare with bitumen. It was confirmed that the bitumen coating layer, rather than dissolved bitumen, was responsible for kaolinite charging. Conversely, when Span 80 was used, kaolinite surface charge was developed by the presence of dissolved Span 80 that formed reverse micelles in cyclohexane. Span 80 may have adsorbed on kaolinite but it did not contribute to the kaolinite surface charge in cyclohexane.

Such a deeper understanding of the charging mechanisms of kaolinite (and by extension, other minerals) in a nonpolar organic solvent opens a range of possible applications of solid-liquid separation in nonaqueous systems.

The main conclusions of this study were:

(1) Kaolinite did not carry a net charge in cyclohexane without any other additives. This was probably due to the instability of charges in such a system. In the absence of charge-stabilizing supramolecular structures in cyclohexane, the charge carriers could not be kept at a distance beyond the Bjerrum length to avoid mutual neutralization.

(2) After being coated by bitumen, asphaltene, or maltene, kaolinite was found to carry net charges in cyclohexane inside an electric field, even when the suspension did not contain any other additives. Thus, bitumen-coated-kaolinite (BCK) and maltene-coated-kaolinite (MCK) were electrophoretic deposited on the anode, and asphaltene-coated-kaolinite (ACK) predominantly deposited on the anode but also deposited on the cathode. The deposited amount increased with kaolinite concentration and deposition time and levelled off after 5 min of electrophoretic deposition.

(3) FTIR spectra showed that the films electrophoretic deposited on the anode from BCK and MCK contained much higher concentrations of carboxyl groups than the anode films deposited from ACK. The presence of carboxyl groups seemed to be the defining character that contributed to the negative charges. In fact, the carboxyl-group-deficient asphaltene was found to deposit mostly to the cathode when it was dissolved in cyclohexane. XPS electron binding energy spectra and surface elemental concentration analyses of the electrodeposited films on both anodes and cathodes showed that, generally, the cathode films had a higher N content, and the anode films showed C and S species with higher oxidation states that were associated with oxygen.

The charging of pristine kaolinite (not previously coated) in cyclohexane was also studied by adding either bitumen or Span 80. It was found that the presence of high

concentrations of Span 80 in the kaolinite-cyclohexane suspension was the pre-requisite for kaolinite to carry positive charges. When the Span 80 was removed, the charges on kaolinite disappeared. This was attributed to the charge-stabilizing function of the Span 80 reverse micelles. When Span 80 was adsorbed on kaolinite, the higher acidity of Span 80 caused it to extract negative charged species (electron donors) from kaolinite surface. The subsequent desorption of the Span 80 removes the negative charge from kaolinite surface, which was stabilized by the Span 80 reverse micelles in the system, thus leaving kaolinite positively charged.

However, the charges developed on pristine kaolinite by adding bitumen to cyclohexane were completely different. Not only was the kaolinite negatively charged after adding bitumen, but the negative charges were resumed when bitumen was removed and the kaolinite re-suspended in fresh cyclohexane. We hypothesize that this was due to the adsorbed bitumen layer on the kaolinite surface. Under the action of an external electric field, part of the adsorbed bitumen layer could desorb, carrying positively charged species. This gave kaolinite a negative surface charge. Therefore, kaolinite surface charge in cyclohexane only depended on the presence of a bitumen coating, but did not depend on whether bitumen was dissolved in cyclohexane or not.

5.2 Original Contributions

The work reported in this thesis contributes to the fundamental understanding of the charging mechanism of clay particles, represented by kaolinite, in NAE bitumen product that was simulated by cyclohexane suspension with the addition of bitumen or bitumen subfractions (asphaltene, maltene). The influence of bitumen and/or bitumen subfractions

on the charging of kaolinite particles and the charging mechanism of kaolinite with adsorbed bitumen components were analyzed. This research was built on accumulated knowledge of particle charging in nonpolar media reported in the open literature over the past several decades. Based on the author's understanding of the relevant literature, the original contributions of this work can be summarized as follows:

(1) The charging mechanism of fine clay minerals such as kaolinite in nonpolar systems such as cyclohexane in the presence of bitumen or bitumen subfractions (asphaltene, maltene) was studied by electrophoretic deposition for the first time.

(2) This research revealed that bitumen adsorbed on kaolinite surface, rather than dissolved bitumen, was responsible for kaolinite charging in cyclohexane. This was different from the widely accepted conventional charging mechanism of fine particles in nonpolar media, which states that in such media, particles become charged due to the formation of reverse micelles from dissolved surfactants.

(3) This research postulated that bitumen-coated kaolinite carries charges in cyclohexane because of the selective dissolution of charge-carrying species from the kaolinite surface. This selective dissolution was induced by an external electric field and could be influenced by the type of solvents, i.e., replacing cyclohexane by a weaker solvent *n*-pentane or a stronger solvent toluene significantly changed the magnitude of the kaolinite surface charges (lower charges in *n*-pentane and higher charges in toluene). The observation lent support to the selective dissolution hypothesis.

(4) Demonstrated that most bitumen-, or bitumen subfractions-coated kaolinite were charged in cyclohexane without the presence of dissolved species. The coating of

asphaltene could make a portion of the kaolinite carry net positive charges and another portion net negative charges, while the coating of maltene and bitumen made kaolinite particles carry negative charges. Overall, asphaltene-, maltene-, and bitumen-coated kaolinite were all predominantly negatively charged, mostly originated from the carboxyl groups and C and S species with high oxidation states.

5.3 Suggestion for Future Work

This work revealed the charging mechanism of fine particle (kaolinite) in nonpolar medium (cyclohexane) in the presence of bitumen or bitumen subfractions. The research into mechanism is expected to help solve the problem of fine solids removal from NAE bitumen product assisted by electric-enhanced fine solids removal techniques. With the understanding of the mechanism revealed by this study, future research could analyze the factors influencing the charging of fine particles in nonpolar media, as well as explore the optimal conditions for particle removal with an applied electric field. In addition, future research could develop an in-situ fine particle removal process using an applied electric field for NAE technique.

Although all the tests for this work were carried out in nonpolar (non-aqueous) system, the "nonpolar" medium and all the materials used in this research were probably not absolutely free of water. Actually, the presence of water may have influence on fine particles charging in nonpolar media. Future research may explore the role of the trace amount of water in fine particles charging in nonpolar media. Studies on absolutely water-free systems may yield interesting discoveries as well. Besides, the charging characterization of fine particles in other solvents, in addition to cyclohexane, is also worth exploring in future works.

Bibliography

[1] Masliyah JH, Czarnecki J. Xu Z. Introduction to the Athabasca oil sands. In: Handbook on theory and practice of bitumen recovery from Athabasca oil sands, volume I: theoretical basis. Kingsley Knowledge Pub; 2011. p. 1-39.

[2] Jin Y, Liu W, Liu Q, Yeung A. Aggregation of silica particles in non-aqueous media. Fuel 2011; 90 (8): 2592-7.

[3] Wang D, Tao H, Wang K, Tan X, Liu Q. The filterability of different types of minerals and the role of swelling clays in the filtration of oil sands tailings. Fuel 2022; 316: 123395.

[4] Alberta Energy Regulator, Alberta energy regulator, available at: https://static.aer.ca/prd/documents/reports/AER2020-21AnnualReport.pdf.

[5] Canadian Association of Petroleum Producers CAPP, 2019 Crude Oil Forecast, Markets and Transportation, available at: https://www.capp.ca/wp-content/uploads/2019/11/2019_Crude_Oil_Forecast_Markets_and_Transportation-338794.pdf.

[6] Regulator-ERCB AE. Alberta's Energy Reserves 2007 and Supply/Demand Outlook 2008-2017. Calgary: Energy Resources Conservation Board. 2008.

[7] Masliyah JH, Czarnecki J. Xu Z. Physical and chemical properties of oil sands. In: Handbook on theory and practice of bitumen recovery from Athabasca oil sands, volume I: theoretical basis. Kingsley Knowledge Pub; 2011. p. 173-256.

[8] Romanova UG, Valinasab M, Stasiuk EN, Yarranton HW, Schramm LL, Shelfantook WE. The effect of oil sands bitumen extraction conditions on froth treatment performance. Journal of Canadian Petroleum Technology. 2006 Sep 1; 45 (09).

[9] Rao F, Liu Q. Froth treatment in Athabasca oil sands bitumen recovery process: A review. Energy & fuels. 2013 Dec 19; 27 (12): 7199-207.

[10] Masliyah J, Zhou ZJ, Xu Z, Czarnecki J, Hamza H. Understanding water‐based bitumen extraction from Athabasca oil sands. The Canadian Journal of Chemical Engineering. 2004 Aug; 82 (4): 628-54.

[11] Oil Sands Magazine, Water usage, available at: https://www.oilsandsmagazine.com/technical/environment/water-usage

[12] Hooshiar A, Uhlik P, Liu Q, Etsell TH, Ivey DG. Clay minerals in nonaqueous extraction of bitumen from Alberta oil sands: Part 1. Nonaqueous extraction procedure. Fuel processing technology. 2012 Feb 1; 94 (1):80-5.

[13] Zhang H, Tan X, Liu Q. Fine solids removal from non-aqueous extraction bitumen: A literature review. Fuel. 2021 Mar 15; 288: 119727.

[14] Avagyan AB. Environmental building policy by the use of microalgae and decreasing of risks for Canadian oil sand sector development. Environmental Science and Pollution Research. 2017 Sep; 24 (25): 20241-53.

[15] Poettmann FH, Kelly JT. Use of a soluble oil in the extraction of hydrocarbons from oil sands. US Patent 3,392,105; 1968.

[16] West RC. Non-aqueous process for the recovery of bitumen from tar sands. US Patent 3,131,141; 1964.

[17] Pal K, Nogueira Branco LDP, Heintz A, Choi P, Liu Q, Seidl PR, et al. Performance of solvent mixtures for non-aqueous extraction of Alberta oil sands. Energy Fuels 2015; 29 (4): 2261–7.

[18] Nikakhtari H, Wolf S, Choi P, Liu Q, Gray MR. Migration of fine solids into product bitumen from solvent extraction of Alberta oilsands. Energy Fuels 2014; 28 (5): 2925–32.

[19] Chen Q, Liu Q. Bitumen coating on oil sands clay minerals: a review. Energy Fuels 2019; 33 (7): 5933-43.

[20] Nikakhtari H, Vagi L, Choi P, Liu Q, Gray MR. Solvent screening for non-aqueous extraction of Alberta oil sands. Can J Chem Eng 2013; 91 (6):1153–60.

[21] Hooshiar A, Uhlik P, Ivey DG, Liu Q, Etsell TH. Clay minerals in nonaqueous extraction of bitumen from Alberta oil sands: Part 2. Characterization of clay minerals. Fuel Process Technol 2012; 96: 183–94.

[22] Russel W. Brownian motion of small particles suspended in liquids. Annu Rev Fluid Mech 1981; 13 (1): 425–55.

[23] Bensebaa F, Kotlyar LS, Sparks BD, Chung KH. Organic coated solids in Athabasca bitumen: Characterization and process implications. Can J Chem Eng 2000; 78 (4): 610–6.

[24] Liu J, Cui X, Huang J, Xie L, Tan X, Liu Q, et al. Understanding the stabilization mechanism of bitumen-coated fine solids in organic media from non-aqueous extraction of oil sands. Fuel 2019; 242: 255–64.

[25] Kaminsky HA, Etsell TH, Ivey DG, Omotoso O. Distribution of clay minerals in the process streams produced by the extraction of bitumen from Athabasca oil sands. Can J Chem Eng 2009; 87 (1): 85–93.

[26] Cullinane JT, Minhas BS. Electrostatic filtration of fine solids from bitumen. US Patent 9,752,079; 2017.

[27] Ohsawa A, Morrow R, Murphy AB. An investigation of a dc dielectric barrier discharge using a disc of glass beads. J Phys D Appl Phys 2000; 33 (12):1487.

[28] Alade O, Mohammed I, Abdel-Azeim S, Shakil Hussain SM, Kamal MS, Mahmoud M, et al. Review on Applications of Ionic Liquids (ILs) for Bitumen Recovery: Mechanisms, Challenges, and Perspectives. Energy & Fuels. 2023.

[29] Joshi VA, Kundu D. Ionic liquid promoted extraction of bitumen from oil sand: A review. Journal of Petroleum Science and Engineering. 2021;199:108232.

[30] Yang Z, He C, Sui H, He L, Li X. Recent advances of CO2-responsive materials in separations. Journal of CO2 Utilization. 2019;30:79-99.

[31] Painter P, Williams P, Mannebach E. Recovery of bitumen from oil or tar sands using ionic liquids. Energy & Fuels. 2010;24(2):1094-8.

[32] Painter P, Williams P, Lupinsky A. Recovery of bitumen from Utah tar sands using ionic liquids. Energy & Fuels. 2010;24(9):5081-8.

[33] Tourvieille J-N, Larachi F, Duchesne C, Chen J. NIR hyperspectral investigation of extraction kinetics of ionic-liquid assisted bitumen extraction. Chemical Engineering Journal. 2017;308:1185-99.

[34] Abdelfatah E, Berton P, Rogers RD, Bryant SL. Low-temperature bitumen recovery from oil-sand reservoirs using ionic liquids. SPE Journal. 2019;24(05):2409-22.

[35] Berton P, Manouchehr S, Wong K, Ahmadi Z, Abdelfatah E, Rogers RD, et al. Ionic liquids-based bitumen extraction: enabling recovery with environmental footprint comparable to conventional oil. ACS Sustainable Chemistry & Engineering. 2019;8(1):632-41.

[36] Holland A, Wechsler D, Patel A, Molloy BM, Boyd AR, Jessop PG. Separation of bitumen from oil sands using a switchable hydrophilicity solvent. Canadian Journal of Chemistry. 2012;90(10):805-10.

[37] Sui H, Xu L, Li X, He L. Understanding the roles of switchable-hydrophilicity tertiary amines in recovering heavy hydrocarbons from oil sands. Chemical Engineering

Journal. 2016;290:312-8.

[38] Latała A, Nędzi M, Stepnowski P. Toxicity of imidazolium and pyridinium based ionic liquids towards algae. Bacillaria paxillifer (a microphytobenthic diatom) and Geitlerinema amphibium (a microphytobenthic blue green alga). Green Chemistry. 2009;11(9):1371-6.

[39] Vanderveen JR, Durelle J, Jessop PG. Design and evaluation of switchable-hydrophilicity solvents. Green Chemistry. 2014;16(3):1187-97.

[40] Plechkova NV, Seddon KR. Applications of ionic liquids in the chemical industry. Chemical Society Reviews. 2008;37(1):123-50.

[41] Geramian M, Liu Q, Ivey DG, Etsell TH. Influence of Oil Sands Composition on Bitumen Quality During Non-Aqueous Bitumen Extraction from the Athabasca Deposit. The Canadian Journal of Chemical Engineering. 2019;97(1):268-80.

[42] Nikakhtari H, Vagi L, Choi P, Liu Q, Gray MR. Solvent screening for non-aqueous extraction of Alberta oil sands. The Canadian Journal of Chemical Engineering. 2013;91(6):1153-60.

[43] Masliyah JH, Czarnecki J, Xu Z. Handbook on theory and practice on bitumen recovery from athabasca oil sands. 2011.

[44] Meadus FW, Sparks BD, Puddington IE, Farnand JR. Separating organic material from tar sands or oil shale. Google Patents; 1977.

[45] Meadus F, Bassaw B, Sparks B. Solvent extraction of athabasca oil-sand in a rotating mill Part 2. Solids—liquid separation and bitumen quality. Fuel Processing Technology. 1982;6(3):289-300.

[46] Kaminsky HA, Uhlik P, Hooshiar A, Shinbine A, Etsell TH, Ivey DG, et al., editors. Comparison of morphological and chemical characteristics of clay minerals in the primary froth and middlings from oil sands processing by high resolution transmission electron microscopy. Proceedings of the first international oil sands tailings conference; 2008.

[47] Hu J, Zhou S, Sun Y, Fang X, Wu L. Fabrication, properties and applications of Janus particles. Chemical Society Reviews. 2012;41(11):4356-78.

[48] Wang S, Liu Q, Tan X, Xu C, Gray MR. Adsorption of asphaltenes on kaolinite as an irreversible process. Colloids and Surfaces A: Physicochemical and Engineering Aspects. 2016;504:280-6.

[49] Gregory J, Barany S. Adsorption and flocculation by polymers and polymer mixtures. Advances in colloid and interface science. 2011;169(1):1-12.

[50] Vajihinejad V, Gumfekar SP, Bazoubandi B, Rostami Najafabadi Z, Soares JB. Water soluble polymer flocculants: synthesis, characterization, and performance assessment. Macromolecular Materials and Engineering. 2019;304(2):1800526.

[51] Madge D, Garner W. Theory of asphaltene precipitation in a hydrocarbon cyclone. Minerals engineering. 2007;20(4):387-94.

[52] Farnand J, Meadus F, Sparks B. Removal of intractable fine solids from bitumen solutions obtained by solvent extraction of oil sands. Fuel processing technology. 1985;10(2):131-44.

[53] Zahabi A, Gray MR, Dabros T. Kinetics and properties of asphaltene adsorption on surfaces. Energy & fuels. 2012;26(2):1009-18.

[54] Long Y, Dabros T, Hamza H. Stability and settling characteristics of solvent-diluted bitumen emulsions. Fuel. 2002;81(15):1945-52.

[55] Lin F, Pang CJ. Impact of a hybrid bitumen extraction process on the destabilization of resulting bitumen froth emulsion diluted with heptane. Minerals Engineering. 2020;145:106069.

[56] Liu J, Cui X, Santander C, Tan X, Liu Q, Zeng H. Destabilization of fine solids suspended in oil media through wettability modification and water-assisted agglomeration. Fuel. 2019;254:115623.

[57] Malladi S. Removal of Particulate Fines from Organic Solvents Using Water as Collector Droplets: University of Toronto (Canada); 2015.

[58] Cosgrove T. Colloid science: principles, methods and applications: John Wiley & Sons; 2010.

[59] Lowe BM, Skylaris C-K, Green NG. Acid-base dissociation mechanisms and

energetics at the silica–water interface: An activationless process. Journal of colloid and interface science. 2015;451:231-44.

[60] Bele M, Kodre A, Arčon I, Grdadolnik J, Pejovnik S, Besenhard J. Adsorption of cetyltrimethylammonium bromide on carbon black from aqueous solution. Carbon. 1998;36(7-8):1207-12.

[61] Gupta SD, Bhagwat SS. Adsorption of surfactants on carbon black-water interface. Journal of dispersion science and technology. 2005;26(1):111-20.

[62] Park S-J, Seo M-K. Intermolecular force. Interface science and technology. 2011;18:1-57.

[63] Bjerrum N. Untersuchungen über Ionenassoziation: AF Høst; 1926.

[64] Tansel B, Sager J, Rector T, Garland J, Strayer RF, Levine L, et al. Significance of hydrated radius and hydration shells on ionic permeability during nanofiltration in dead end and cross flow modes. Separation and Purification Technology. 2006;51(1):40-7.

[65] Volkov A, Paula S, Deamer D. Two mechanisms of permeation of small neutral molecules and hydrated ions across phospholipid bilayers. Bioelectrochemistry and bioenergetics. 1997;42(2):153-60.

[66] Dukhin A, Parlia S. Ions, ion pairs and inverse micelles in non-polar media. Current opinion in colloid & interface science. 2013;18(2):93-115.

[67] Kraus CA, Hooper GS. The Dielectric Properties of Solutions of Electrolytes in a Non-Polar Solvent. Proceedings of the National Academy of Sciences. 1933;19(11):939-43.

[68] Geddes JA, Kraus CA. Properties of electrolytic solutions. XVIII. Molecular polarisations and polar moments of some electrolytes in benzene solutions. Transactions of the Faraday Society. 1936;32:585-93.

[69] Wohlfarth C. CRC Handbook of Phase Equilibria and Thermodynamic Data of Aqueous Polymer Solutions: CRC Press; 2012.

[70] Myers D. Surfactant science and technology: John Wiley & Sons; 2020.

[71] Baruwati B. Studies on the synthesis, characterization, surface modification and application of nanocrystalline nickel ferrite. India Institute of Chemical Technology Hyderabad. 2007.

[72] Nelson S, Pink R. 322. Solutions of metal soaps in organic solvents. Part III. The aggregation of metal soaps in toluene, iso butyl alcohol, and pyridine. Journal of the Chemical Society (Resumed). 1952:1744-50.

[73] Singleterry C, Weinberger LA. The Size of Soap Micelles in Benzene from Osmotic Pressure and from the Depolarization of Fluorescence1. Journal of the American Chemical Society. 1951;73(10):4574-9.

[74] Kaufman S, Singleterry CR. The critical range for micelle formation by an oil-dispersible soap in a hydrocarbon solvent. Journal of Colloid Science. 1952;7(5):453-64.

[75] Gacek M, Brooks G, Berg JC. Characterization of mineral oxide charging in apolar media. Langmuir. 2012;28(5):3032-6.

[76] Michor EL, Berg JC. Temperature effects on micelle formation and particle charging with span surfactants in apolar media. Langmuir. 2015;31(35):9602-7.

[77] Sainis SK, Merrill JW, Dufresne ER. Electrostatic interactions of colloidal particles at vanishing ionic strength. Langmuir. 2008;24(23):13334-7.

[78] Espinosa CE, Guo Q, Singh V, Behrens SH. Particle charging and charge screening in nonpolar dispersions with nonionic surfactants. Langmuir. 2010;26(22):16941-8.

[79] Keir RI, Quinn A, Jenkins P, Thomas JC, Ralston J, Ivanova O. Electrokinetic properties of copper phthalocyanine pigment dispersions. Journal of Imaging Science and Technology. 2000;44(6):528-33.

[80] Mattei M, Kontogeorgis GM, Gani R. Modeling of the critical micelle concentration (CMC) of nonionic surfactants with an extended group-contribution method. Industrial & Engineering Chemistry Research. 2013;52(34):12236-46.

[81] Ruckenstein E, Nagarajan R. Aggregation of amphiphiles in nonaqueous media. The Journal of Physical Chemistry. 1980;84(11):1349-58.

[82] Shrestha LK, Sato T, Aramaki K. Phase behavior and self-organized structures of

diglycerol monolaurate in different nonpolar organic solvents. Langmuir. 2007;23(12):6606-13.

[83] Eicke H. Aggregation and micellization. Top Curr Chem. 1980;87:85-9.

[84] Ravey J, Buzier M, Picot C. Micellar structures of nonionic surfactants in apolar media. Journal of colloid and interface science. 1984;97(1):9-25.

[85] Shrestha LK, Kaneko M, Sato T, Acharya DP, Iwanaga T, Kunieda H. Phase behavior of diglycerol fatty acid esters− nonpolar oil systems. Langmuir. 2006;22(4):1449-54.

[86] Shrestha LK, Sato T, Acharya DP, Iwanaga T, Aramaki K, Kunieda H. Phase behavior of monoglycerol fatty acid esters in nonpolar oils: Reverse rodlike micelles at elevated temperatures. The Journal of Physical Chemistry B. 2006;110(25):12266-73.

[87] Eicke HF, Christen H. Is water critical to the formation of micelles in apolar media?? Helvetica Chimica Acta. 1978;61(6):2258-63.

[88] Alexandridis P, Andersson K. Reverse micelle formation and water solubilization by polyoxyalkylene block copolymers in organic solvent. The Journal of Physical Chemistry B. 1997;101(41):8103-11.

[89] Kawai T, Hamada K, Shindo N, Kon-No K. Formation of AOT reversed micelles and W/O microemulsions. Bulletin of the Chemical Society of Japan. 1992;65(10):2715-9.

[90] Giddings LD, Olesik SV. A study of AOT reverse micelles in liquids at ambient and high pressure. Langmuir. 1994;10(9):2877-83.

[91] Manoj KM, Jayakumar R, Rakshit S. Physicochemical studies on reverse micelles of sodium bis (2-ethylhexyl) sulfosuccinate at low water content. Langmuir. 1996;12(17):4068-72.

[92] Falcone RD, Correa NM, Biasutti MA, Silber JJ. Properties of AOT aqueous and nonaqueous microemulsions sensed by optical molecular probes. Langmuir. 2000;16(7):3070-6.

[93] Roberts GS, Sanchez R, Kemp R, Wood T, Bartlett P. Electrostatic charging of

nonpolar colloids by reverse micelles. Langmuir. 2008;24(13):6530-41.

[94] McNamee CE, Tsujii Y, Matsumoto M. Interaction forces between two silica surfaces in an apolar solvent containing an anionic surfactant. Langmuir. 2004;20(5):1791-8.

[95] Cao H, Cheng Y, Huang P, Qi M. Investigation of charging behavior of PS particles in nonpolar solvents. Nanotechnology. 2011;22(44):445709.

[96] Dukhin AS, Goetz PJ. How non-ionic “electrically neutral” surfactants enhance electrical conductivity and ion stability in non-polar liquids. Journal of Electroanalytical Chemistry. 2006;588(1):44-50.

[97] Patel MN, Smith Jr PG, Kim J, Milner TE, Johnston KP. Electrophoretic mobility of concentrated carbon black dispersions in a low-permittivity solvent by optical coherence tomography. Journal of colloid and interface science. 2010;345(2):194-9.

[98] Briscoe WH, Horn RG. Direct measurement of surface forces due to charging of solids immersed in a nonpolar liquid. Langmuir. 2002;18(10):3945-56.

[99] Mukherjee K, Moulik S, Mukherjee D. Langmuir1993, 9, 1727− 1730. Google Scholar There is no corresponding record for this reference.

[100] Eicke H-F. Surfactants in nonpolar solvents. Micelles. 1980:85-145.

[101] Eicke H-f, Shepherd JC, Steinemann A. Exchange of solubilized water and aqueous electrolyte solutions between micelles in apolar media. Journal of colloid and interface science. 1976;56(1):168-76.

[102] Rharbi Y, Winnik MA. Solute exchange between surfactant micelles by micelle fragmentation and fusion. Advances in colloid and interface science. 2001;89:25-46.

[103] Arrhenius S. Über die Dissociation der in Wasser gelösten Stoffe. Zeitschrift für physikalische Chemie. 1887;1(1):631-48.

[104] Brönsted JN. Einige bemerkungen über den begriff der säuren und basen. Recueil des Travaux Chimiques des Pays-Bas. 1923;42(8):718-28.

[105] Lowry T. The uniqueness of hydrogen. Journal of the Society of Chemical

Industry. 1923;42(3):43-7.

[106] Lewis GN. Valence and the Structure of Atoms and Molecules: Chemical Catalog Company, Incorporated; 1923.

[107] Berg JC. The importance of acid-base interactions in wetting, coating, adhesion and related phenomena. Nordic Pulp & Paper Research Journal. 1993;8(1):75-85.

[108] Sun C, Berg JC. A review of the different techniques for solid surface acid–base characterization. Advances in Colloid and Interface Science. 2003;105(1-3):151-75.

[109] Sposito G. Surface-reactions in natural aqueous colloidal systems. Chimia. 1989;43(6):169-76.

[110] Yukselen Y, Kaya A. Zeta potential of kaolinite in the presence of alkali, alkaline earth and hydrolyzable metal ions. Water, Air, and Soil Pollution. 2003;145(1):155-68.

[111] Yukselen-Aksoy Y, Kaya A. A study of factors affecting on the zeta potential of kaolinite and quartz powder. Environmental Earth Sciences. 2011;62(4):697-705.

[112] West LJ, Stewart DI, editors. Effect of zeta potential on soil electrokinesis. Geoenvironment 2000: Characterization, Containment, Remediation, and Performance in Environmental Geotechnics; 2000: ASce.

[113] Dwari R, Mishra B. Evaluation of flocculation characteristics of kaolinite dispersion system using guar gum: a green flocculant. International Journal of Mining Science and Technology. 2019;29(5):745-55.

[114] Pugh R, Fowkes F. The dispersibility and stability of coal particles in hydrocarbon media with a polyisobutene succinamide dispersing agent. Colloids and surfaces. 1984;11(3-4):423-7.

[115] Heavens S. Electrophoretic deposition as a processing route for ceramics. Noyes Publications, Advanced Ceramic Processing and Technology. 1990;1:255-83.

[116] Besra L, Liu M. A review on fundamentals and applications of electrophoretic deposition (EPD). Progress in materials science. 2007;52(1):1-61.

[117] Taylor SE. The electrodeposition of asphaltenes and implications for asphaltene

structure and stability in crude and residual oils. Fuel. 1998;77(8):821-8.

[118] Khvostichenko DS, Andersen SI. Electrodeposition of asphaltenes. 1. Preliminary studies on electrodeposition from oil− heptane mixtures. Energy & fuels. 2009;23(2):811-9.

[119] Krylova I. Painting by electrodeposition on the eve of the 21st century. Progress in Organic Coatings. 2001;42(3-4):119-31.

[120] Gurrappa I, Binder L. Electrodeposition of nanostructured coatings and their characterization—a review. Science and Technology of Advanced Materials. 2008.

[121] Hasegawa K, Kunugi S, Tatsumisago M, Minami T. Preparation of thick films by electrophoretic deposition using surface modified silica particles derived from sol-gel method. Journal of sol-gel science and technology. 1999;15(3):243-9.

[122] Du C, Heldbrant D, Pan N. Preparation and preliminary property study of carbon nanotubes films by electrophoretic deposition. Materials Letters. 2002;57(2):434-8.

[123] Shan W, Zhang Y, Yang W, Ke C, Gao Z, Ye Y, et al. Electrophoretic deposition of nanosized zeolites in non-aqueous medium and its application in fabricating thin zeolite membranes. Microporous and Mesoporous Materials. 2004;69(1-2):35-42.

[124] Yum J-h, Seo S-Y, Lee S, Sung Y-E. Y 3Al5 O 12: Ce0. 05 phosphor coatings on gallium nitride for white light emitting diodes. Journal of the Electrochemical Society. 2003;150(2):H47.

[125] Shane MJ, Talbot JB, Kinney BG, Sluzky E, Hesse K. Electrophoretic deposition of phosphors: II. Deposition experiments and analysis. Journal of colloid and interface science. 1994;165(2):334-40.

[126] Shane MJ, Talbot JB, Schreiber RD, Ross CL, Sluzky E, Hesse K. Electrophoretic deposition of phosphors: I. Conductivity and zeta potential measurements. Journal of colloid and interface science. 1994;165(2):325-33.

[127] Hayashi K, Furuya N. Preparation of gas diffusion electrodes by electrophoretic deposition. Journal of the Electrochemical Society. 2004;151(3):A354.

[128] Maiti HS, Datta S, Basu RN. High-Tc Superconductor Coating on Metal Substrates

by an Electrophoretic Technique. Journal of the American Ceramic Society. 1989;72(9):1733-5.

[129] Yau J, Sorrell C. High-Jc (Bi, Pb) 2Sr2Ca2Cu3O10+ x tapes fabricated by electrophoretic deposition. Physica C: Superconductivity and its applications. 1997;282:2563-4.

[130] Wei M, Ruys A, Milthorpe B, Sorrell C, Evans J. Electrophoretic deposition of hydroxyapatite coatings on metal substrates: a nanoparticulate dual-coating approach. Journal of Sol-Gel Science and Technology. 2001;21(1):39-48.

[131] Sridhar T, Mudali UK. Development of bioactive hydroxyapatite coatings on Type 316L stainless steel by electrophoretic deposition for orthopaedic applications. Transactions of the Indian Institute of Metals. 2003;56(3):221-30.

[132] Poortinga AT, Bos R, Busscher HJ. Controlled electrophoretic deposition of bacteria to surfaces for the design of biofilms. Biotechnology and bioengineering. 2000;67(1):117-20.

[133] Lovsky Y, Lewis A, Sukenik C, Grushka E. Atomic-force-controlled capillary electrophoretic nanoprinting of proteins. Analytical and bioanalytical chemistry. 2010;396(1):133-8.

[134] Boccaccini A, Keim S, Ma R, Li Y, Zhitomirsky I. Electrophoretic deposition of biomaterials. Journal of the Royal Society Interface. 2010;7(suppl_5):S581-S613.

[135] Jaiswal A, Smoukov S, Poggi M, Grzybowski B, editors. Quartz crystal microbalance with dissipation monitoring (QCM-D): real-time characterization of nano-scale interactions at surfaces. Proceedings of the 2008 NSTI Nanotechnology Conference and Trade, Bosten; 2008.

[136] Irwin E, Ho J, Kane S, Healy K. Analysis of interpenetrating polymer networks via quartz crystal microbalance with dissipation monitoring. Langmuir. 2005;21(12):5529-36.

[137] Olanya G, Iruthayaraj J, Poptoshev E, Makuska R, Vareikis A, Claesson PM. Adsorption characteristics of bottle-brush polymers on silica: Effect of side chain and charge density. Langmuir. 2008;24(10):5341-9.

[138] Nguyen TH, Elimelech M. Adsorption of plasmid DNA to a natural organic matter-

coated silica surface: kinetics, conformation, and reversibility. Langmuir. 2007;23(6):3273-9.

[139] Guzman E, Ortega F, Baghdadli N, Cazeneuve C, Luengo GS, Rubio RG. Adsorption of conditioning polymers on solid substrates with different charge density. ACS applied materials & interfaces. 2011;3(8):3181-8.

[140] Wayment-Steele HK, Johnson LE, Tian F, Dixon MC, Benz L, Johal MS. Monitoring N3 dye adsorption and desorption on TiO2 surfaces: a combined QCM-D and XPS study. ACS Applied Materials & Interfaces. 2014;6(12):9093-9.

[141] Abudu A, Goual L. Adsorption of crude oil on surfaces using quartz crystal microbalance with dissipation (QCM-D) under flow conditions. Energy & Fuels. 2009;23(3):1237-48.

[142] Xiang B, Truong NTV, Feng L, Bai T, Qi C, Liu Q. Study of the role of sodium citrate in bitumen liberation. Energy & Fuels. 2019;33(9):8271-8.

[143] Masliyah JH, Czarnecki J. Xu Z. Oil sands composition: bitumen, mineral solids, and inorganic ions. In: Handbook on theory and practice of bitumen recovery from Athabasca oil sands, volume I: theoretical basis. Kingsley Knowledge Pub; 2011. p. 177-96.

[144] Lin F, Stoyanov SR, Xu Y. Recent advances in nonaqueous extraction of bitumen from mineable oil sands: a review. Org Process Res Dev 2017; 21 (4): 492-510.

[145] Dixon DV, Stoyanov SR, Xu Y, Zeng H, Soares JB. Challenges in developing polymer flocculants to improve bitumen quality in non-aqueous extraction processes: an experimental study. Pet Sci 2020: 1-11.

[146] Graham R, Helstrom J, Mehlberg R. A solvent extraction process for tar sand. Eastern Oil Shale Symposium 1987: 93-9.

[147] Alquist HE, Ammerman AM. Process for extracting bitumen from tar sands. US Patent 4, 229, 281; 1980.

[148] Crittenden JC, Trussell R, Rhodes H, David W, Howe KJ, Tchobanoglous G. Stability of particles in water. In: MWH's water treatment – principles and design (3rd Edition). John Wiley Sons; 2012. p. 546-57.

[149] Lee J, Zhou ZL, Alas G, Behrens SH. Mechanisms of particle charging by surfactants in nonpolar dispersions. Langmuir 2015; 31 (44): 11989-99.

[150] Moritz R, Zardalidis G, Butt HJ, Wagner M, Mullen K, Floudas G. Ion size approaching the Bjerrum length in solvents of low polarity by dendritic encapsulation. Macromolecules 2014; 47 (1): 191-96.

[151] Ponto BS, Berg JC. Clay particle charging in apolar media. Applied Clay Sci 2018; 161: 76-81.

[152] Lee J, Zhou ZL, Behrens SH. Charging mechanism for polymer particles in nonpolar surfactant solutions: influence of polymer type and surface functionality. Langmuir 2016; 32 (19): 4827-36.

[153] Smith GN, Eastoe J. Controlling colloid charge in nonpolar liquids with surfactant. Phys Chem Chem Phys 2013; 15 (2): 424-439.

[154] Smith PG, Patel MN, Kim J, Milner TE, Johnston KP. Effect of surface hydrophilicity on charging mechanism of colloids in low-permittivity solvents. J Phys Chem C 2007; 111 (2): 840-8.

[155] Guo Q, Lee J, Singh V, Behrens SH. Surfactant mediated charging of polymer particles in a nonpolar liquid. J Colloid Interface Sci 2013; 392: 83-9.

[156] Gacek MM, Berg JC. Investigation of surfactant mediated acid-base charging of mineral oxide particles dispersed in apolar systems. Langmuir 2012; 28 (51): 17841-5.

[157] Wang S, Liu Q, Tan X, Xu C, Gray MR. Study of asphaltene adsorption on kaolinite by X-ray photoelectron spectroscopy and time-of-flight secondary ion mass spectroscopy. Energy Fuels 2013; 27 (5): 2465-73.

[158] Rosenholm JB. Evaluation of particle charging in non-aqueous suspensions. Adv Colloid Interface Sci 2018; 259: 21-43.

[159] Li X, Bai Y, Sui H, He L. Understanding desorption of oil fractions from mineral surfaces. Fuel. 2018 Nov 15; 232: 257-66.

[160] Adams JJ. Asphaltene adsorption, a literature review. Energy & Fuels. 2014 May 15; 28(5): 2831-56.

[161] Goual L, Horváth-Szabó G, Masliyah JH, Xu Z. Characterization of the charge carriers in bitumen. Energy Fuels. 2006; 20(5): 2099-108.

[162] Berkowitz N, Speight JG. The oil sands of Alberta. Fuel. 1975; 54(3):138-49.

[163] Wu J, Dabros T. Process for solvent extraction of bitumen from oil sand. Energy & fuels. 2012; 26(2):1002-8.

[164] Poovarodom S, Berg JC. Effect of particle and surfactant acid–base properties on charging of colloids in apolar media. Journal of colloid and interface science. 2010; 346(2):370-7.

[165] Ponto BS, Berg JC. Charging of Oxide Nanoparticles in Media of Intermediate Dielectric Constant. Langmuir. 2019; 35(47):15249-56.

[166] Ponto BS. Exploring new avenues of surfactant mediated particle charging in apolar media 2019.

[167] Zhang H, Tan X, Wang K, Liu Q. Electrodeposition of bitumen-, asphaltene-, or maltene-coated kaolinite from cyclohexane suspensions. Fuel. 2022; 311: 122582.

[168] Chen Q, Xu S, Liu Q, Masliyah J, Xu Z. QCM-D study of nanoparticle interactions. Advances in colloid and interface science. 2016; 233: 94-114.

[169] Tamiz Bakhtiari M, Harbottle D, Curran M, Ng S, Spence J, Siy R, et al. Role of caustic addition in bitumen–clay interactions. Energy & Fuels. 2015; 29(1):58-69.

[170] Bai T, Xiang B, Li M, Manica R, Liu Q. Mechanism of modification of bitumen zeta potential by sodium citrate: Interactions between bitumen metal content and ligands. Colloids and Surfaces A: Physicochemical and Engineering Aspects. 2022; 653: 130007.

[171] Pugh RJ, Matsunaga T, Fowkes FM. The dispersibility and stability of carbon black in media of low dielectric constant. 1. Electrostatic and steric contributions to colloidal stability. Colloids and Surfaces. 1983; 7(3):183-207.

[172] Pugh RJ, Fowkes FM. The dispersibility and stability of carbon black in media of low dielectric constant. 2. Sedimentation volume of concentrated dispersions, adsorption and surface calorimetry studies. Colloids and surfaces. 1984; 9(1):33-46.

[173] Gacek MM, Berg JC. The role of acid–base effects on particle charging in apolar media. Advances in colloid and interface science. 2015; 220: 108-23.

[174] Gacek MM, Berg JC. Investigation of surfactant mediated acid–base charging of mineral oxide particles dispersed in apolar systems. Langmuir. 2012; 28(51):17841-5.

[175] Gacek M, Bergsman D, Michor E, Berg JC. Effects of trace water on charging of silica particles dispersed in a nonpolar medium. Langmuir. 2012; 28(31):11633-8.

[176] Hsu MF, Dufresne ER, Weitz DA. Charge stabilization in nonpolar solvents. Langmuir. 2005; 21(11):4881-7.

[177] Teng F, Liu Q, Zeng H. In situ kinetic study of zinc sulfide activation using a quartz crystal microbalance with dissipation (QCM-D). Journal of colloid and interface science. 2012; 368(1):512-20.

[178] Ekholm P, Blomberg E, Claesson P, Auflem IH, Sjöblom J, Kornfeldt A. A quartz crystal microbalance study of the adsorption of asphaltenes and resins onto a hydrophilic surface. Journal of colloid and interface science. 2002; 247(2):342-50.

Appendix: Publication related to this thesis work*

A literature review has been published during the author's Ph.D. study, which provided much of the background information related to this thesis work. The following is a copy of the published paper.

Fine Solids Removal from Nonaqueous Extraction Bitumen: A Literature Review

Decreasing fine mineral solids content in bitumen product generated from nonaqueous extraction (NAE) of oil sands is an important requirement to ensure that the product quality meets the downstream process requirements. Two approaches may be used, one is to remove the fine solids from bitumen product after NAE extraction, and the other is to try to directly obtain low-solid-content bitumen during NAE extraction. The post NAE extraction clean-up methods include the use of polymers, antisolvents, water, surface functionalized magnetic particles with or without an electric field, a magnetic field, and a hydrothermal treatment. Methods that may be able to directly yield clean bitumen product during NAE extraction include the use of small amount of water or ionic liquid, or the use of wettability-switchable solvents. Directions for future research are proposed.

1 Introduction

Nonaqueous extraction (NAE) process to recover bitumen from the Alberta oil sands, which has been studied since the 1960s [1, 2], is an alternative to the commercial Clark hot water extraction (CHWE) process [3]. The CHWE process was patented by Karl Clark

* Zhang H, Tan X, Liu Q. Fine solids removal from non-aqueous extraction bitumen: A literature review. Fuel. 2021 Mar 15; 288: 119727

in the 1920s [4], and after years of laboratory and field tests, has been used in commercial bitumen extraction since 1960s. After decades of development, the CHEW process has been significantly improved and continues to be used today [5]. However, the CHWE process has an inherent issue that becomes increasingly problematic. The issue is that after recovering bitumen, the CHWE process generates a tailings stream containing sands and most of the fine clays together with a large quantity of process water and a small amount of residual bitumen. This tailings stream is extremely difficult to dewater, creating the two most pressing problems associated with the commercial hot water extraction process today: large tailings ponds, and high fresh water and energy consumption [6,7]. Large tailings ponds are required to contain the slow-settling tailings, posing serious long-term risks to migrating birds and ecological system [6-8]. Since the process water locked in the slow-settling tailings cannot be recycled, large amount of fresh river water needs to be heated to the required temperature of about 50ºC and used in the extraction, leading to high energy consumption and greenhouse gas emissions [9].

The process to extract bitumen from oil sands by nonaqueous solvents instead of hot water, i.e., the NAE process, holds the potential to overcome these problems. In an NAE process, schematically shown in **Fig. 1**, surface mined oil sands ore is crushed and mixed with a nonaqueous solvent to extract bitumen. After a follow-up solid-liquid separation, a solvent-diluted-bitumen stream and a dry stackable extraction tailings stream can be produced. No water is needed in this process, thus eliminating the inherent issue associated with the CHWE process.

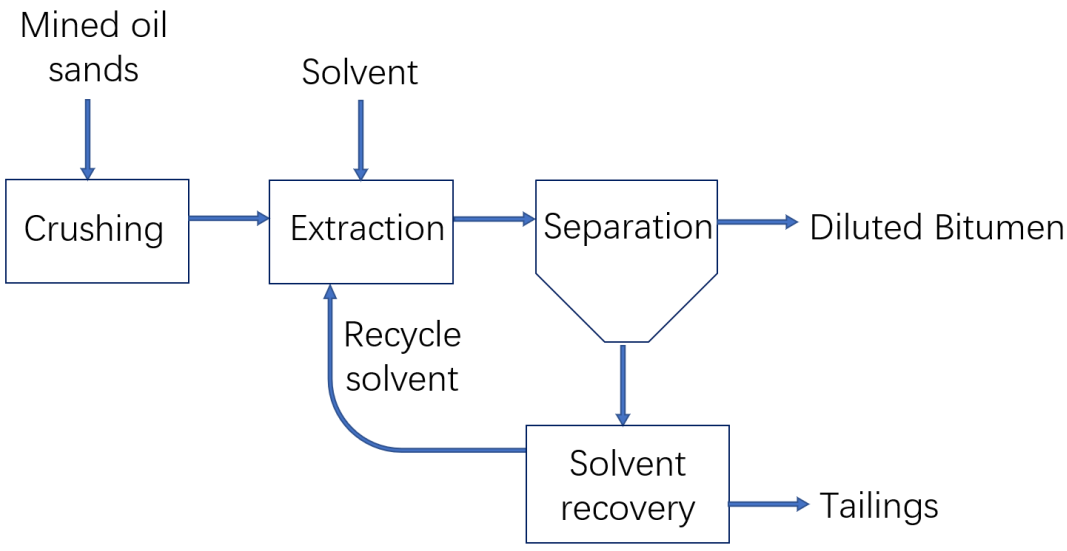

Fig. 1. Schematic flow diagram of a nonaqueous extraction (NAE) process.

Although the study on NAE of Alberta oil sands was initiated more than 50 years ago, it has been on and off in lockstep with changing political, economic and environmental climate of the industry, and has not gained serious traction. To this day, there has not been a commercial NAE process. While the non-technical factors are difficult to predict or control, the NAE process does have two technical challenges that need to be overcome before it can be seriously considered. One is the solvent recovery from the extraction tailings, and the other is the clean-up of the generated bitumen product so that it meets market specs regarding water and mineral solids content [10, 11].

For economic and environmental reasons, the solvent contained in the NAE tailings stream needs to be recovered and re-used. The solvent is most likely more valuable than bitumen so that its loss to the tailings is not desirable. Unrecovered solvent in the tailings also poses environmental hazard. Since there has not been a NAE plant, there is yet no regulation regarding solvent content in NAE tailings. If the regulations on the solvent concentrations in oil sands froth treatment tailings in the CHWE process can be used as a reference, then

it is specified that for every 1000 units of recovered bitumen, 4 units of solvent are allowed to be trapped in the tailings [12]. By this standard, assuming a medium grade ore that contains about 13 wt% bitumen, the maximum concentration of solvent in the extraction tailings cannot exceed 260 g/t, or 260 ppm. Solvent migration, diffusion, and evaporation from fines-dominated NAE extraction tailings that also contain residual bitumen are challenging scientific problems, so that although complete solvent recovery by a high temperature under vacuum is doable, how to make the process economical and less energy-intensive is a major challenge [13].

The solvent-diluted-bitumen product after the solid-liquid separation in an NAE process will unavoidably contain water (from oil sands connate water) and fine clay solids. Pipeline transport of the bitumen requires that it contains less than 0.5 wt% of water+solids combined. To sell the bitumen to a high conversion refinery, it needs to contain less than 0.03 wt% solids [10, 11]. If the mineral solids content is higher than 0.03 wt%, the bitumen needs to be cleaned/upgraded in an upgrader. The use of an upgrader would make the NAE process unattractive due to the high capital and operating costs of the upgrader as well as the high energy consumption and greenhouse gas emissions. In order to reduce the suspended mineral solids content of NAE bitumen product, many fine solids removal processes were studied based on the physical, chemical and physicochemical properties of the solvent-bitumen-fines system.

It is to be noted that the CHWE process generates a “bitumen froth” product that also needs to be cleaned to remove water and fine solids before transport and sale to market. There are currently two such bitumen froth treatment processes: the naphthenic froth treatment (NFT) process, and the paraffinic froth treatment (PFT) process. NFT is a process in which

naphtha is used to dilute the bitumen froth to lower its viscosity, followed by gravity and centrifugal separation to remove mineral solids and water from the bitumen froth. The final bitumen product of NFT typically contains about 0.5 wt% fine solids and 1-2 wt% water [14], therefore it does not meet market specs and needs to be upgraded. On the other hand, in PFT a paraffinic solvent such as hexane or pentane is used to dilute the bitumen froth and at the right solvent-to-bitumen (S/B) ratio, the paraffinic solvent triggers asphaltene precipitation, and the precipitated asphaltene agglomerates with fine solids and water and settles out from the diluted bitumen. As a result, the PFT process generates a much cleaner bitumen product that can be used directly as a high conversion refinery feed, but at a lower bitumen recovery due to the precipitation and removal of about 50% of the asphaltenes [14].

It will be seen in this review that some of the proposed or studied fine solids removal methods from NAE bitumen are similar to or based on methods that are used in NFT or PFT. In fact, the possible differences in the properties of the constituents in bitumen froth and NAE bitumen, and their effects on the clean-up process, remain obscure.

2 Mineral Particles in NAE Bitumen

Nikakhtari et al. [11] reported the mineralogical composition of the suspended fine solids after NAE extraction of an oil sands ore sample. The sample was a low-fines Alberta oil sands ore sample. The solvent used in the process was cyclohexane. The oil sands sample was mixed with the solvent for 10 min and then settled for 30 min. Afterwards, the sediment was treated by the solvent again. The coarse solids (larger than 45 μm) was removed by a 45 μm aperture sieve. The fine solids suspended in the product bitumen

solution (the undersize product from the sieve) was collected by centrifugation (4000 RCF, 1 h). **Table 1** shows the composition of collected centrifuge solids. As can be seen, the suspended fine solids were dominated by fine quartz, kaolinite, illite and feldspar.

Table 1. Composition of fine solids of NAE bitumen. Reproduced from reference [11] with permission from American Chemical Society.

Mineral	Weight % (normalized)
Nonclays	
Quartz	38.6
Potassium feldspar	8.0
Calcite	2.4
Dolomite	0.8
Siderite	3.2
Pyrite	0.7
Hematite	0.2
Anatase	0.2
Total nonclays	**54.1**
Clays	
Kaolinite (disordered)	27.2
Illite	16.8
Chlorite	1.8
Total clays	**45.9**
Total	**100.0**

Table 1 shows the mineralogical composition of the fine solids in NAE bitumen from a specific oil sands ore. In reality, the composition will be different depending on the source of crude ore (ore grade, fine solids content, water content of the ore), the extraction-separation equipment and specific operating parameters used in the operation, and the solvent used in the process [5, 7, 10, 11, 13, 15, 16]. Yet it has been widely accepted that the fine solids are mainly comprised of quartz, kaolinite and illite clays, with trace amount of siderite, pyrite, calcite and chlorite. In addition, the mixed layer swelling clays, such as illite-smectite and kaolinite-smectite, are also important even when present in low

quantities due to their unique properties such as high cation exchange capacity, high charge density and high specific surface areas [9, 11, 12, 17-19].

Although "fine solids" in oil sands industry generally refer to mineral solids with diameters less than 45 μm, the fine solids in NAE bitumen that are problematic to remove are usually much smaller than 45 μm. They normally have particle sizes ranging from 10 nm to 10 μm [9-11, 13]. These small sized particles in NAE bitumen are susceptible to Brownian motion [20]. Therefore, the fine particles can remain suspended indefinitely, or settle at undetectable low velocity in solvents. This is one of the reasons that the fine particles are difficult to remove from NAE bitumen.

A more important reason is that the fine mineral particles in NAE bitumen are mostly coated by organic matters (mainly asphaltenes) [21]. Much of the mineral particles in oil sands ore have been coated by organic matters before mining. During NAE process, the mineral particles are exposed to an organic solution containing dissolved bitumen components, and can adsorb these components to form a surface coating [22-24]. As a result, the solids are rendered hydrophobic which increases the possibility for them to remain stabilized in NAE bitumen product. In addition to surface hydrophobization, the coated organic layer can extend outward in good solvents of asphaltenes, leading to a steric repulsion which prevents particles from aggregating [25, 26]. Since the usual industrial solid-liquid separation methods such as filtration and centrifugation are only suitable for slurries with particle size larger than about 100 μm [18], and the organic coating keeps the particles dispersed in solvent-diluted-bitumen with sizes ranging from 10 nm to 10 μm, these methods are ineffective in removing the fine solids from the bitumen product unless the suspended fine solids can be destabilized to form aggregates, or other forces (e.g.,

electrostatic force or magnetic force) are applied to help the solid-liquid separation.

3 Fine Solids Removal Methods from NAE Bitumen Product

3.1 Polymer flocculation

A direct way to aggregate suspended fine solids is by adding polymer flocculants. The effects of polymers on the stability of a dispersion is schematically described in **Fig. 2** [27]. At low polymer concentration (lower than saturation adsorption), bridging flocculation is the main function of the polymer [27, 28]. Since most fine solid partilces in NAE bitumen are usually coated by bitumen components (mainly asphaltene), bridging heteroflocculation, i.e., particles that have been coated with organic matters that are flocculated together by another polymer [27], is an important form of bridging flocculation. At high concentration of the polymer flocculants, particle surface can reach saturation adsorption leading to steric repulsion in a good solvent [25-27]. In a poor solvent, if the sterically stabilizing coating layer is thin, the short-range van der Waals interaction between the particles may result in weak coagulation [26, 27]. In an aqueous suspension, strong coagulation may occur when an electrolyte is added to the system to cause particle surface charge neutralization [27, 29]. Finally, non-adsorbing polymers may lead to depletion flocculation at high concentration, both for bare particles and coated particles which are stabilized by steric repulsion [27, 30].

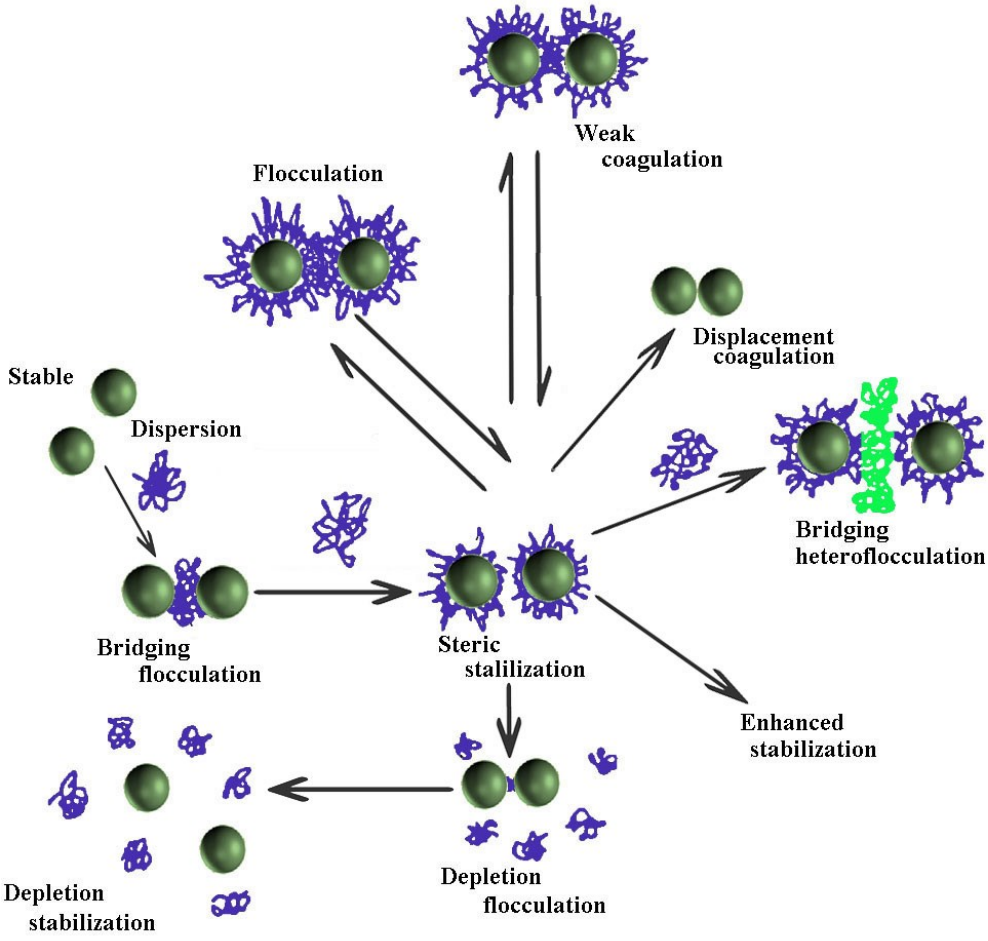

Fig. 2. Schematic of polymer's influences on the stability of disperse system.

Reproduced from reference [27] with permission from Elsevier.

Bridging flocculation and electrostatic effects are the main mechanism for polymer flocculation. During bridging flocculation process, the polymer adsorbs on the surface of a particle, the tail and loop of the adsorbed polymer extend into the solution and adsorb to other particle(s) [28]. There should be unoccupied sites on particles' surfaces in order to adsorb polymers attached to other particles. That is why low polymer concentration (thus low particle surface coverage) is required. Bridging flocculation promotes the formation of flocs that settle faster than the discrete particles. Electrostatic effects include charge

neutralization and electrostatic patching. Although electrostatic effects are prominent mainly in aqueous suspensions, they play a role in nonaqueous system as well [31]. Relevant details of electrostatic effects of polymer flocculation are available in Szilagyi et al.'s review [29], which will not be discussed here.

Polymer flocculants have been widely used to remove fine particles in wastewater treatment, pulp and paper industry [32]. In oil sands industry, they have been used in the treatment of fluid fine tailings (FFT) and mature fine tailings (MFT) [33]. Dixon et al. [34] reported their study about fine solids removal from NAE bitumen by polymer flocculants. They agreed with Mowla and Naderi [35] regarding the selection of polymer flocculants. The desired polymers should have a molecular weight greater than 10^6 g/mol, and soluble in oil (organic solvent) [34, 35]. Furthermore, the oil-soluble polymers should contain some polar end groups or blocks in order to adsorb to fine particles [34]. Ngnie et al. [36] took organic coated kaolinite and dry MFT as models of fine solids in bitumen product, and suspended them in cyclohexane. They reported that polyethylene glycol (PEG_{1000}) was able to aggregate the fine solids. Although the flocculation process did not reach the low solids content required by the industry, it was a good starting point of research on fine solids removal from NAE bitumen. NAE bitumen is a unique system, it is organic coated particles suspended in nonpolar medium. Future research could focus on the mechanism of formation of bridging flocculation/heteroflocculation between polymers and organic coated particles. In addition, more efficient, commercially availble, and environmentally friendly polymers should be sought.

3.2 Aggregation by antisolvent

Antisolvent here refers to a poor solvent of asphaltenes, which can precipitate asphaltenes from solution. Asphaltene is the largest, densest, and most polar component in bitumen [37]. Its concentration in heavy crude varies from source to source and is up to 19 wt% in Canadian oil sands bitumen [38]. Many studies have shown that asphaltene is stabilized by resin, which is thought to bind to asphaltene by van der Waals interaction. Asphaltenes therefore stabilize in oil in the form of an emulsion or dispersion rather than a true solution [38-41], even in a good solvent such as toluene. This form of asphaltene is capable of stabilizing suspended fine solids. When an antisolvent (poor solvent of asphaltenes) is added, bonds between asphaltene and resin will break and the polyaromatic clusters in asphaltene molecules tend to bind together via π-π interaction and therefore form "network" structured aggregates* [38, 42, 43]. This process can trap and collect fine solids, which are removed together with the precipitated and aggregated asphaltenes [12, 38, 44]. The suspended fine solids particles can also function as nuclei for asphaltene precipitation when an antisolvent is added. In this case, the asphaltenes adsorb on the surface of the particles that act as nucleation centres [45, 46]. This will enhance mineral solids removal by increasing the particle size [47] and forming bonding bridges between particles, resulting in the formation of large asphaltene-solid flocs [48]. In addition, when asphaltene is precipitated by antisolvent from diluted bitumen, the viscosity of the solution will decrease. This can cause an increase in the settling velocity of fine solids, which is helpful for fine solids removal [47].

The precipitation and aggregation of asphaltenes by an antisolvent is used in one of the

* The resins also dissolve in a good solvent such as toluene. But the strong solvating effect of toluene to asphaltenes would keep the asphaltenes dispersed.

two methods, called paraffinic froth treatment (PFT), in the treatment of bitumen froth generated by the CHWE process to remove water and fine solids from the bitumen froth [49]. PFT performances well in froth treatment and can result in virtually solids free bitumen product [50]. However, the disadvantage of lower bitumen recovery caused by the precipitation of asphaltene is an unavoidable issue of PFT. Graham et al. [15] used a similar process to remove fine solids from NAE extracted bitumen. Pentane was used to precipitate asphaltenes and remove fine solids from heptane extracted bitumen. Unfortunately, this process failed to meet the ideal requirement for fine solids content of the bitumen product. In addition, using one solvent for bitumen extraction while another for fine solids removal would bring complication for industrial application.

Subsequent studies analyzed related process parameters in order to improve the fine solids removal performance. The influence of carbon number of solvents, S/B ratio, mixing temperature, and mixing speed were discussed. The selected antisolvents were mainly aliphatic hydrocarbons alone or in combination, such as pentane, hexane, heptane or their mixture at S/B ratio higher than a certain value depending on the type of solvent and operating conditions. It was found that a light alkane performed better on the settling of suspended fine solids than a heavier alkane at the same S/B ratio [14, 49, 51]. Usually the bitumen solution in light alkane had a relatively low density and viscosity, which could improve settling performance. However, the comparison between experimental results of settling rate and the calculated effects of medium density and viscosity indicated that the density and viscosity were not the main driving force for sedimentation in this case. The lighter alkane precipitated more asphaltenes, and more asphaltene precipitation always led to better fine solids removal performance [51]. The influence of S/B ratio also showed

similar peculiarity in that higher S/B ratio led to more asphaltene precipitation, which resulted in better fine solids removal performance [49, 51, 52]. More precipitated asphaltenes seemed to cause the aggregates to settle more quickly, while the reason behind was still unclear. Based on the Stokes law, the settling rate of aggregates formed by precipitated asphaltenes and fine solids in diluted bitumen, a laminar flow regime, can be evaluated according to eq. (1) [51]:

$$u_0 = \frac{g\Delta\rho D^2}{18\eta} \quad (1)$$

where g is the gravitational constant, $\Delta\rho$ the effective density difference between the aggregates and medium, D the diameter of the aggregates, and η the viscosity of medium. More asphaltene precipitation was likely to result in changes in aggregates structure, increasing their size and density. This point was proven by relevant studies [51, 53]. Further studies investigated the influence of solvent-diluted bitumen mixing temperature and mixing speed (energy input) on settling. The influence of temperature on the precipitation amount of asphaltene was not obvious, but a high mixing temperature caused the formation of large aggregates, thus increasing the sedimentation efficiency [54]. Unlike the influence of mixing temperature, mixing energy could not enlarge aggregates size. In contrast, the aggregate size would become smaller at higher mixing energy input, although high energy input could significantly increase the density of the asphaltene aggregates, which was helpful for fine solids removal [55].

Many developments have been achieved on fine particles removal from diluted bitumen by the controlled use of antisolvent, albeit mostly in the bitumen froth treatment area rather

than NAE bitumen. However, there are still the needs for further study. While precipitated asphaltenes can form a network structure and collect fine particles from NAE bitumen, which sub-fraction of asphaltenes works for this process is unclear. Exploring the function of sub-fractions of asphaltenes on this process separately should be an interesting direction for future research. On the technological side, relevant parameters like carbon number of solvents, S/B ratio, mixing temperature and energy input have been investigated, but these findings are not enough to achieve the purpose of removing the fine solids without losing too much bitumen due to asphaltene precipitation. Adding process aids to precipitate asphaltene together with the antisolvent is also likely to improve the fine solids removal performance. The use of suitable process aids may also reduce the dosage of antisolvent required for asphaltene precipitation, and remove all fine mineral solids without the need to precipitate all asphaltenes, thus lowering bitumen loss. These process aids could be a polymer, an inorganic additive, or CO_2 gas to enhance aggregation of fine particles. Using oil-soluble polymers could be considered as a combination of antisolvent with polymer flocculation, discussed in previous section. Inorganic additives such as NaOH would be a choice with reference to the bitumen froth treatment process [56]. CO_2 is known to promote asphaltene precipitation in enhanced oil recovery (EOR) processes, which may be useful in combination with an antisolvent for fine solids removal process [57-59].

3.3 Agglomeration by water-in-oil emulsion droplets

This is a process of using water droplets with dissolved additives to remove fine particles from NAE bitumen product. When water is added to the solvent diluted bitumen suspension, it will disperse into water droplets under agitation. The water droplets can collect the fine particles and form large aggregates that are easier to settle. A schematic

description of the collection of fine solids particles by water droplets is shown in **Fig. 3**. Hydrophilic particles may be absorbed into the water droplets by penetration through the solvent-water interface [60], while amphiphilic particles tend to remain at the solvent-water interface [44]. If the water droplet contains a dissolved surfactant, the hydrocarbon tail of the surfactant will extend into the solvent. The suspended hydrophobic particles (e.g. particles coated by bitumen component) could be collected by the hydrocarbon tail of surfactant molecules and thus remain at the solvent-water interface [61]. Another approach for enhancing the collection of hydrophobic particles is to modify their surface and make it hydrophilic before the addition of water droplets [62].

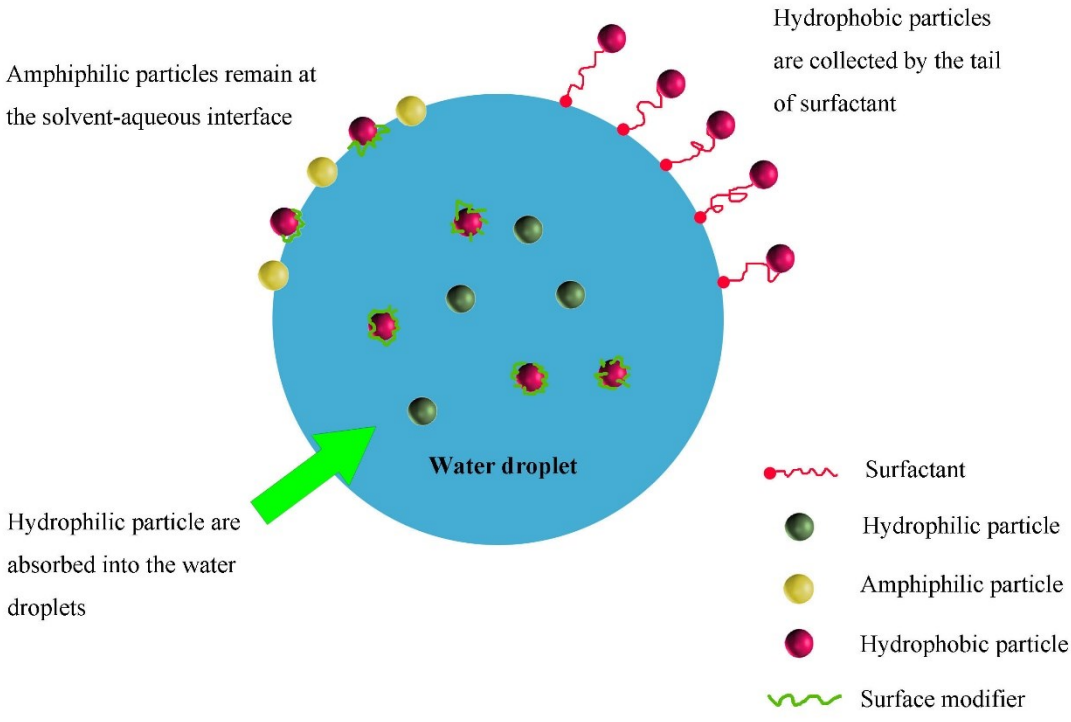

Fig. 3. Schematic diagram of how a water droplet traps fine particles.

Alquist et al. were awarded a patent for a bitumen extraction process from oil sands using organic solvents in 1978 [61], in which the fine solids suspended in diluted bitumen were

removed by added water containing a cationic surfactant. Their process is schematically shown in **Fig. 4** [61]. As can be seen, crushed oil sands ore and organic solvent (toluene and xylene were preferred in this patent) were mixed and transported to settling zone, where the mixture was separated into a coarse particle phase and a diluted bitumen phase containing fine solid particles. The coarse particle phase was removed, and the diluted bitumen phase was collected for next step of treatment where the fine particles were removed by mixing with water containing a cationic surfactant. The mixture was fully agitated and then transferred to the settler, where the mixture was separated into three phases, an aqueous phase at the bottom, a diluted bitumen phase at the top, and the fine particles concentrated between these two layers. Water was collected for recycle, the fine particles were withdrawn for disposal or further treatment, and the diluted bitumen would be pumped to recover solvent. This patent also described the appropriate concentration of the cationic surfactant and the recommended operating temperature. Under the optimal conditions, the solids content in final bitumen product was reduced to about 0.2 wt%.

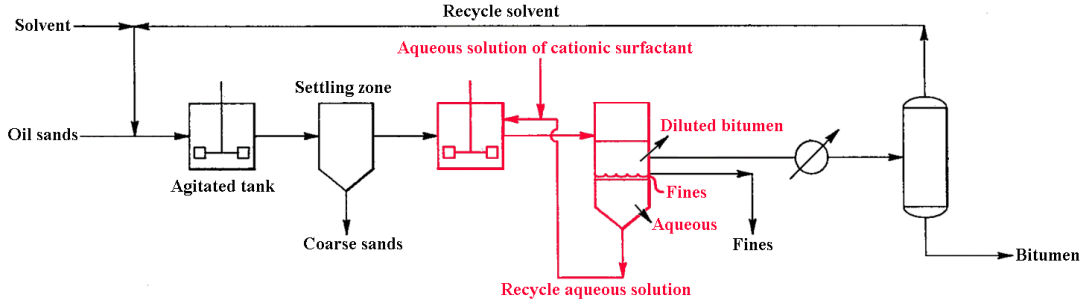

Fig. 4. Flowsheet of a NAE process and fine solids removal from NAE bitumen by aqueous solution of cationic surfactant, patented by Alquist et al. [61]. The diagrams and texts shown in red is the fine solids removal process.

However, Farnand et al. [44] suggested that surfactant usually led to the formation of stable

water-in-oil emulsions which were detrimental to the separation of fine solids particles. In contrast, water-soluble organic compounds with low molecular weight, such as resorcinol, formic acid, catechol, and chloral hydrate, can modify the surface wettability of the bitumen-coated particles suspended in diluted bitumen, making these particles amenable for collection by water droplets which can then be readily separated. It should be noted that Alquist's patent [61] also mentioned that the surfactant should be carefully selected. Nonionic and anionic surfactant were not effective for removing the fine solids from diluted bitumen [61, 63]. On this point, there seemed to be no contradiction between Alquist et al.'s patent and Farnand et al.'s approaches. The water-soluble low molecular weight organic compounds performed well in assisting water droplets to collect fine particles, but the concentrations of these compounds needed to be extremely high (>50 wt%) in the aqueous solution in order to achieve satisfactory degree of fine solids removal. Farnand et al.'s work also proposed a combination technique of using the water-soluble additive and antisolvent, which showed a dramatic improvement in settling rate of the fine solids at much lower reagent dosages. The solids content in bitumen product was decreased to 0.1 wt% [44]. However, such a process would require a two-solvent system as the authors used naphtha in the NAE process and an antisolvent in the fine solids removal process. Liu et al. [62] explored this method and put forward a two-stage agglomeration process to separate bitumen-coated fine particles from cyclohexane by modifying the particle's surface using the amphiphilic polymer poly(ethylene glycol)-block-poly(propylene glycol)-block-poly(ethylene glycol), i.e., PEG-PPG-PEG, and then adding small amount of water to collect the surface modified particles to form large aggregates. The tow-stage method required small amount of the amphiphilic polymer and performed

better than one-stage addition of only the polymer or only water. The solids content in bitumen product of this two-stage method could be lowered to 0.01 wt% under laboratory conditions for a very dilute cyclohexane solution of bitumen. Malladi [60] studied the influence of velocity and size of the collector (water) droplets on particle capture efficiency using a microfluidic aspiration device. Although the particles used in the research, hollow glass beads, were different from bitumen-coated particles, the results provided reference for an understanding of influencing factors on the performance of the water droplets collection process.

There are many factors that affect the performance of this process. For example, the degree of mixing, the operating temperature, water chemistry (surfactant/polymer/salt concentrations and pH), drop and suspending fluid viscosities, and the interfacial tension between the water drop and the suspending phase. They all worth further investigation. There is also the opportunity to combine the uses of antisolvent and water droplets with water-soluble additives to remove the fine solids from NAE bitumen.

3.4 Filtration in an electric field

Electrostatic interaction has long been used to separate fine particles from a fluid phase. Experiments using electric field to remove suspended particles from air were reported as early as 1800s [64, 65]. The electrostatic filtration process using glass bead bed to remove fine particles from oil medium was described in a recent patent by Fritsche et al. [66]. The glass beads were packed into a hollow container where electric field was applied by a pair of electrodes, with one electrode located in the center while the counter electrode surrounded the shell of the container. During the separation process, the potential

difference between the electrodes can be maintained across the glass beads bed and/or the separation volume, which can lead to a spatially varying electric field because of the dielectric character of the glass beads [67]. When oil flew through this electric field, the dispersed fine particles, which were assumed charged [68, 69], would be retained by the glass beads and removed from oil.

Cullinane et al. [70] received a patent about removing fine particle form NAE bitumen using electrostatic filtration in 2017. The process was similar to Fritsche's work [66] and it introduced the separation and filter media regeneration process as depicted in **Fig. 5** [70]. The raw material, bitumen product of NAE process, was passed through a coarse filter. The filtrate from the filter was then pumped to an electrostatic separator where the fine sands in the bitumen could be adsorbed by the glass beads in the separator. Afterwards, the clean bitumen with 0.1 wt% fine solids content was sent for solvent recovery. Heat exchangers were used to control the temperature during the process. When the filter media reached its maximum capacity, the applied voltage was turned off and the filter media were flushed with solvent. Inert fluid (such as nitrogen) could be used to purge the residue from the electrostatic separator between filtration and wash cycles in order to avoid product and solvent loss.

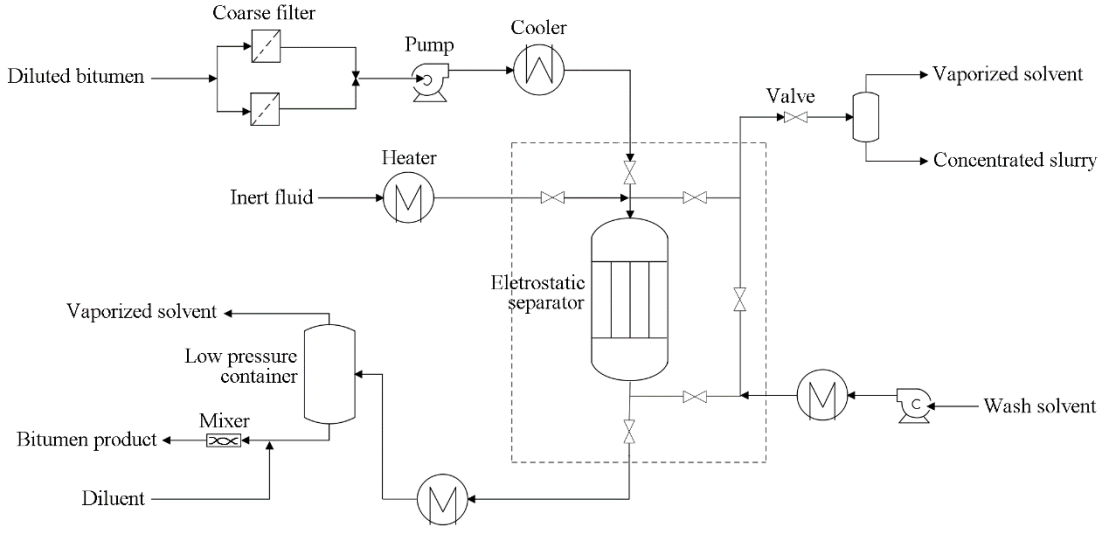

Fig. 5. Flowsheet of fine solids removal process from NAE bitumen by electrostatic filtration patented by Cullinane et al. [70].

Using electrostatic filtration to remove fine solids from NAE bitumen is a novel concept, although the process has been successfully applied in other systems. To make the electrostatic filtration cleaning of NAE bitumen feasible, future research can focus on the relevant properties of the components in the system, for example, to reveal why and how fine mineral particles acquire charges in NAE process, to understand the influence of applied electric field on particles in NAE bitumen, both for motion and electrification, and to find out ways to increase the particle charges in NAE bitumen in order to improve the fine solids removal performance.

3.5 Filtration after hydrothermal treatment

Removing fine solids from bitumen by filtration after hydrothermal treatment has been tested on bitumen froth samples from CHWE process [71]. Although there is not yet any report of this method on the treatment of NAE bitumen, the sufficient similarity between

these two systems makes it reasonable to discuss this method here. In this process, hydrothermal treatment at a moderate temperature and pressure is required to make bitumen amenable to filtration [72, 73]. At high temperature and pressure, many properties of water change significantly compared with at ambient conditions. For example, the dielectric constant of water at ambient conditions is about 80 while this number becomes about 5 at water's critical point (T_c = 374℃, P_c = 22.1 MPa) [74], which means that the high temperature and pressure can increase water's dissolution ability for nonpolar organic compounds. In addition, water has higher concentrations of H^+ and OH^- at high temperature and pressure than at ambient conditions [75]. This can promote chemical reactions in water like hydrolysis and hydration. These favorable properties of water at high temperature and pressure make hydrothermal technology useful in the treatment of hydrocarbon resources such as coal [76], heavy oil [77], oil shale [78] and oil sands bitumen [71]. In the application of treating bitumen froth, hydrothermal treatment made the wettability of fine particles in bitumen froth more uniform, which was shown to improve the filterability of the fine particles [73].

Chen et al. [71] used the combination of hydrothermal treatment and hot filtration to treat bitumen froth. As shown in **Fig. 6** [71], bitumen froth was treated in an autoclave. After the treatment, the vapors were vented off and separated into gas and water. Fine particles in the remaining bitumen solution were removed by hot filtration. During their research, the temperature and pressure of hydrothermal treatment were 300-420℃ and 8.6-19.3 MPa, respectively. The vapors were vented out from the hydrothermal reactor at 270℃ and the hot filtration was performed at 200℃. It was found that this combination process was feasible to remove fine particles from bitumen froth. The solids content in the bitumen

product was lowered to 0.08 wt%.

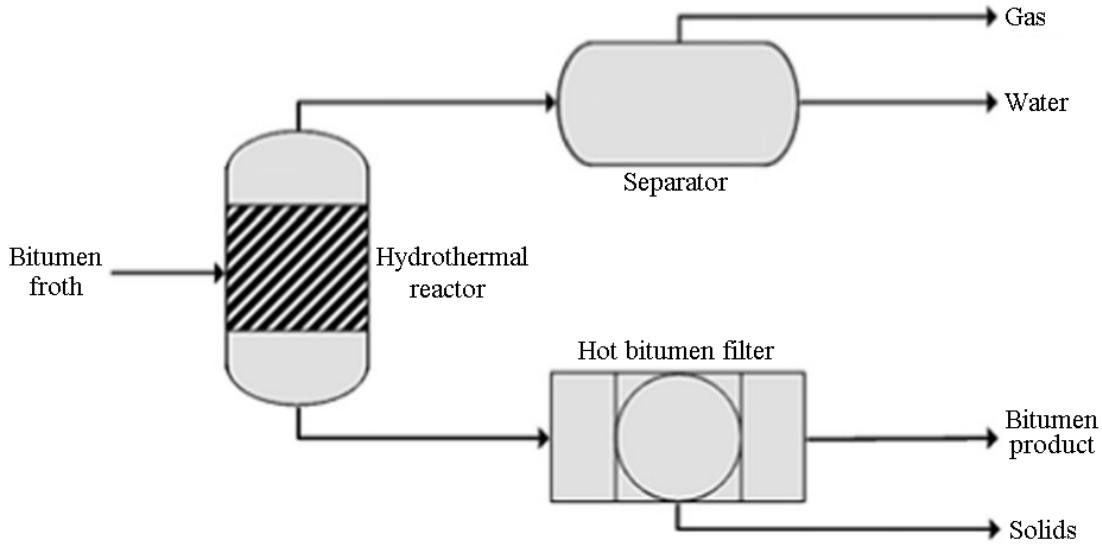

Fig. 6. Schematics of the combination of hydrothermal treatment and hot filtration of bitumen froth. Reproduced from reference [71] with permission from Elsevier.

As mentioned earlier, the fine particles removal from NAE bitumen has a lot of similarities with bitumen froth treatment from both system composition and the fundamental sciences that it entails. Therefore, filtration after hydrothermal treatment is also a promising method to remove fine particles from NAE bitumen, but it is worth noting that usually NAE bitumen contains less water than bitumen froth product of CHWE, which means the hydrothermal treatment for NAE bitumen may require the addition of water. Similar methods such as direct thermal treatment, and thermal treatment with (supercritical) carbon dioxide are also worth investigating.

3.6 Collecting fine solids by surface functionalized particles

Surface functionalized particles are the particles coated by polymers or chemicals with specific functional groups. When the surface properties of the particles are suitably

modified, these surface functionalized particles can collect the fine solids suspended in bitumen solution due to the attractive interactions between the surface functionalized particles and the suspended fine solids. As the fine solids particles are now piggy-backed on the larger functionalized particles, they can be removed together by filtration, gravitational settling, centrifugation, magnetic separator (if the functionalized particles are magnetic), or skimming (if the density of the particles is lower than the liquid).

Berg et al. [79] first used surface functionalized particles to remove fine solids from oil sands tailings generated from the CHWE process. The fine particles that were difficult to separate from the tailings were coated by bitumen components and had a very small size, similar to the fine solids in NAE bitumen. Therefore, this method was a valuable reference for fine solids removal from NAE bitumen. In the patent, Berg et al. suggested that the particles suitable for modification can include organic (such as starch, modified starch, solid or hollow polymeric spheres and the like) or inorganic particles (such as kaolin, silica and sand recovered from the bitumen extraction process itself), or their mixtures. The size of the particles can range from nanometers to few hundred microns, and the density of the particles can be larger than the fluids or less than the fluids. The surface modifier should contain at least one amine functional group. Lupamin, chitosan, branched polyethyleneimine (BPEI), and poly diallyldimethylammonium chloride (PDAC) were some recommended options. In addition, an activation treatment of the fine particles in oil sands tailings was needed. The “activation” step was to treat the suspended fine solids in the tailings by an activating material, such as flocculants or other polymeric substances, to promote the attractive interactions between the surface functionalized particles and the suspended fine solids. In the fine solids removal practice of this patent, an oil sands tailings

sample (containing 7 wt% solids) was first activated by Magnafloc LT30, then mixed with the surface functionalized particles, which were sea sands coated by PDAC. After agitation, the solids were removed by filtration and the fine solids content of the liquid product was reduced to less than 1 wt%. The patented process was similar to a flocculation process, except that larger pre-treated particles were used to aggregate the fine solids in the tailings, making the subsequent filtration more effective.

When taking this method to treat NAE bitumen, it should be noted that the main component of continuous phase of oil sands tailings is water, while the medium of NAE bitumen is an organic solvent. The operating conditions should be adjusted according to the properties of the media. In addition, future research can also consider using surface functionalized magnetic particles to collect and remove fine solids from NAE bitumen product. External magnetic field can be applied when magnetic particles are introduced. Removing suspended particles by external magnetic field is more selective, efficient, and often much faster than centrifugation or filtration [80, 81]. This technology has been widely used as a value recovery and pollutant removal process in many environmental, biomedical and industrial applications, such as the recovery of magnetic minerals, remediation of ground water contamination, removal of yeast from process streams, purification of drinking water [82]. It is also widely used in the extraction of coronavirus RNA for subsequent identification and analysis. It is reasonable that this method would be promising for removing fine particles from NAE bitumen.

The fine solids removal methods discussed above are additional process steps that need to be appended to a NAE process. These methods are suitable for the solvent-alone extraction (SAE) process, which is a traditional NAE process that use organic solvent or solvent

mixture alone to extract bitumen from oil sands. If NAE process can be modified to obtain the product with low fine solids content directly, the additional fine solids removal process step may be avoided to reduce costs and process complexity. These modified NAE processes are discussed below.

4 Fine Solids Removal by Modified NAE Processes

4.1 Solvent extraction spherical agglomeration

Solvent extraction spherical agglomeration (SESA) process is one of the common modified NAE processes. It uses a solvent to extract bitumen followed by agglomeration of the fine particles in order to improve solid-liquid separation performance [83, 84]. In the SESA process, bitumen is extracted by a nonaqueous solvent, a second liquid, which is immiscible with the nonaqueous solvent and which can displace the organic solvent from the surface of suspended fine particles is added to treat the fine particles [17]. Water meets both requirements and has the advantages of low cost and no pollution, and is therefore the best choice of the second liquid. It is worth noting that SESA process is different from aqueous-nonaqueous hybrid extraction process, which consumes a large amount of water [85]. The aqueous-nonaqueous hybrid extraction process is not technically a NAE process, it cannot reduce fresh water consumption and save energy usage [86]. Therefore, the detail of aqueous-nonaqueous hybrid extraction process will be not discussed in this review.

The reason why SESA process perform well in fine solids removal is when the small amount of water is added in the extraction process, the resulting oil-water interface network can trap fine particles and the water droplets can form liquid bridge between the

suspended fine particles during agitation [17]. The effectiveness of fine solids collection is influenced by the wettability of the fine solids, which can be adjusted by the wetting agent addition. The trapped fine particles and water droplets can form loose three-dimensional structures which will collapse and become dense solid-water spherical agglomerates by strong capillary forces [12]. The spherical agglomerates can further grow by the coalescence of individual agglomerates and the adsorption of fine particles on the surfaces of agglomerates, further reducing the difficulty of solids removal. Therefore, SESA has the advantages in fine solids removal and is especially suitable for treating oil sands with high fine solids content [17, 87].

Sparks et al. [88] described a SESA process of oil sands extraction. As shown in **Fig. 7** [88], the crushed oil sands ore sample was fed into the extractor, where it was mixed with a small amount of water and recycled dilute bitumen solution. The fine particles that were suspended in the oil sands agglomerated under the action of the small amount of water in the extractor. Then the agglomerated solids were removed via solid-liquid separation. Afterwards, the solvent was recovered from both liquid phase and solid phase and reused to the extraction process. According to Sparks et al., naphtha fractions from bitumen upgrading was the suitable solvent for bitumen extraction. The amount of solvent should make the content of the oil sands ore sample in mixture in the range of 40 to 60 wt%, i.e., that the mass ratio of solvent to oil sands ore is around 1:1. The mass ratio of the added water and solids was selected in the range of 0.08 to 0.15, and the desirable pH of the added water was about 8 to 10. The fine solids can form removable agglomerates with the size of about 0.1 mm to 2 mm during the extraction. After extraction, the solids content, based on the extracted bitumen in solution, was less than 2 wt%. The solids content in the

product was lower than that of SAE product, but still far from meeting the requirement of less than 0.03 wt%. Reports showed that the agglomeration occurring in SESA process benefited solid-liquid separation, which increased bitumen recovery together with a decrease in the fine solids content in bitumen product [17, 86, 89, 90]. However, most reported work mainly focused on bitumen recovery. The factors that influenced bitumen recovery have been analyzed by many reports. The feedstock properties and operating parameter which influence solids content in bitumen product worth further investigation in future research.

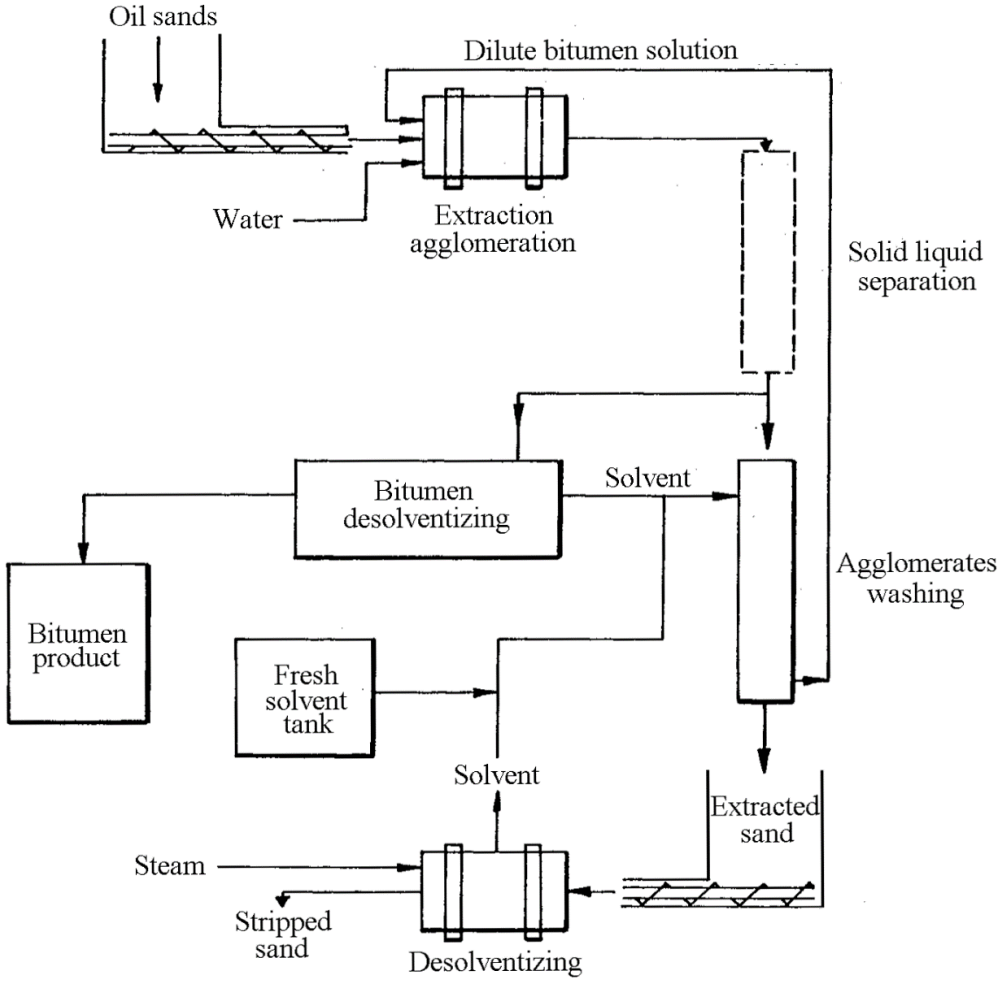

Fig. 7. Flowsheet of a SESA process patented by Sparks et al. [88].

4.2 Ionic liquid assisted solvent extraction

Ionic liquid (IL) is usually defined as materials that are composed of cations and anions which melt at or below 100℃ (ionic liquids exist at other temperatures as well but the ILs with low melt points are preferred in industrial applications) [91]. The IL was initially observed by Paul Walden as early as 1914 [91]. However, using IL to help bitumen extraction from oil sands, i.e., the ionic liquid assisted solvent extraction (ILASE) process, was initially developed by Painter et al. and published in 2010 [92]. As depicted in **Fig. 8**, the ILASE process entails mixing the crushed oil sands ore with IL and organic solvent. Under the assistance of IL, bitumen is extracted by solvent and the mixture is separated into three layers: bitumen-solvent layer at the top, IL layer in the middle, and solids-IL layer at the bottom. The top layer is separated as the bitumen product. The middle layer is used as the recycled IL. The bottom layer is collected to separate the solids and IL by the addition of water. IL usually has a high viscosity and therefore the solids are difficult to separate from IL [86]. The viscosity can be significantly decreased when the IL is dissolved in water, leading to an easy separation of solids and IL. Water and IL can be separated by evaporation because the vapor pressure of IL is almost zero [91, 93] and both the water and IL can be recycled.

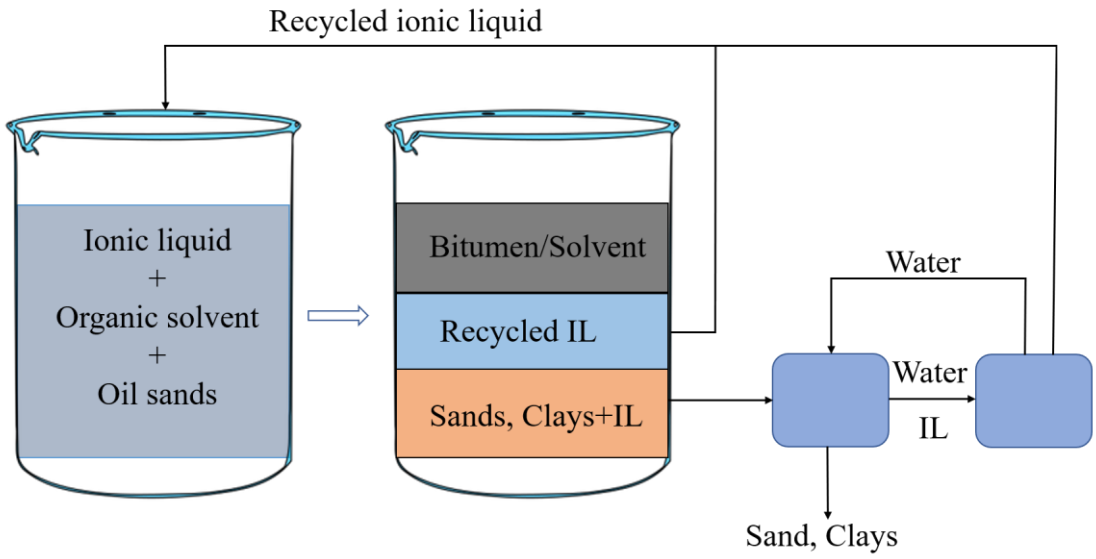

Fig. 8. Schematic plot of an ILASE process.

Regarding the mechanism behind the function of IL on improving bitumen extraction efficiency of organic solvent, several researchers investigated the nature of interactions between ILs and the components (both organic and inorganic) of oil sands [94-96]. Liu et al. [94] suggested that electrostatic forces played very important role. IL had strong electrostatic interactions with the surface of mineral particles in oil sands and thus was able to assist in the release of bitumen from mineral surface [92]. Hogshead et al. [97] measured the interaction forces between silica and bitumen suspended either in 1-butyl-2,3-dimethyl-imidazolium tetrafluoroborate ([bmmim][BF_4], an IL) or in water. Their results showed that under ambient temperature, the interaction forces between silica and bitumen surface were almost an order of magnitude weaker in IL than in aqueous medium. Li et al. [98] analyzed surface interactions between bitumen fractions (saturates, aromatics, resins, asphaltenes), organic solvent, IL, and silica by the COSMOtherm software which is based on surface free energy and oil fraction solubility. It was found that the surface free energy at IL-organic solvent interface was much lower than at IL-bitumen fractions

interface. Further calculations also suggested that IL had a stronger interaction with the silica surface than with oil fractions. Therefore, IL improved the bitumen extraction performance by promoting the transfer of bitumen from mineral surface to solvent phase.

Painter's group took toluene as organic solvent, [bmmim][BF_4] and the like as ILs, and studied bitumen extraction from Alberta and Utah oil sands [92, 99, 100]. Together with a good recovery of bitumen, according to the reports, no detectable quantities of fine solids were found in bitumen products in most experiments. Only when extracting Utah oil sands, small amounts of carbonates were found in the bitumen product at extended extraction time although the bitumen produced at initial stage were solids free.

Despite the excellent performance on bitumen extraction, there were some disadvantages of using IL in bitumen extraction which limited its extensive application. The major issues were (i) the selected ILs had a high viscosity, which would make them adhere onto the inner wall of pipelines, leading to the difficulty of transport and also to increased IL loss, and (ii) high cost and environmental issues caused by the selected ILs and organic solvent (toluene). In consideration of the first issue, Li et al. [101] used IL with low viscosity, 1-ethyl-3-methyl imidazolium tetrafluoroborate ([Emim][BF_4]), to extract bitumen from Alberta oil sands. Toluene, acetone, or n-heptane were used as solvents in their research. It seemed that [Emim][BF_4] was not as good as [bmmim][BF_4] when it comes to the performance of reducing solids content in bitumen product. A small amount of mineral solids was found in the bitumen product, and toluene performed the best among the organic solvents tested in their research. Regarding the environmental impact, IL has historically been considered as "green solvent" since it has zero vapor pressure, and hence cannot be distilled [91] (note: later research proved that the vapor pressure of IL was not absolutely

zero, that it was difficult to evaporate but still could be distilled [93]). Having almost zero vapor pressure means that IL has low risk of air pollution. However, the potential toxicity and inaccessible biodegradability of IL may lead to water contamination if released to aquatic environments [102]. Therefore, “green solvent” must meet different criteria such as biodegradability, non-toxicity, and recyclability.

A new family of ILs, called deep eutectic solvent (DES), was discovered in the last two decades. It usually consists of two or three environmentally friendly components which can associate with each other via hydrogen bonds and form a eutectic mixture. Unlike conventional IL, the DES is relatively cheap, non-toxic and easy to degrade [103, 104]. Pulati et al. [105] reported the use of DES to extract bitumen from oil sands. Naphtha was used as the organic solvent. Their result showed that only 0.5 wt% mineral fine solids were found in the bitumen product. It performed much better than SAE process but still not enough to meet the requirement of downstream process. In addition, similar to most of the ILs, DESs also have a high viscosity [103], which may bring issues for the process as discussed above.

Therefore, although different types of ILs showed good performance, further research is needed to find the ILs that meet the requirements of low viscosity, environmental acceptability, and capable of generating bitumen product with very low solids content.

Future research should also focus on the mechanism study. It has only been a decade since IL was first used to extract bitumen from oil sands. The function mechanism by which IL reduces the solids content in bitumen product is not clear, and the relevant impact factors are worth exploring. In addition, more than one million simple ILs, which can be easily

prepared in the laboratory, have been found during the past 100 years [106]. It is a promising research direction to select ILs with superior comprehensive performance based on an understanding of the function mechanisms. In addition, ILASE process performed well in transferring solids from bitumen to IL, but after removing solids from IL by adding water, it needs large amount of energy to evaporate water from IL [107]. Reducing this energy consumption would enable the likelihood of industrial application of ILASE.

4.3 Switchable hydrophilicity solvent extraction

Switchable hydrophilicity solvent extraction (SHSE) process is also a novel NAE process. The first "switchable solvent" was discovered by Philip Jessop in 2004. After that, Jessop's group developed many switchable solvents and classified them into switchable polarity solvent (SPS), switchable hydrophilicity solvent (SHS), and switchable water (SW) [108, 109]. SHS is the type of solvent that can "switch" the property between hydrophobic and hydrophilic with the addition and removal of "switch agent" (usually CO_2) [110]. For example, $CyNMe_2$ is a common SHS, which is hydrophobic at normal condition, but becomes a hydrophilic solvent, $[CyNMe_2H][HCO_3]$, when mixed with water and CO_2. Holland et al. [111] used $CyNMe_2$ to extract bitumen from oil sands. As described in **Fig 9** [111], crushed oil sands ore sample was mixed with hydrophobic $CyNMe_2$, and bitumen was dissolved in $CyNMe_2$ and could be easily separated from mineral solids. After removing the solids, the addition of water and CO_2 to the bitumen-$CyNMe_2$ solution turned the solvent hydrophilic, thus bitumen could be separated easily. Removing CO_2 from the water/$CyNMe_2$/CO_2 mixture by heating could switch the solvent back to the hydrophobic state. In this state, water and solvent can be separated from each other and recycled. The result of bench-scale experiment showed a high bitumen recovery and low solvent loss.

Moreover, it was reported that within experimental error, the solids content in the extracted bitumen product was zero.

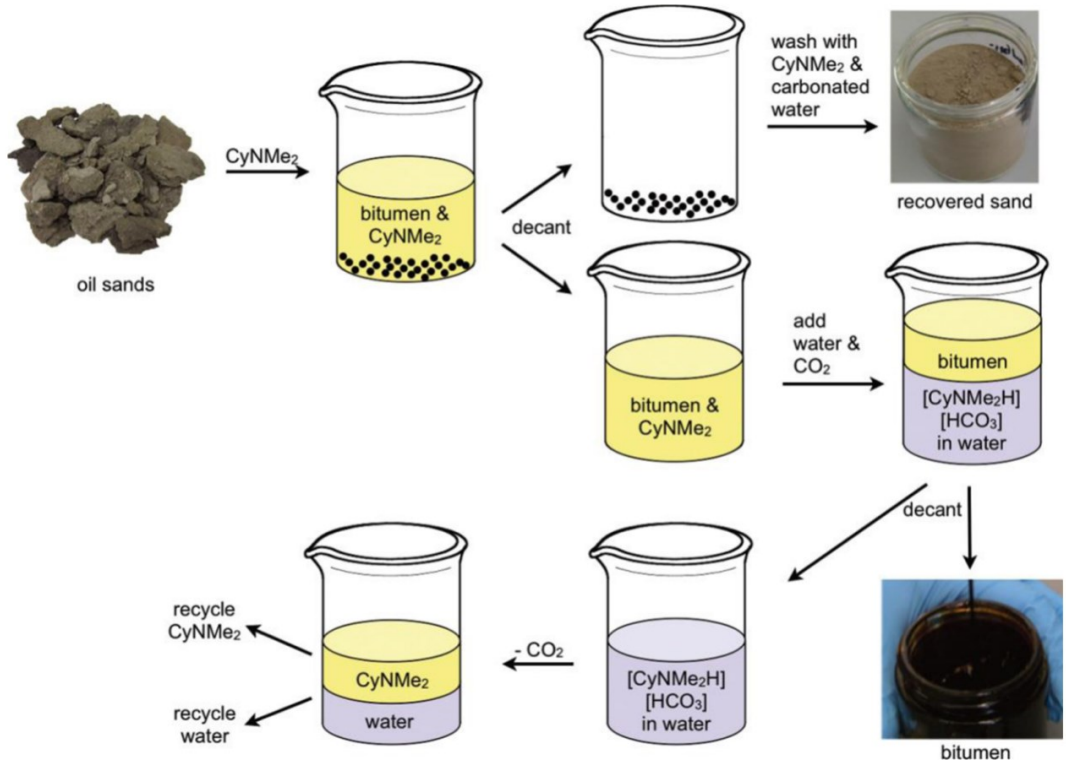

Fig. 9. Schematics of a SHSE process. Reproduced from reference [111].

Sui et al. [112] explored the roles of SHS in extracting bitumen from oil sands. Switchable hydrophilicity tertiary amines (SHTAs, such as triethylamine, N,N-dimethylcyclohexylamine, and N,N-dimethylbenzylamine) were used as SHS in their work. The surfaces of bitumen and solids were characterized by FT-IR, SEM/EDS, wettability test, zeta potential measurements, and QCM-D. It was found that the reason why SHS (SHTAs in their work) improved extraction performance was that the SHS could modify the surfaces of both bitumen and solids. The cation of SHS could adsorb on bitumen surface and form ions pairs. The ion pairs reduced the interactions between bitumen and solids and thus increased the wettability of solids surfaces. Therefore, the

separation of bitumen from solids surface became easier. The generated bitumen product contained 0.12 wt% fine solids according to their report. It can be seen that the SHSE process performed much better than the SAE process on reducing solids content in bitumen product, but the particular result was influenced by experimental conditions. It did not lead to bitumen product with solids content less than 0.03 wt%. In addition, as a new method, SHSE also face the issues such as cost and toxicity of SHS [113]. Future research could focus on developing new, better performing SHS with low toxicity, volatility, flammability, and eutrophication potential. The classification of SHS and the establishment of database on this type of solvent are also important for the industrial application of this process.

5 Conclusions

The bitumen product of nonaqueous extraction (NAE) of Alberta oil sands contains higher mineral solids content than what is required in downstream processes. The suspended mineral solids have very fine particle sizes and are usually coated by organic matters, which makes the fine particles difficult to remove by conventional separation methods. Research to remove the fine solids from bitumen products can be divided into two categories. One is to remove the fine solid particles from the diluted bitumen product after the NAE extraction, which focuses on improving separation efficiency by adding chemical additives in combination with physical separation techniques. The other category of the methods aims at directly obtaining bitumen product with low solids content by modifying the NAE process.

Methods in the first category, i.e., post extraction fine solids removal, include the addition of polymers, antisolvents, and water and by using electric field, hydrothermal treatment,

and surface functionalized particles.

• Polymers can cause bridging flocculation of the fine solids thus increasing their sizes and facilitating their removal. The proper polymers, such as polyethylene glycol (PEG_{1000}), was thought useful for enhancing fine solids removal performance from NAE bitumen. More efficient, commercially availble, and environmentally friendly polymers are still to be identified.

• Antisolvents, such as pentane, hexane, heptane or their mixture, were used to precipitate asphaltenes from the bitumen solution. The precipitated asphaltenes can form network structured aggregates and trap and remove the fine solids. This method was used in bitumen froth treatment (paraffinic froth treatment) of hot water extracted bitumen but have not been used in NAE extracted bitumen due to the loss of bitumen recovery. Relevant parameters like carbon number of solvents, S/B ratio, mixing temperature and energy input have been systematically studied. Future research could investigate mixing the anti-solvent with inorganic or organic additives to remove fine solids art lower bitumen losses.

• Water droplets together with additives can be used for removing fine solids from NAE bitumen. When water is added into the solvent, the fine solids tend to be absorbed into the water droplets or remain at the solvent-aqueous interface. The collected solids can then be removed together with the added water. Many papers in the open literature discussed the choice of additives, including cationic surfactant and water-soluble organic compounds with low molecular weight, such as resorcinol, formic acid, catechol, and chloral hydrate. This method also can work together with antisolvents to significantly improve the fine

solids removal efficiency.

• Electrostatic filtration was reported in fine solids removal from NAE bitumen in recent patent literature. The fine solids in NAE bitumen can be collected when the bitumen was passed through an electrostatic separator in the presence of electric field. The solids content in the final bitumen product can be reduced to 0.1 wt%. Further research on the mechanism and influencing factors of fine particles charge in diluted bitumen would improve the performance of this method.

• Enhancing fine solids removal by hydrothermal treatment or use surface functionalized particles have been studied on the applications of treating bitumen froth and oil sands tailings. These two methods should have potential to remove fine solids from NAE bitumen due to the similarities of the system composition.

The methods that directly obtain bitumen product with low fine solids content by modifying the traditional NAE process, including solvent extraction spherical agglomeration (SESA), ionic liquid assisted solvent extraction (ILASE), and switchable hydrophilicity solvent extraction (SHSE) process, are also reviewed in this work.

• SESA combines the addition of organic solvent and small amount of water which can agglomerate the fine particles and form removable solid-water spherical agglomerates, and therefore reducing the difficulty of solids removal and obtaining bitumen product with low solids content. Reports showed that the solids content in bitumen product of this process can be less than 2 wt%, which was still too high for NAE bitumen. The feedstock properties and operating parameter which influence solids content in bitumen product worth further explore by future research.

• In ILASE process an appropriate ionic liquid (IL) is used to assist the extraction of bitumen from oil sands by an organic solvent. IL has strong interaction with the surface of mineral solids in oil sands, so it can promote the release of bitumen and therefore increase extraction recovery and decrease fine solids content in bitumen product. ILASE can generate fine solids free bitumen product from the oil sands under specific conditions. However, there is a struggle of ILASE between extraction performance and environmental concern. Future research would aim at solving this issue.

• SHSE is a novel bitumen extraction process that uses switchable hydrophilicity solvent (SHS) to achieve better extraction performance than normal solvent alone extraction (SAE) process. It was reported that the solids content in final bitumen product was zero within experimental error. Similar to ILASE process, SHSE process also has environment and cost issues to be solved by future research.

Acknowledgements

During the preparation of this review, helpful advices have been received from Xuyang Liu and Menatalla Ahmed. The authors also have productive discussion with Xianfeng Sun. The authors acknowledge the financial support from the Natural Sciences and Engineering Research Council of Canada (NSERC). H.Z. would like to thank China Scholarship Council (CSC) for providing a scholarship for his PhD study at the University of Alberta.

References

[1] Poettmann FH, Kelly JT. Use of a soluble oil in the extraction of hydrocarbons from oil sands. US Patent 3,392,105; 1968.

[2] West RC. Non-aqueous process for the recovery of bitumen from tar sands. US Patent 3,131,141; 1964.

[3] Leung H, Phillips CR. Solvent extraction of mined Athabasca oil sands. Industrial & Engineering Chemistry Fundamentals. 1985; 24(3): 373-379.

[4] Adolf CK. Process and apparatus for separating and treating bituminous sands. US Patent 1,791,797; 1931.

[5] Czarnecki JA, Masliyah JH, Xu Z, Dabros M. Slurry preparation and conditioning. In: Handbook on Theory and Practice of Bitumen Recovery from Athabasca Oil Sands, Volume II: Industrial Practice; Kingsley Knowledge Pub, 2013: pp 71-114.

[6] Hooshiar A, Uhlik P, Liu Q, Etsell TH, Ivey DG. Clay minerals in nonaqueous extraction of bitumen from Alberta oil sands: Part 1. Non aqueous extraction procedure. Fuel Processing Technology 2012; 94(1): 80-85.

[7] Wu J, Dabros T. Process for solvent extraction of bitumen from oil sand. Energy & Fuels 2012; 26(2): 1002-1008.

[8] Cormack DE, Kenchington JM, Phillips CR, Leblanc PJ. Parameters and mechanisms in the solvent extraction of mined Athabasca oil sand. The Canadian Journal of Chemical Engineering 1977; 55(5): 572-580.

[9] Hooshiar A, Uhlik P, Ivey DG, Liu Q, Etsell TH. Clay minerals in nonaqueous extraction of bitumen from Alberta oil sands: Part 2. characterization of clay minerals. Fuel Processing Technology 2012; 96: 183-194.

[10] Pal K, Nogueira Branco LDP, Heintz A, Choi P, Liu Q, Seidl PR, Gray MR. Performance of solvent mixtures for non-aqueous extraction of Alberta oil sands. Energy & Fuels 2015; 29(4): 2261-2267.

[11] Nikakhtari H, Wolf S, Choi P, Liu Q, Gray MR. Migration of fine solids into product bitumen from solvent extraction of Alberta oilsands. Energy & Fuels 2014; 28(5): 2925-2932.

[12] Lin F, Stoyanov SR, Xu Y. Recent advances in nonaqueous extraction of bitumen from mineable oil sands: a review. Organic Process Research & Development 2017; 21(4): 492-510.

[13] Nikakhtari H, Vagi L, Choi P, Liu Q, Gray MR. Solvent screening for non-aqueous extraction of Alberta oil sands. The Canadian Journal of Chemical Engineering 2013; 91(6): 1153-1160.

[14] Rao F, Liu Q. Froth treatment in Athabasca oil sands bitumen recovery process: A review. Energy & Fuels 2013; 27(12): 7199-7207.

[15] Graham R, Helstrom J, Mehlberg R. A solvent extraction process for tar sand. Eastern Oil Shale Symposium 1987: 93-99.

[16] Meadus FW, Sparks BD, Puddington IE, Farnand JR. Separating organic material from tar sands or oil shale. US Patent 4,057,486; 1977.

[17] Meadus F, Bassaw B, Sparks B. Solvent extraction of Athabasca oil-sand in a rotating mill part 2. Solids-liquid separation and bitumen quality. Fuel Processing Technology 1982; 6(3): 289-300.

[18] Kaminsky HA, Etsell TH, Ivey DG, Omotoso O. Distribution of clay minerals in the process streams produced by the extraction of bitumen from Athabasca oil sands. The Canadian Journal of Chemical Engineering 2009; 87(1): 85-93.

[19] Kaminsky HAW, Uhlik P, Hooshiar A, Shinbine A, Etsell TH, Ivey DG, Liu Q, Omotoso O. Comparison of morphological and chemical characteristics of clay minerals in the primary froth and middlings from oil sands processing by high resolution transmission electron microscopy. In: Proceedings of the First International Oil Sands Tailings Conference, Edmonton, Canada. 2008: pp 102-111.

[20] Russel W. Brownian motion of small particles suspended in liquids. Annual Review of Fluid Mechanics 1981; 13(1): 425-455.

[21] Bensebaa F, Kotlyar LS, Sparks BD, Chung KH. Organic coated solids in Athabasca bitumen: Characterization and process implications. The Canadian Journal of Chemical Engineering 2000; 78(4): 610-616.

[22] Buckley J, Liu Y. Some mechanisms of crude oil/brine/solid interactions. Journal of Petroleum Science and Engineering 1998; 20(3-4): 155-160.

[23] Liu Q, Dong M, Asghari K, Tu Y. Wettability alteration by magnesium ion binding in heavy oil/brine/chemical/sand systems—analysis of electrostatic forces. Journal of Petroleum Science and Engineering 2007; 59(1-2): 147-156.

[24] Tian C, Lu Q, Liu Y, Zeng H, Zhao Y, Zhang J, Gupta R. Understanding of physicochemical properties and formation mechanisms of fine particular matter generated from Canadian coal combustion. Fuel 2016; 165: 224-234.

[25] Jin Y, Liu W, Liu Q, Yeung A. Aggregation of silica particles in non-aqueous media. Fuel 2011; 90(8): 2592-2597.

[26] Liu J, Cui X, Huang J, Xie L, Tan X, Liu Q, Zeng H. Understanding the stabilization mechanism of bitumen-coated fine solids in organic media from non-aqueous extraction of oil sands. Fuel 2019; 242: 255-264.

[27] Dickinson E, Eriksson L. Particle flocculation by adsorbing polymers. Advances in Colloid and Interface Science 1991; 34: 1-29.

[28] Ruehrwein R, Ward D. Mechanism of clay aggregation by polyelectrolytes. Soil Science 1952; 73(6): 485-492.
[29] Szilagyi I, Trefalt G, Tiraferri A, Maroni P, Borkovec M. Polyelectrolyte adsorption, interparticle forces, and colloidal aggregation. Soft Matter 2014; 10(15): 2479-2502.

[30] Lekkerkerker HN, Tuinier R. Depletion interaction. In: Colloids and the Depletion Interaction. Springer Netherlands, 2011: pp 57-108.

[31] Berg JC. Fluid interfaces and capillarity. In: An Introduction to Interfaces & Colloids: The Bridge to Nanoscience. World Scientific: Singapore, 2010: pp 30-80.

[32] Gregory J, Barany S. Adsorption and flocculation by polymers and polymer mixtures. Advances in Colloid and Interface Science 2011; 169(1): 1-12.

[33] Vajihinejad V, Gumfekar SP, Bazoubandi B, Rostami Najafabadi Z, Soares JB. Water soluble polymer flocculants: synthesis, characterization, and performance assessment. Macromolecular Materials and Engineering 2019; 304(2): 1800526.

[34] Dixon DV, Stoyanov SR, Xu Y, Zeng H, Soares JB. Challenges in developing polymer flocculants to improve bitumen quality in non-aqueous extraction processes: an experimental study. Petroleum Science 2020: 1-11.

[35] Mowla D, Naderi A. Experimental study of drag reduction by a polymeric additive in slug two-phase flow of crude oil and air in horizontal pipes. Chemical Engineering Science 2006; 61(5): 1549-1554.

[36] Ngnie G, Baitan D, Dedzo GK, Detellier C. Sedimentation of fine particles of

kaolinite and polymer-coated kaolinite in cyclohexane: Implications for fines removal from extracted bitumen in non-aqueous processes. Fuel 2018; 234: 218-224.

[37] Chopra S, Lines L. Introduction to this special section: heavy oil. The Leading Edge 2008; 27(9): 1104-1106.

[38] Madge D, Garner W. Theory of asphaltene precipitation in a hydrocarbon cyclone. Minerals Engineering 2007; 20(4): 387-394.

[39] Buckley JS, Wang J, Creek JL. Solubility of the least-soluble asphaltenes. In: Asphaltenes, Heavy Oils, and Petroleomics. Springer, 2007: pp 401-437.

[40] Andreatta G, Bostrom N, Mullins OC. High-q ultrasonic determination of the critical nanoaggregate concentration of asphaltenes and the critical micelle concentration of standard surfactants. Langmuir 2005; 21(7): 2728-2736.

[41] Buenrostro-Gonzalez E, Groenzin H, Lira-Galeana C, Mullins OC. The overriding chemical principles that define asphaltenes. Energy & Fuels 2001; 15(4): 972-978.

[42] Gonz´alez G, Neves GB, Saraiva SM, Lucas EF, dos Anjos de Sousa M. Electrokinetic characterization of asphaltenes and the asphaltenes- resins interaction. Energy & Fuels 2003; 17(4): 879-886.

[43] Pereira JC, L´opez I, Salas R, Silva F, Fern´andez C, Urbina C, López JC. Resins: The molecules responsible for the stability/instability phenomena of asphaltenes. Energy & Fuels 2007; 21(3): 1317-1321.

[44] Farnand J, Meadus F, Sparks B. Removal of intractable fine solids from bitumen solutions obtained by solvent extraction of oil sands. Fuel Processing Technology 1985; 10(2): 131-144.
[45] Zahabi A, Gray MR, Dabros T. Kinetics and properties of asphaltene adsorption on surfaces. Energy & Fuels 2012; 26(2): 1009-1018.

[46] Abudu A, Goual L. Adsorption of crude oil on surfaces using quartz crystal microbalance with dissipation (QCM-D) under flow conditions. Energy & Fuels 2009; 23(3): 1237-1248.

[47] Henry Jr JD, Prudich ME, Vaidyanathan KR. Novel separation processes for solid/liquid separations in coal derived liquids. Separation and Purification Methods 1979; 8(2): 81-118.

[48] Zahabi A, Gray MR, Czarnecki J, Dabros T. Flocculation of silica particles from a model oil solution: effect of adsorbed asphaltenes. Energy & fuels 2010; 24(6): 3616-3623.

[49] Long Y, Dabros T, Hamza H. Stability and settling characteristics of solvent-diluted bitumen emulsions. Fuel 2002; 81(15): 1945-1952.

[50] Lin F, Pang CJ. Impact of a hybrid bitumen extraction process on the destabilization of resulting bitumen froth emulsion diluted with heptane. Minerals Engineering 2020; 145: 106069.

[51] Long Y, Dabros T, Hamza H. Selective solvent deasphalting for heavy oil emulsion treatment. In: Asphaltenes, Heavy Oils, and Petroleomics. Springer, 2007: pp 511-547.

[52] Kosior D, Ngo E, Dabros T. Determination of the settling rate of aggregates using the ultrasound method during paraffinic froth treatment. Energy & Fuels 2016; 30(10): 8192-8199.

[53] Tang P, Raper JA. Modelling the settling behaviour of fractal aggregates: a review. Powder Technology 2002; 123(2-3): 114-125.

[54] Long Y, Dabros T, Hamza H. Structure of water/solids/asphaltenes aggregates and effect of mixing temperature on settling rate in solvent diluted bitumen. Fuel 2004; 83(7-8): 823-832.

[55] Zawala J, Dabros T, Hamza HA. Settling properties of aggregates in paraffinic froth treatment. Energy & Fuels 2012; 26(9): 5775-5781.

[56] Romanova UG, Yarranton HW, Schramm LL, Shelfantook WE. Investigation of oil sands froth treatment. The Canadian Journal of Chemical Engineering 2004; 82(4): 710-721.

[57] Gonzalez DL, Vargas FM, Hirasaki GJ, Chapman WG. Modeling study of CO_2-induced asphaltene precipitation. Energy & Fuels 2008; 22(2): 757-762.

[58] Okwen RT. Formation damage by CO_2 asphaltene precipitation. In: SPE International Symposium and Exhibition on Formation damage control. Society of Petroleum Engineers, 2006.

[59] Srivastava R, Huang S, Dong M, Dong M. Asphaltene deposition during CO_2 flooding. SPE Production & Facilities 1999; 14(04): 235-245.

[60] Malladi S. Removal of Particulate Fines from Organic Solvents Using Water as Collector Droplets. Ph.D. Thesis; 2015.

[61] Alquist HE, Ammerman AM. Process for extracting bitumen from tar sands. US Patent 4,229,281; 1980.

[62] Guymon EP. Solvent and water/surfactant process for removal of bitumen from tar sands contaminated with clay. US Patent 4,968,412; 1990.

[63] Liu J, Cui X, Santander C, Tan X, Liu Q, Zeng H. Destabilization of fine solids suspended in oil media through wettability modification and water-assisted agglomeration. Fuel 2019; 254: 115623.

[64] Hohlfeld M. Das niederschlagen des rauches durch elektricitat. Kastner Arch Gesammte Naturl 1824; 2: 205-206.

[65] Guitard C. Condensation by electricity. The Mechanics Magazine, London 1850; 53: 346.

[66] Fritsche GR, Bujas RS, Caprioglio GC. Electrostatic separator using a bead bed. US Patent 5,308,586, 1994.

[67] Ohsawa A, Morrow R, Murphy AB. An investigation of a dc dielectric barrier discharge using a disc of glass beads. Journal of Physics D: Applied Physics 2000; 33(12): 1487.

[68] Rosenholm JB. Evaluation of particle charging in non-aqueous suspensions. Advances in Colloid and Interface Science 2018; 259: 21-43.

[69] Morrison ID. Electrical charges in nonaqueous media. Colloids and Surfaces A: Physicochemical and Engineering Aspects 1993; 71(1): 1-37.

[70] Cullinane JT, Minhas BS. Electrostatic filtration of fine solids from bitumen. US Patent 9,752,079; 2017.

[71] Chen Q, Stricek I, Cao M, Gray MR, Liu Q. Influence of hydrothermal treatment on filterability of fine solids in bitumen froth. Fuel 2016; 180: 314-323.

[72] Chen Q. Organically-Modified Clay Minerals in Oil Sands: Characterization and Effect of Hydrothermal Treatment. PhD. Thesis; 2017.

[73] Zhao J, Liu Q, Gray MR. Characterization of fine solids in Athabasca bitumen froth before and after hydrothermal treatment. Energy& Fuels 2016; 30(3): 1965-1971.

[74] Guo Y, Wang S, Xu D, Gong Y, Ma H, Tang X. Review of catalytic supercritical water gasification for hydrogen production from biomass. Renewable and Sustainable Energy Reviews 2010; 14(1): 334-343.

[75] Akiya N, Savage PE. Roles of water for chemical reactions in high temperature water. Chemical Reviews 2002, 102(8), 2725-2750.

[76] Sakaguchi M, Laursen K, Nakagawa H, Miura K. Hydrothermal upgrading of loy yang brown coal|effect of upgrading conditions on the characteristics of the products. Fuel Processing Technology 2008; 89(4): 391-396.

[77] Dejhosseini M, Aida T, Watanabe M, Takami S, Hojo D, Aoki N, Arita T, Atsushi K, Adschiri T. Catalytic cracking reaction of heavy oil in the presence of cerium oxide nanoparticles in supercritical water. Energy & Fuels 2013; 27(8): 4624-4631.

[78] Zhang Z, Chai J, Zhang H, Guo L, Zhan JH. Structural model of longkou oil shale kerogen and the evolution process under steam pyrolysis based on reaxff molecular dynamics simulation. Energy Sources, Part A: Recovery, Utilization, and Environmental Effects 2019: 1-14.

[79] Berg MC, Dise JH, Petersen KT, Soane DS, Stokes KK, Ware Jr W, Thakrar AC. Systems and methods for removing finely dispersed particulate matter from a fluid stream. US Patent 10,570,037; 2000.

[80] Giakisikli G, Anthemidis AN. Magnetic materials as sorbents for metal/metalloid preconcentration and/or separation. A review. Analytica Chimica Acta 2013; 789: 1-16.

[81] Pamme N. Magnetism and microfluidics. Lab on a Chip 2006; 6(1): 24-38.

[82] Hejazian M, Li W, Nguyen NT. Lab on a chip for continuous-flow magnetic cell separation. Lab on a Chip 2015; 15(4): 959-970.

[83] Sparks B, Meadus F. A combined solvent extraction and agglomeration technique for the recovery of bitumen from tar sands. Energy Processing Canada 1979; 72(1): 55-61.

[84] Capes CE, McIlhinney A, Sirianni AF. Agglomeration from liquid suspension-research and applications. Agglomeration 1977; 77: 910-930.

[85] Harjai SK, Flury C, Masliyah J, Drelich J, Xu Z. Robust aqueous-nonaqueous hybrid process for bitumen extraction from mineable Athabasca oil sands. Energy & Fuels 2012; 26(5): 2920-2927.

[86] Yang H, Wang Y, Ding M, Hu B, Ren S. Water-assisted solvent extraction of bitumen from oil sands. Industrial & Engineering Chemistry Research 2012; 51(7): 3032-3038.

[87] Irani CA, Funk EW, Gomez E, Espino RL. Tar sands extraction process. US Patent 4,036,732; 1977.

[88] Sparks BD, Meadus FW, Hoefele EO. Solvent extraction spherical agglomeration of oil sands. US Patent 4,719,008; 1988.

[89] Sparks, B.; Meadus, F. A study of some factors affecting solvent losses in the solvent extraction—spherical agglomeration of oil sands. Fuel Processing Technology 1981, 4(4), 251-264.

[90] Majid, A.; Sirianni, A. F.; Ripmeester, J. A. Comparative study of three laboratory methods for the extraction of bitumen from oil sands. Fuel 1982, 61(5), 477-479.

[91] Plechkova, N. V.; Seddon, K. R. Applications of ionic liquids in the chemical industry. Chemical Society Reviews 2008, 37(1), 123-150.

[92] Painter, P.; Williams, P.; Mannebach, E. Recovery of bitumen from oil or tar sands using ionic liquids. Energy & Fuels 2010, 24(2), 1094-1098.

[93] Earle MJ, Esperanca JM, Gilea MA, Lopes JNC, Rebelo LP, Magee JW, Seddon KR, Widegren JA. The distillation and volatility of ionic liquids. Nature 2006; 439(7078): 831-834.

[94] Liu J, Xu Z, Masliyah J. Studies on bitumen- silica interaction in aqueous solutions by atomic force microscopy. Langmuir 2003; 19(9): 3911-3920.

[95] Dai Q, Chung KH. Bitumen-sand interaction in oil sand processing. Fuel 1995; 74(12): 1858-1864.

[96] Ji D, Liu G, Zhang X, Zhang C, Yuan S. Molecular dynamics study on adsorption of heavy oil drops on silica surface with different hydrophobicity. Energy & Fuels 2020.

[97] Hogshead CG, Manias E, Williams P, Lupinsky A, Painter P. Studies of bitumen- silica and oil- silica interactions in ionic liquids. Energy & Fuels 2011; 25(1): 293-299.

[98] Li X, Wang J, He L, Sui H, Yin W. Ionic liquid-assisted solvent extraction for unconventional oil recovery: Computational simulation and experimental tests. Energy & Fuels 2016; 30(9): 7074-7081.

[99] Williams P, Lupinsky A, Painter P. Recovery of bitumen from low grade oil sands using ionic liquids. Energy & Fuels 2010; 24(3): 2172-2173.

[100] Painter P, Williams P, Lupinsky A. Recovery of bitumen from Utah tar sands using ionic liquids. Energy & Fuels 2010; 24(9): 5081-5088.

[101] Li X, Sun W, Wu G, He L, Li H, Sui H. Ionic liquid enhanced solvent extraction for bitumen recovery from oil sands. Energy & Fuels 2011; 25(11): 5224-5231.

[102] Zhao D, Liao Y, Zhang Z. Toxicity of ionic liquids. Clean-Soil, Air, Water 2007; 35(1): 42-48.

[103] Zhang Q, Vigier KDO, Royer S, Jerome F. Deep eutectic solvents: syntheses, properties and applications. Chemical Society Reviews 2012; 41(21): 7108-7146.

[104] Pulati N, Tighe T, Painter P. Bitumen-silica interactions in a deep eutectic ionic liquid analogue. Energy & Fuels 2016; 30(1): 249-255.

[105] Pulati N, Lupinsky A, Miller B, Painter P. Extraction of bitumen from oil sands using deep eutectic ionic liquid analogues. Energy & Fuels 2015; 29(8): 4927-4935.

[106] Seddon K. The International George Papatheodorou Symposium: Proceedings. Boghosian, S 1999: 131-135.

[107] Berton P, Manouchehr S, Wong K, Ahmadi Z, Abdelfatah E, Rogers RD, Bryant SL. Ionic liquids-based bitumen extraction: Enabling recovery with environmental footprint comparable to conventional oil. ACS Sustainable Chemistry & Engineering 2019; 8(1): 632-641.

[108] Jessop PG, Heldebrant DJ, Li X, Eckert CA, Liotta CL. Reversible nonpolar-to-polar solvent. Nature 2005; 436(7054): 1102-1102.

[109] Jessop PG. Switchable solvents. Bioresource Technology 2012; 118: 628-632.

[110] Jessop PG, Phan L, Carrier A, Robinson S, D¨urr CJ, Harjani JR. A solvent having switchable hydrophilicity. Green Chemistry 2010; 12(5): 809-814.

[111] Holland A, Wechsler D, Patel A, Molloy BM, Boyd AR, Jessop PG. Separation of bitumen from oil sands using a switchable hydrophilicity solvent. Canadian Journal of Chemistry 2012; 90(10): 805-810.

[112] Sui H, Xu L, Li X, He L. Understanding the roles of switchable hydrophilicity tertiary amines in recovering heavy hydrocarbons from oil sands. Chemical Engineering Journal 2016; 290: 312-318.

[113] Vanderveen JR, Durelle J, Jessop PG. Design and evaluation of switchable-hydrophilicity solvents. Green Chemistry 2014; 16(3): 1187-1197.